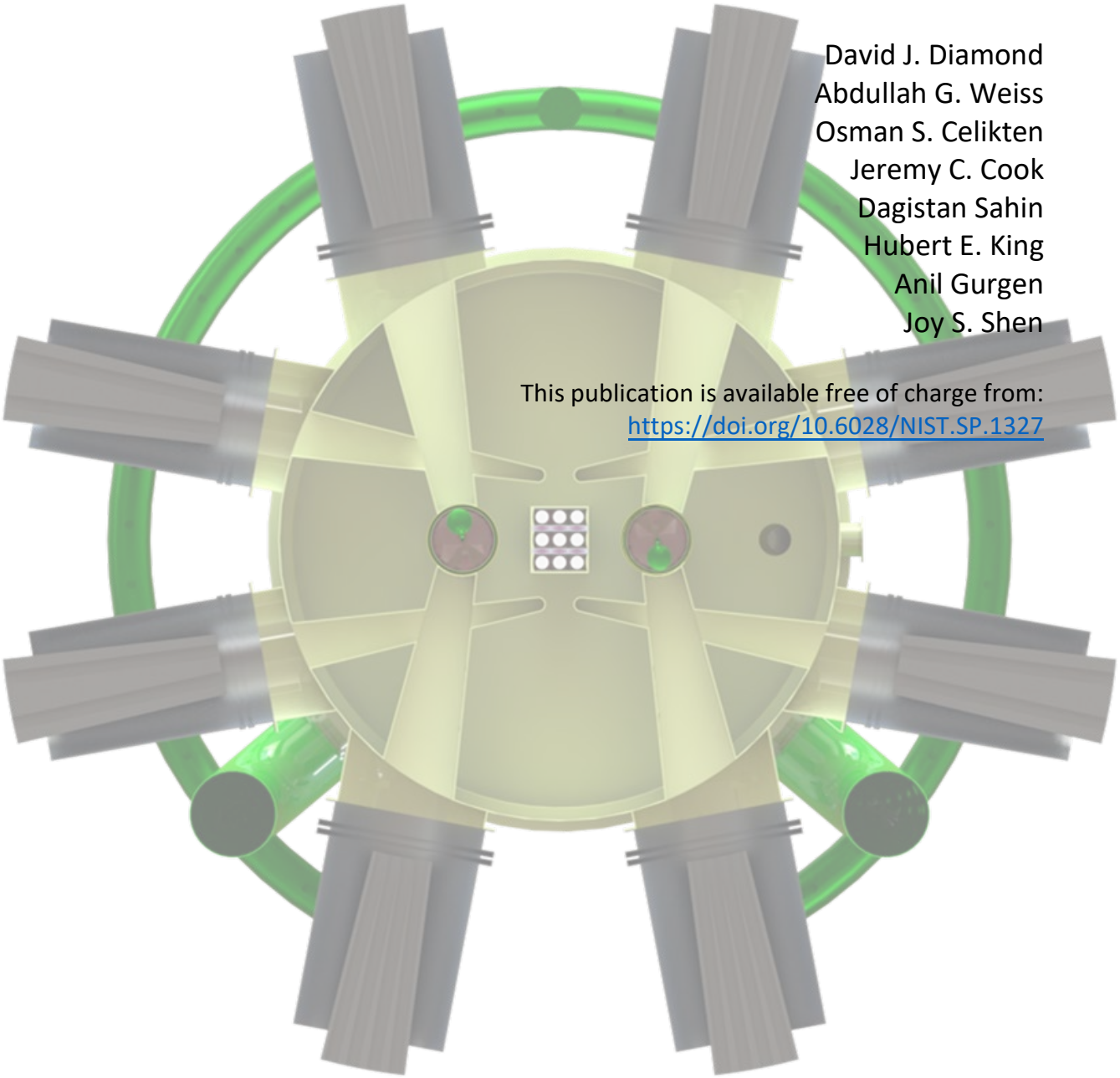
Check for updates

NIST Special Publication
NIST SP 1327

# NIST Neutron Source Pre-Conceptual Design



David J. Diamond
Abdullah G. Weiss
Osman S. Celikten
Jeremy C. Cook
Dagistan Sahin
Hubert E. King
Anil Gurgen
Joy S. Shen

This publication is available free of charge from:
https://doi.org/10.6028/NIST.SP.1327

NIST NATIONAL INSTITUTE OF STANDARDS AND TECHNOLOGY
U.S. DEPARTMENT OF COMMERCE

**NIST Special Publication**
**NIST SP 1327**

# NIST Neutron Source Pre-Conceptual Design

David J. Diamond
Abdullah G. Weiss
Osman Ş. Çelikten
Dağıstan Şahin
Anil Gurgen
Joy S. Shen
*Reactor Operations and Engineering*
*NIST Center for Neutron Research*

Jeremy C. Cook
*Research Facilities Operations*
*NIST Center for Neutron Research*

Hubert E. King
*Neutron Condensed Matter Science*
*NIST Center for Neutron Research*

This publication is available free of charge from:
https://doi.org/10.6028/NIST.SP.1327

February 2025




U.S. Department of Commerce
*Jeremy Pelter, Acting Secretary of Commerce*

National Institute of Standards and Technology
*Craig Burkhardt, Acting Under Secretary of Commerce for Standards and Technology and Acting NIST Director*

Certain equipment, instruments, software, or materials, commercial or non-commercial, are identified in this paper in order to specify the experimental procedure adequately. Such identification does not imply recommendation or endorsement of any product or service by NIST, nor does it imply that the materials or equipment identified are necessarily the best available for the purpose.

**NIST Technical Series Policies**
Copyright, Use, and Licensing Statements
NIST Technical Series Publication Identifier Syntax

**Publication History**
Approved by the NIST Editorial Review Board on 2025-02-10

**How to Cite this NIST Technical Series Publication**
Diamond DJ, Weiss AG, Celikten OS, Cook JC, Sahin D, King HE, Gurgen A, Shen JS (2025) NIST Neutron Source Pre-Conceptual Design. (National Institute of Standards and Technology, Gaithersburg, MD), NIST Special Publication (SP) NIST SP 1327. https://doi.org/10.6028/NIST.SP.1327

**Author ORCID iDs**
Abdullah G. Weiss: 0000-0003-1134-1735
Osman Ş. Çelikten: 0000-0002-4499-8699
Jeremy C. Cook: 0000-0002-6348-1812
Dağistan Şahin: 0000-0002-5256-1809
Hubert E. King: 0000-0002-9536-3802
Anil Gurgen: 0000-0002-2304-8061
Joy S. Shen: 0009-0004-8046-8945

**Contact Information**
abdullah.weiss@nist.gov
dagistan.sahin@nist.gov

NIST SP 1327
February 2025

## Abstract

A pre-conceptual design has been completed for a NIST Neutron Source (NNS). It would replace the existing facility at the NIST Center for Neutron Research (NCNR) to enable significantly more thermal and cold neutrons to be used in many more experiments than possible currently. The scientific community through several organizations has made recommendations to improve access to neutrons and Congress has requested that a strategic plan for the future of the NCNR be written. This report is in support of that plan.

At the heart of the NNS is a 20 MW compact reactor core cooled and moderated by light water. The fuel assemblies use uranium-molybdenum plates and reactivity is controlled with hafnium blades. The core is surrounded by a reflector tank containing heavy water and cold neutron sources (CNSs) which use liquid deuterium. Cold neutron guides extend out from the reflector tank to experimental stations as do thermal neutron beams. The reactor has a 40-day fuel cycle and is cooled with three out of the four pumps that are part of the design. The design has acceptable reactivity feedback from increases in temperature or voiding and is within thermal limits for both normal operation and transients or accidents where the instrumentation and control system protects the reactor.

The cold neutrons (wavelengths greater than 4 Å) that this design will deliver have an integral neutron brightness 3.5 times that at the present NCNR facility. For the two CNSs at least 15 kW of cooling would be necessary. Neutron currents at instruments will depend on future guide tube design. However, calculations of neutron currents entering guides from one CNS show that there will be a factor of 10 increase relative to the current NCNR cold source. The number of cold neutron guides from each CNS will increase to 16 whereas the single large CNS at the NCNR currently has 12. A proposed set of instruments for both cold and thermal neutron beams is presented as part of the design.

## Key Words

Neutron science; research; reactor; neutronics; thermal-hydraulics; guides; instruments; safety; beam.

# Table of Contents

Table of Figures ..... v
Foreword ..... ix
Acknowledgements ..... ix
Executive Summary ..... x
1 Introduction ..... 1-1
1.1 Background ..... 1-1
1.2 Objective ..... 1-3
1.3 Outline of Report ..... 1-4
1.4 References ..... 1-5
2 Design Philosophy ..... 2-1
2.1 Functions and Requirements ..... 2-1
2.2 Design Down-Selection ..... 2-6
2.3 References ..... 2-8
3 Reactor Design ..... 3-1
3.1 Summary Description ..... 3-1
3.2 Reactor Core and Reflector Components ..... 3-2
3.2.1 Core Assembly ..... 3-2
3.2.2 Fuel Assemblies ..... 3-4
3.2.3 Control Blades ..... 3-6
3.2.4 Reflector Tank ..... 3-6
3.3 Primary Cooling System ..... 3-8
3.3.1 General description ..... 3-8
3.3.2 Pumps ..... 3-10
3.4 Reactor Pool and Service Pool Cooling System ..... 3-10
3.5 References ..... 3-10
4 Nuclear Design ..... 4-1
4.1 Design-Basis ..... 4-1
4.2 Neutronic Steady-State and Burnup Model ..... 4-1
4.3 Neutron Flux Distribution and Spectrum ..... 4-7
4.4 Power Density and Fission Density Distributions ..... 4-9
4.5 Reactivity of Control Blades ..... 4-13
4.6 Reactivity Coefficients ..... 4-16

4.7 Reflector Dump ..... 4-18
4.8 Kinetics Parameters ..... 4-19
4.9 References ..... 4-20
5 Core Thermal-Hydraulic Design ..... 5-1
5.1 Design-basis ..... 5-1
5.2 Thermal-Hydraulic Methodology ..... 5-1
5.2.1 System Model ..... 5-1
5.2.2 Primary Coolant Pumps ..... 5-3
5.2.3 Heat Exchangers ..... 5-3
5.2.4 Flap Valves ..... 5-4
5.2.5 Shutdown Cooling System ..... 5-5
5.2.6 Core Models ..... 5-5
5.3 Computing Safety Margins ..... 5-8
5.4 Steady-State Analysis ..... 5-9
5.5 References ..... 5-12
6 Instrumentation and Control ..... 6-1
6.1 Introduction ..... 6-1
6.2 Design Philosophy ..... 6-2
6.3 Reactor Control System (RCS) ..... 6-3
6.4 Reactor Protection System (RPS) ..... 6-4
6.5 Radiation Monitoring System (RMS) ..... 6-5
6.6 Condition Monitoring System (CMS) ..... 6-6
6.7 Emergency Control Station (ECS) ..... 6-7
7 Safety Analysis ..... 7-1
7.1 Safety Philosophy ..... 7-1
7.2 Methodology ..... 7-2
7.3 Loss of Power Accident (LOPA) ..... 7-3
7.4 Loss of Heat Sink Accident ..... 7-6
7.5 Loss of Flow Accident (LOFA) ..... 7-7
7.6 Reactivity Insertion Accident (RIA) ..... 7-10
7.7 Loss of Coolant Accident (LOCA) ..... 7-12
7.8 Misloaded Fuel Assembly ..... 7-16

7.9 References ..... 7-17
8 Cold and Thermal Neutron Beam Production ..... 8-1
8.1 Cold and Thermal Neutrons ..... 8-1
8.2 CNS Design and Performance ..... 8-1
8.2.1 Liquid Deuterium CNS Cold Neutron Brightness ..... 8-2
8.2.2 CNS Size and Neutron Guide Illumination ..... 8-9
8.2.3 $LD_2$ CNS Diameter and Nuclear Heat Load ..... 8-11
8.3 Nuclear Heating of Al-Substrate Cold Neutron In-Pile Guides ..... 8-12
8.4 Thermal Beams ..... 8-13
8.4.1 Thermal Spectral Brightness at Thermal Guide Entrance and Dependence on Tube Position 8-13
8.4.2 Performance of Thermal Neutron Guides ..... 8-15
8.5 References ..... 8-18
9 Neutron Science Facilities ..... 9-1
9.1 Introduction ..... 9-1
9.2 Cold Neutron Beam Tube and Guide Network Layout ..... 9-1
9.3 Thermal Instruments ..... 9-4
9.4 Neutron Activation Analysis ..... 9-7
9.5 References ..... 9-7
Appendix A List of Acronyms / Abbreviations ..... 9-1

## Table of Figures

Figure 1-1 NCNR Mission [2] ..... 1-2
Figure 2-1 Alternative Designs Considered ..... 2-8
Figure 3-1 Reflector Tank with Core, Cold Sources and Beam Tubes ..... 3-1
Figure 3-2 Overview of NNS ..... 3-2
Figure 3-3 Planar View of the Core ..... 3-3
Figure 3-4 Reactor Core; Exploded View on the Right Showing Assemblies, Guide Boxes and Control Blade ..... 3-4
Figure 3-5 Fuel Management Scheme ..... 3-4
Figure 3-6 Fuel Assembly with 21 Fuel Plates ..... 3-5
Figure 3-7 Control Blade Inside Guide ..... 3-6
Figure 3-8 Reflector Tank; Internal Beam Tubes Shown on the Right ..... 3-7
Figure 3-9 Cutaway Showing Reflector Tank Internals ..... 3-8
Figure 4-1 Planar View of MCNP Model (a) with Details (b-e) ..... 4-2
Figure 4-2 Planar View of MCNP Model ..... 4-3
Figure 4-3 Elevation View of MCNP Model ..... 4-3
Figure 4-4 Methodology for Calculating Each Fuel Cycle ..... 4-6
Figure 4-5 Cycle States and Cycle Points ..... 4-7
Figure 4-6 Planar Views of Neutron Flux in Four Energy Groups at MOC ..... 4-8
Figure 4-7 Elevation Views of Neutron Flux in Four Energy Groups at MOC ..... 4-9
Figure 4-8 Normalized Fuel Assembly Power During a Fuel Cycle ..... 4-10
Figure 4-9 Relative Power in Each Fuel Stripe ..... 4-11
Figure 4-10 Axial Power in Fuel Plates and for FA Average in FAs with Maximum Peaking ..... 4-12
Figure 4-11 Power Density versus Fission Density for Six Cycle States ..... 4-13
Figure 4-12 Control Blade Positions in Core ..... 4-14
Figure 4-13 Worth of Safety Blades at Different Fuel Cycle States ..... 4-15
Figure 4-14 Worth of Regulating Control Blades at Different Fuel Cycle States ..... 4-15
Figure 4-15 Reactivity as a function of $D_2O$ in the Pool at SU and EOC ..... 4-17
Figure 4-16 Reactivity as a Function of $H_2O$ in Reflector at SU and EOC ..... 4-18
Figure 4-17 Effective Multiplication Factor as a Function of Reflector Dump Level ..... 4-19
Figure 5-1 Primary Coolant System Modeled in TRACE ..... 5-2
Figure 5-2 Core Representation Used in the TRACE System Model ..... 5-6
Figure 5-3 Power Parameters at Startup ..... 5-7
Figure 5-4 Core Representation with Detailed Core Model ..... 5-8
Figure 5-5 Hot Channel Temperature Distributions for Both Core Models ..... 5-10
Figure 5-6 Core Channel Axial Pressure Distributions ..... 5-11
Figure 7-1 Hot Channel Coolant Flow Rate During a Loss of Power Accident ..... 7-4

Figure 7-2 Temperatures During a Loss of Power Accident. ..... 7-4
Figure 7-3 Minimum CHFR During a Loss of Power Accident ..... 7-5
Figure 7-4 Minimum OFIR During Loss of Power Accident ..... 7-6
Figure 7-5 Temperatures in Hot Channel During a Loss of Heat Sink Accident ..... 7-7
Figure 7-6 Hot Channel Flow Rate During Loss of Flow Accident (Pump Seizure) ..... 7-8
Figure 7-7 Temperatures in Hot Channel During LOFA (Pump Seizure) ..... 7-8
Figure 7-8 Reactor Power During Loss of Flow Accident (Pump Seizure) ..... 7-9
Figure 7-9 Hot Channel Flow Rate During LOFA (Trip of Two Pumps) ..... 7-10
Figure 7-10 Temperatures in Hot Channel During LOFA (Trip of Two Pumps) ..... 7-10
Figure 7-11 Reactor Power During Reactivity Insertion Accident ..... 7-11
Figure 7-12 Temperatures in Hot Channel During Reactivity Insertion Accident ..... 7-12
Figure 7-13 Temperatures in Hot Channel During LOCA (78.5 $cm^2$ Break) ..... 7-13
Figure 7-14 Mass Flow Rate and Minimum CHFR During LOCA (78.5 $cm^2$ Break) ..... 7-14
Figure 7-15 Temperatures in Hot Channel During LOCA (314 $cm^2$ Break) ..... 7-15
Figure 7-16 Mass Flow Rate and Minimum CHFR During LOCA (314 $cm^2$ Break) ..... 7-16
Figure 7-17 Normalized Fuel Assembly Power with Misloaded Fuel Assembly ..... 7-17
Figure 8-1 Schematic Showing Access to the Two Cold Neutron Sources and Thermal Beam Tubes ..... 8-2
Figure 8-2 Brightness Spectrum of the NBSR and NNS ..... 8-3
Figure 8-3 Comparison of the Core Thermal Flux Distributions of the NBSR and NNS ..... 8-4
Figure 8-4 Brightness for the NNS with Various $LD_2$ Vessel Diameters and for the NBSR $LD_2$ Unit 3 CNS ..... 8-6
Figure 8-5 Brightness Ratios with Respect to the Present NBSR $LH_2$ Unit 2 CNS for Different NNS $LD_2$ Vessel Diameters ..... 8-7
Figure 8-6 Brightness Ratios with Respect to the Future NBSR $LD_2$ Unit 3 CNS for Different CNS $LD_2$ Vessel Diameters ..... 8-7
Figure 8-7 Planar View of the CNS with One Cavity ..... 8-8
Figure 8-8 Neutron Brightness Gain at the Cavity Side with Respect to the Non-Cavity Side of the CNS ..... 8-9
Figure 8-9 Schematic of Full-Illumination (top) and Under-Illumination (bottom) of an ideal, Long, Straight Neutron Guide ..... 8-10
Figure 8-10 Contributing Regions of a Rectangular Cross-Section Source ..... 8-11
Figure 8-11 Cryogenic System Radiation Heat Load as a Function of CNS Vessel Diameter ..... 8-12
Figure 8-12 Nuclear Heating for Al-Substrate In-Pile Cold Neutron Guides ..... 8-13
Figure 8-13 Plan View Showing Placement of Thermal Beam Tubes ..... 8-14
Figure 8-14 Thermal Neutron Brightness vs Neutron Wavelength for NNS and NBSR BT6 at the Shield Exit ..... 8-15

Figure 8-15 Flux Gains Using a Thermal Neutron Guide Over an Empty Penetration Through the Biological Shield ..... 8-17
Figure 9-1 Schematic Showing Access to the Two Cold Neutron Sources and Eight Thermal Beam Tubes [2] ..... 9-2
Figure 9-2 Possible Instrument Layout for Groups 1-4 [2] ..... 9-3
Figure 9-3 Beam Guide Configuration and Thermal Instruments ..... 9-6

## Table of Tables

Table 4-1 Reactivity for Different Blade Configurations ..... 4-14
Table 4-2 Neutron Generation Time for each Cycle State ..... 4-19
Table 4-3 Delayed Neutron Fractions and Decay Constants ..... 4-20
Table 5-1 Hydraulic Diameters for Portions of the Primary System ..... 5-2
Table 5-2 Geometry for Core Coolant Channels ..... 5-6
Table 5-3 Maximum Hot Channel Temperatures and Location for Both Core Models ..... 5-10
Table 5-4 Core Pressure Drop ($\Delta P$) for Both Steady State Models ..... 5-11
Table 5-5 Thermal Margins for Steady State Operation ..... 5-12
Table 6-1: Reactor Trip Inputs ..... 6-5
Table 6-2: Reactor Rundown Inputs ..... 6-5
Table 7-1 Safety Blades Reactivity vs Time After Reactor Trip ..... 7-3
Table 8-1 Integrals of Neutron Brightness in Figure 8-2 for All ..... 8-3
Table 8-2 Transmittable Neutron Currents Entering the Cold Neutron Guide Networks for the NBSR Unit 2 CNS ($LH_2$) versus the NNS CNS with 6 cm × 15 cm Guide Entrances ..... 8-4
Table 8-3 Transmittable Neutron Currents Entering the Cold Neutron Guide Networks for the NBSR Unit 2 CNS ($LH_2$) versus the NNS CNS with 6 cm × 20 cm Guide Entrances ..... 8-5
Table 8-4 Transmittable Neutron Currents Entering the Cold Neutron Guide Networks for the NBSR Unit 3 CNS ($LD_2$) versus the NNS CNS with 6 cm × 15 cm Guide Entrances ..... 8-5
Table 8-5 Transmittable Neutron Currents Entering the Cold Neutron Guide Networks for the NBSR Unit 3 CNS ($LD_2$) versus the NNS CNS with 6 cm × 15 cm Guide Entrances ..... 8-5
Table 8-6 Heating Contributions from Radiation Components and Total Minimum Cryogenic Heat Loads ..... 8-12
Table 9-1 Cold Instruments for Guide Halls ..... 9-4
Table 9-2 Thermal Instruments Currently Being Considered ..... 9-5

## Foreword

The use of neutrons as an essential tool in scientific discovery has increased exponentially in the nearly 100 years since their discovery. The unique properties of neutrons allow them to interact with matter in a way that no other technique can. Neutrons have been the primary driver in discovery and development of hundreds if not thousands of major achievements in virtually all scientific fields over the years and has significantly contributed to work resulting in the awarding of many Nobel prizes. For the U.S. to have any hope of leading the world in science, robust and vibrant neutron sources are an essential component of our scientific infrastructure, and it is apparent that the aging facilities in the U.S. cannot continually sustain the vast scientific demand of neutron sources over the long term.

The preconceptual design of a neutron source for NIST described in the pages that follow is the result of several years of effort by a dedicated and talented staff with one goal in mind: design of a relatively simple but world-leading neutron source that greatly enhances long-term scientific capabilities of the U.S.

Although the design will undoubtedly evolve with more detailed engineering effort, it is evident that the team has greatly succeeded in their efforts. Of note, this design features two large, high-flux cold sources which will provide a greater supply of essential cold neutrons than any existing facility in the world. The reactor, consisting of nine fuel assemblies, will be eminently licensable and easy to maintain and operate. Additionally, the facility is built with flexibility in mind, allowing it to accommodate future scientific and engineering improvements.

When built, this innovative neutron source design will provide the measurement capacity and capabilities required for the U.S. to achieve world leadership in neutron research and maintain it for decades to come, likely well into the 22$^{nd}$ century. We can only imagine the immense impact this would have on science and society.

Thomas H. Newton, Ph.D.
Deputy Director and Chief of Reactor Operations and Engineering
NIST Center for Neutron Research

## Acknowledgements

The principal authors are indebted to the encouragement and contributions made by many coworkers at the NIST Center for Neutron Research, specifically, Idan R. Baroukh, Noura R.A. Elsalamouny, Steven R. Kline, Yun Liu, Charles Majkrzak, Eliezer Nahmani, Patrick Park, Thomas Newton, Yaniv Shaposhnik, Danyal Turkoglu, and Robert Williams, and from Brookhaven National Laboratory, specifically, Lap-Yan Cheng. The authors would also like to acknowledge and recognize technical support and reviews from Argonne National Laboratory, specifically, John Stillman, Erik Wilson, and Dhongik Yoon.

# Executive Summary

The NIST Center for Neutron Research (NCNR) serves as one of the nation's primary resources for research using neutron techniques. The National Bureau of Standards Reactor (NBSR) at NCNR provides a safe and reliable neutron source for the thousands of researchers that come every year to utilize the facility. However, the NBSR is ageing and current NCNR facilities fall short of accommodating scientific demand. The National Academies of Sciences, Engineering, and Medicine, and the American Physical Society have recognized that a new facility is needed, and Congress has asked for a conceptual design of a new reactor and accompanying facilities. This report provides a pre-conceptual design of a new NIST Neutron Source (NNS) that will provide the neutron science community with higher neutron fluxes for more scientific instruments than at the NBSR using a reactor that can be operated safely and reliably.

The design of the NNS follows from the functions and requirements deemed important for its mission. Several potential designs were considered before detailed analysis was done for the current proposed NNS design. The design documented in this report is a 20 MW compact reactor core cooled and moderated by light water. It is surrounded by a reflector tank containing heavy water and cold neutron sources which use liquid deuterium. Cold neutron guides extend out from the reflector tank to experimental stations as do thermal neutron beams.

The core consists of a three-by-three array of fuel assemblies each containing 21 curved fuel plates fitted into side plates. The fuel plates contain monolithic uranium-molybdenum foils with a zirconium interlayer in an aluminum alloy cladding. The uranium is enriched to the maximum allowed, 19.75%. The side plates contain cadmium wires to minimize power peaking in fresh assemblies. Three of the fuel assemblies are fresh and stay in the reactor for three cycles. Four hafnium safety blades provide shutdown, and two hafnium blades provide reactivity control during operation.

The nuclear design was analyzed with the MCNP Monte Carlo neutronics code which has been validated for use on similar reactors. Calculations show that the reactor would have the target fuel cycle length of 40 days with acceptable power peaking, and high thermal neutron fluxes in the reflector where they are needed. Excess reactivity, shutdown reactivity, and maximum fission density are within expected Technical Specification limits. Increases in power and/or coolant temperature, the inadvertent mixing of light and heavy water, or the boiling of liquid deuterium in the cold neutron sources, all lead to negative reactivity feedback.

The thermal design, like the nuclear design, is meant to assure the safety of the reactor. The primary cooling system includes four centrifugal pumps, with only three needed for operation. Each is connected to a plate-type heat exchanger capable of removing a third of the reactor power. Thermal-hydraulic calculations were done using the well-validated TRACE code. Calculations for normal operation showed the fuel having significant margin to limiting conditions such as critical heat flux, onset of flow instability, departure from nucleate boiling or

the temperature at which blistering might occur. The design safety margin extended to transient/accident conditions that were analyzed due to postulated reactivity insertions, flow disruptions from problems with pumps or valves, or pipe breaks.

The transient/accident analysis takes into account reactor protection system setpoints which generate reactor shutdown using the safety blades or a backup shutdown system that drains water from the reflector tank. The reactor protection system includes measurement of core power and reactor period (from detectors in the reflector tank), primary coolant flow and temperature and reflector tank water level. Three other primary instrumentation and control systems are considered: the reactor control system and plant process control system which monitor and control operation and the radiation monitoring system.

With the reactor design, the NNS can deliver cold (below 5 meV) and thermal neutrons to experimentalists. Two cold neutron sources are placed in the reflector tank at the location of the maximum unperturbed thermal flux. They use liquid deuterium cryogenically cooled outside the tank with a helium heat exchanger. For the two cold sources at least 15 kW of cooling would be necessary. Calculations using MCNP show that the integral of neutron brightness for wavelengths greater than 4 Å is 3.5 times that presently at the NBSR liquid hydrogen cold source. Neutron currents at instruments will depend on future guide tube design. However, calculations of neutron currents entering cold neutron guides show that there will be a factor of 10 increase in the NNS relative to the current NBSR cold source.

Beam tube location for thermal beams that will exit from the reflector tank have not been optimized. However, initial calculations show that the thermal neutron brightness at the entrance to beam tubes at the NNS is at least a factor of two greater than at the NBSR.

Existing beam guide technology will be combined with today's cold neutron instruments. The number of cold neutron guides would be increased relative to the NBSR from 12 to 16. Instrument advances can be accomplished by customizing the neutron optics to transmit the beam area and divergence interval used by a particular instrument more efficiently. This also has the advantage of increasing the instrument signal-to-noise ratio. A proposed set of instruments for both cold and thermal neutron beams is presented.

It is noted that NNS design information herein is of a conceptual nature and does not include many systems that will eventually be added. For example, the confinement building, ultimate heat sink, positions for neutron activation, reflector tank cooling all will need to be added. The NNS design will mature with continued input from experimenters/users, architect-engineers, the regulatory body, and other stakeholders.

# 1 Introduction

## 1.1 Background

The NIST Center for Neutron Research (NCNR) serves as one of the nation's primary resources for research using neutron techniques. The National Bureau of Standards Reactor (NBSR) at NCNR provides a safe and reliable neutron source for the thousands of researchers that come every year to utilize the facility. The NBSR has a long history of successful operation [1] that began in 1967. It is licensed to operate by the U.S. Nuclear Regulatory Commission until 2029 at which point it will be relicensed. It is now one of only two major steady-state neutron scattering facilities in the U.S.

Through advanced instrumentation at the NCNR, thermal and sub-thermal (cold) neutrons are employed to conduct measurements in condensed matter science, biological sciences, fundamental physics, technology, and analytical chemistry. This is because neutrons reveal physical properties not readily probed by other techniques including photon or electron beams:

- They display wave-like properties with wavelengths comparable with interatomic spacings allowing determination of atomic and molecular structures.
- Their kinetic energy is comparable with that of atoms in solids and liquids, allowing atomic motions and their energy levels to be resolved by measuring neutron energy and momentum changes in the scattering process.
- Their electrical neutrality and very short-range nuclear interaction means that neutrons are penetrating, allowing bulk property measurements. This also allows encapsulation of samples in neutron-transparent materials permitting measurements under diverse conditions of chemistry, temperature, pressure, magnetic field or electrical bias. Their weak interaction also facilitates accurate interpretation of scattering data.
- The neutron magnetic moment couples to externally applied magnetic fields, such that the neutron scattering is sensitive to unpaired electron spins.
- Hydrogen has a particularly large thermal neutron scattering cross-section, which greatly facilitates the measurement of hydrogen locations and dynamics in heavy (higher atomic number) materials.
- The isotopic sensitivity of neutron scattering allows contrast variation, particularly involving hydrogen-deuterium isotope substitution.

The mission of the NCNR, outlined in Figure 1-1 [2] is to "assure the availability of neutron measurement capabilities to meet the needs of U.S. researchers from industry, academia and other government agencies." In answering the central question of how the NCNR can best fulfill this mission, one strategy is to "provide a source of neutrons into the future." To this end, an investment priority of the NCNR must be to "develop a long-term plan for providing

neutrons to the U.S. research community." Using the NBSR to provide this capability has limitations. The demand for time has been more than double with respect to the time available for the last five years of operation. Existing user facilities are at capacity and cannot be expanded. Furthermore, the NBSR reactor core components, structures and essential systems has recently required longer outages and larger expenditures due to material limitations and aging.

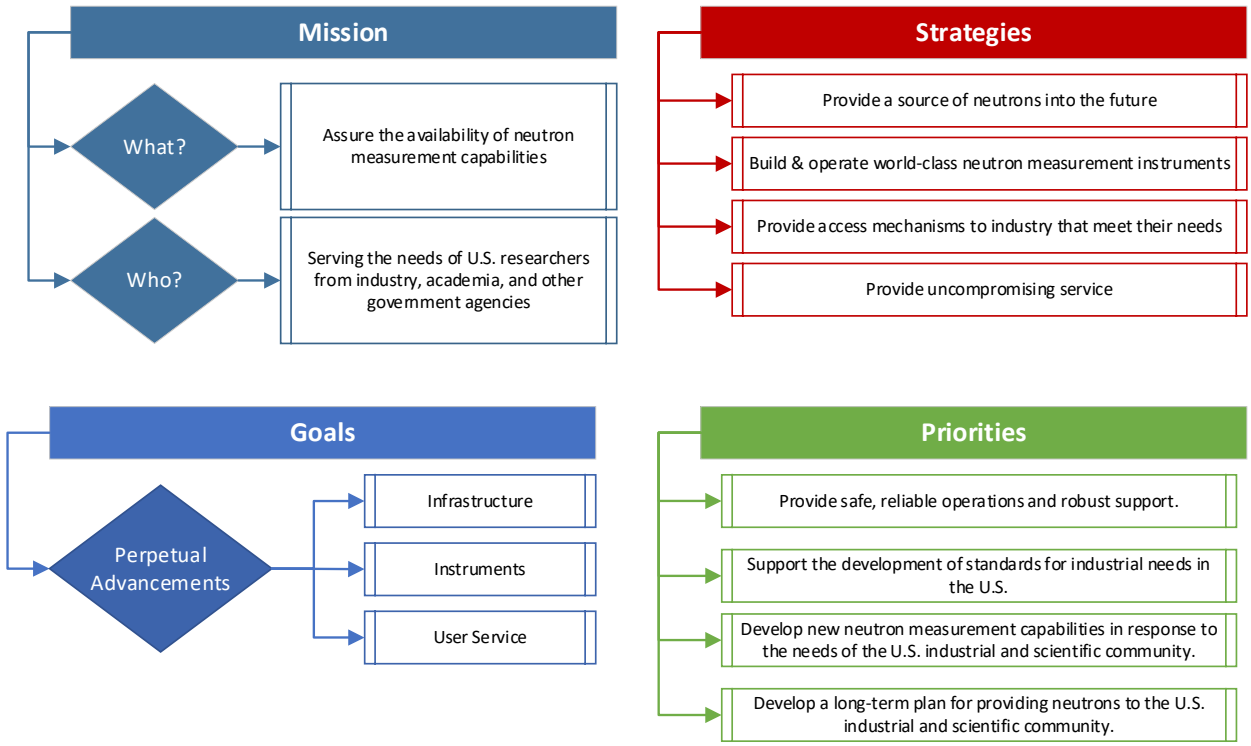



**Figure 1-1 NCNR Mission [2]**

A study on future options for the NCNR neutron source [3] found that a replacement reactor is the best option to ensure a reliable neutron source in the long term. Another option considered was a rehabilitated NBSR. This would address the issue of aging and possibly expand user facilities. However, this option requires replacement of core internals. The many unknowns involved with removing and replacing the reactor vessel, and the long downtime required, make this option undesirable. A third option, keeping the existing reactor operational, was also deemed undesirable because of the long-term uncertainty in the condition of the reactor structures, the vessel and primary systems such as the thermal shield, and furthermore, because it would not allow for expansion of neutron beams.

A new reactor within the NCNR can be built while the NBSR continues to operate and would take advantage of the infrastructure and personnel in place at the NCNR with a proven track record of running a world-class and cost-effective neutron science facility. A new state-of-the-art neutron source at the NCNR would greatly enhance neutron science capabilities and increase the scientific productivity measured by the long-standing abundance of scientific

publications and research participants. The new nuclear reactor would directly provide thermal neutron beams and, also cold neutron beams through cryogenically cooled moderator inserts (cold neutron sources).

It is encouraging to note that the process of transitioning from an aging neutron source to a new state-of-the-art facility has precedent. Three recent examples are:

1) Forschungsreaktor München II (FRM II) [4], a beam-tube research reactor that replaced the research reactor FRM at Garching, Germany in 2004 after more than 40 years of operation.
2) Open Pool Australian Lightwater (OPAL) reactor [5] a multi-purpose research reactor that replaced the High Flux Australian Reactor (HIFAR) in 2007 after nearly 50 years of operation at the Australian Nuclear Science and Technology Organization (ANSTO) Research Establishment.
3) Pallas Reactor [6] replacing the previous High Flux Reactor (HFR) in Netherlands.

An assessment of the NCNR by the National Academies of Sciences, Engineering, and Medicine in 2018 [7] recognized that "Loss of this facility [the NBSR] would have a strongly negative impact on neutron science within the United States and the scientific disciplines that the NCNR serves." Furthermore, "NCNR should commission a detailed assessment of the current facility and begin the conceptual design of a new reactor." The American Physical Society in their 2019 report [8] on neutron sources had the following recommendation: "The United States should initiate an effort to competitively design and build a new generation of LEU-fueled [low-enriched uranium fueled] high-performance research reactors that would satisfy all needs presently met by current HEU-fueled [highly enriched uranium fueled] U.S. high-performance research reactors and provide new capabilities." Other recent reports that highlight the important contributions of neutron scattering and imaging techniques to a broad range of scientific disciplines and technology have been issued by the Swiss Academies [9], the U.S. Department of Energy [10] and recently again, the National Academies of Sciences [11].

Additionally, the NCNR supports NIST's role as the nation's reference laboratory for measurements and standards of chemical composition. Neutron activation analysis carried out at the NBSR serves as one of the two independent measurements required for the certification of Standard Reference Materials®. This service must also continue in the future.

## 1.2 Objective

This report provides a pre-conceptual design for a NIST Neutron Source (NNS) that will satisfy the needs of the neutron science community for the remainder of this century. It is a prelude to a conceptual design for an NNS that will include a replacement reactor concept and the cold neutron sources, neutron guides and thermal neutron beam tubes that satisfy the needs of experimentalists. The objective of this report is to discuss the functional requirements for the proposed NNS and explain how those requirements could be met. For the reactor, the report focuses on the neutronic and thermal-hydraulic design, the mechanical design of associated

components, and the instrumentation and control that would be required. The report shows how the reactor would respond to operational events and hypothetical accidents to understand the inherent safety of the design. In terms of neutron science user facilities, the report provides the path forward for the cold and thermal neutron sources and the beam tube and guide network taking into account the instruments that are likely to be used by experimentalists.

Another important objective is to help satisfy a portion of the 2022 NIST Appropriations Act [12] that has taken into account the recommendations described in Section 1.1 above. In that congressional legislation (Sec. 211, "Neutron Scattering") it is stated:

*(a) STRATEGIC PLAN FOR THE INSTITUTE NEUTRON REACTOR. — The [NIST] Director shall develop a strategic plan for the future of the Institute Center for Neutron Research after the current neutron reactor is decommissioned, including—*

*(1) a succession plan for the reactor, including a roadmap with timeline and milestones;*
*(2) conceptual design of a new reactor and accompanying facilities, as appropriate; and*
*(3) a plan to minimize disruptions to the user community during the transition.*

*(b) COORDINATION WITH THE DEPARTMENT OF ENERGY. — The Secretary, acting through the Director, shall coordinate with the Secretary of Energy on issues related to Federal support for neutron science, including estimation of long-term needs for research using neutron sources, and planning efforts for future facilities to meet such needs.*

*(c) REPORT TO CONGRESS. — Not later than 30 months after the enactment of this Act, the Director shall submit to Congress the plan required under subsection (a), and shall notify Congress of any substantial updates to such plan in subsequent years.*

This report satisfies (a)(2).

## 1.3 Outline of Report

Chapter 2, Design Philosophy, provides the functions for the NNS, that is, what it is designed to do. The requirements or specific parameters that satisfy each function are discussed as are design features that are desirable but not requirements. Chapter 2 also provides the design down-selection; the designs, that might have satisfied the functions and requirements and that eventually led to the pre-conceptual design documented in this report. A description of the replacement reactor pre-conceptual design is given in Chapter 3. This includes the core and reflector components, the primary cooling system and other features. Chapter 4 explains the nuclear design and includes a summary of the neutronics methodology and key parameters such as the reactivity of control elements, reactivity feedback coefficients, and power distributions. The thermal-hydraulic design is described in Chapter 5. The margin to thermal limits during operation is given along with the description of the methodology used. Chapter 6, Instrumentation and Control provides the design philosophy and details of the relevant industrial control systems. An abbreviated safety analysis is given in Chapter 7 along with the

methods used for the analysis. The objective is to show that the transients/accidents analyzed lead to acceptable consequences. Chapter 8 explains the cold and thermal beams that are included for experimentalists. A proposed design of the cold neutron sources is provided. The improvement in beams' performance with respect to existing facilities is given. Lastly, Chapter 9, Neutron Science Facilities, discusses the beam tubes and neutron guides and the resulting instrumentation which they enable.

## 1.4 References

[1] J. J. Rush and R. L. Cappelletti, "The NIST Center for Neutron Research: Over 40 Years Serving NIST/NBS and the Nation," National Institute of Standards and Technology, Gaithersburg, MD, NIST SP 1120, 2011 2011. Accessed: 2023-04-12 16:28:19.

[2] R. Dimeo, "NCNR All Hands Presentation," February 26, 2019. [Online]. Available: https://www-i.ncnr.nist.gov/admin/NCNR_AllHands2019.pdf.

[3] T. H. Newton, P. C. Brand, and D. Hughes, "Future Options for the Neutron Source at the NIST Center for Neutron Research," National Institute for Standards and Technology, 2017.

[4] W. Gläser and W. Petry, "The new neutron source FRM II," (in en), *Physica B: Condensed Matter,* vol. 276-278, pp. 30-32, March 1, 2000 2000, doi: 10.1016/S0921-4526(99)01460-X.

[5] S.-J. Kim, "The OPAL (open pool Australian light-water) reactor in Australia," (in en), *Nuclear Engineering and Technology,* vol. 38, no. 9, pp. 443–448, 2006.

[6] Unknown, "Pallas Reactor." [Online]. Available: https://www.pallasreactor.com/en.

[7] National Academies of Science, "An Assessment of the Center for Neutron Research at the National Institute of Standards and Technology: Fiscal Year 2018," The National Academies Press, Washington, DC, 2018.

[8] J. D. Wells, *Neutrons for the Nation: Discovery and Applications while Minimizing the Risk of Nuclear Proliferation*. American Physical Society Panel on Public Affairs, 2019.

[9] "Neutron Science Roadmap for Research Infrastructures 2025–2028 by the Swiss Neutron Science Community, Swiss Academies Reports, Vol. 16, No. 7," 2021. [Online]. Available: https://boris.unibe.ch/156933/1/327_Neutron_Science_Roadmap_2021.pdf

[10] "Scientific Justification for a U.S. Domestic High-Performance Reactor-Based Research Facility, Report of the Basic Energy Sciences Advisory Committee, U.S. Department of Energy, Office of Science.," 2020.

[11] National Academies of Science, "An Assessment of the National Institute of Standards and Technology Center for Neutron Research: Fiscal Year 2023," Washington, DC, 2024.

[12] U. S. Congress, "NIST Appropriations Act," February 28, 2022.

# 2 Design Philosophy

## 2.1 Functions and Requirements

The functions and requirements for the NIST Neutron Source are defined by the NCNR and the scientific community that utilizes the NCNR and are consistent with those of the Department of Commerce. The functions identify what the NNS should be designed to do, and the requirements are the specific parameters that will satisfy the functions. When possible, the requirements are quantified as either a bounding value or a range of values. Requirements may be modified (and certainly will be added) in the future when more feedback is obtained from experimenters/users, architect-engineers, the regulatory body, and other stake holders. There are design features that, although not requirements, are desirable and they are discussed herein as well.

There are five functions that the NNS must satisfy:

F1. Neutron Science: The NNS must: (1) Provide cold and thermal neutron beams[a] that meet the current and anticipated needs of the neutron science community with high availability (capacity factor); (2) alleviate present and future over-subscription of scientific instruments; (3) be competitive and complementary with other premier neutron scattering facilities; (4) provide future expansion capabilities; and (5) provide irradiation capability with negligible detriment to item (1).

F2. Reactor Safety: The NNS must be able to be licensed by the U.S. Nuclear Regulatory Commission (NRC).

F3. Reactor Manufacturability: The neutronic, thermal-hydraulic, and mechanical design, and the materials chosen to build the reactor must not challenge the manufacturability of the NNS and add risk to the project. They must also be chosen to help minimize the cost of construction and lifetime cost of the NNS.

F4. Operational Reliability: The neutronic, thermal-hydraulic, and mechanical design, and the materials chosen to build the reactor must not challenge operational reliability; that is, the ability to operate without interruption in each fuel cycle and the ability to do routine maintenance in a fixed schedule between fuel cycles.

F5. Adequacy of Balance-of-Plant: The reactor supplies the neutrons and is the central system. There are many structures, systems, and components (SSC) that complete the plant and allow the reactor to be a useful neutron source. The balance-of-plant SSC must be consistent with all functional requirements above.

---

[a] Thermal neutrons are defined herein as having energies less than 1 eV and cold neutrons are defined as having wavelengths greater than 4 Å.

The following explains how those functions can be attained through requirements on the design of the NNS.

Requirements for F1, Neutron Science

The NNS will be tailored for neutron science involving thermal and cold neutron beams. The NNS should be both (1) competitive with other premier neutron science facilities that utilize continuous neutron sources, such as FRM-II in Germany and ILL in France, and (2) complementary of premier neutron science facilities that have pulsed neutron sources, such as European Spallation Source in Sweden and Spallation Neutron Source at Oak Ridge National Laboratory.

Presently, the NCNR offers world-class capabilities owing to the NBSR design and investments in upgrades of the cold neutron sources, neutron guides and instruments. At the initial startup (commissioning), the NNS should at least deliver the capabilities that exist with the NBSR as the neutron source. Once at full capacity, the facility should alleviate the over-subscription of scientific instruments through the combination of an increased number of instruments and the intensities of the neutron beams. Additional capacity (i.e., available neutron guide end positions, particularly those involving cold neutrons) is desired to allow for expansion of capabilities to meet increased demand from anticipated growth in the user base and to accommodate additional novel scientific instruments that will arise in the future.

R1.1. Surrounding the reactor core, a reflector vessel should be filled with heavy water and have ample space to accommodate multiple cold neutron sources (CNSs), beam tubes and irradiation facilities. The determining factor for the performance of a cold neutron source or a beam tube is the unperturbed thermal neutron flux at its location in the reflector. At a given reactor power, the unperturbed neutron flux is inversely correlated with the active core volume. The ultra-compact FRM II core, enabled by use of highly-enriched uranium fuel, has a peak unperturbed neutron flux in the reflector of $8\times10^{14}$ $cm^{-2}s^{-1}$ at a 20 MW power level. The compact OPAL reactor core has a peak unperturbed neutron flux in the reflector of $4\times10^{14}$ $cm^{-2}s^{-1}$ at a 20 MW power level. The NBSR, which does not have a compact core, has a peak unperturbed neutron flux in the reflector of $2\times10^{14}$ $cm^{-2}s^{-1}$ at a 20 MW power level.

R1.2. The NNS core should be sufficiently compact to produce a minimum peak unperturbed thermal neutron flux in the reflector of $5\times10^{14}$ $cm^{-2}s^{-1}$ at a 20 MW power level.

R1.3. Cold neutrons, with wavelengths greater than 4 Å, should be the primary output from the CNSs because they are used by most experimentalists. As many as 50 total beam instruments are targeted for this design. Preliminary assessments for the number of cold neutron instruments is, at minimum, 16. To accommodate each instrument with an end position of a cold neutron guide, an equal number of neutron guides, 16 at a minimum, is required. With additional spare capacity, a minimum of 20 cold neutron guides are envisioned, each having an in-pile entrance at a distance of 1.5 m or less from each cold neutron source. With each neutron guide having an entrance window of 20 cm by 6 cm in size, the large solid angle

subtended by the in-pile neutron guides likely requires multiple large-volume cold neutron sources, which have cryostats filled with liquid deuterium at 20 K, and multiple beam tubes viewing each cold neutron source. To allow installation and maintenance of cold neutron sources to be independent of the in-pile neutron guides, they should occupy vertical thimbles. The cold neutron source designs and their locations should be optimized to maximize cold neutron source brightness within the practical constraints of cooling the cold neutron source and having safe and stable operation.

R1.4. It is desired, at minimum, to sustain the existing suite of thermal neutron beam instruments currently at the NCNR (six instruments). It is possible that additional thermal neutron instruments (at least two), such as a Materials Diffractometer, may be accommodated with the use of thermal neutron guides. The use of thermal neutron guides may facilitate instrument layout and, in some cases, place the affected instruments in areas of lower background radiation. Thermal beam tubes of appropriate geometry, likely intersecting the cold neutron conduits, allow placement of the thermal beam entrances close to the unperturbed thermal neutron flux peak in the reflector. The locations of thermal beam tubes should maximize the performance of thermal neutron instruments without reducing the flux in the cold moderator by more than 5%.

R1.5. Near-core irradiation facilities (i.e., thimbles, ports and tubes) of various sizes in the reflector tank should be included for pneumatic irradiation facilities and experiment facilities and should not detract from cold and thermal neutron facilities or significantly impact reactor availability.

Requirements for F2, Reactor Safety

The NNS will obtain a construction permit and initial operating license from the NRC as a Class 104 non-power reactor (NPR, aka non-power production or utilization facility). NPRs are licensed after providing a Safety Analysis Report (SAR) to the NRC that demonstrates their safety and acceptable risk to the public. The NRC report, NUREG-1537, “Guidelines for Preparing and Reviewing Applications for the Licensing of Non-Power Reactors,” provides guidance for “Format and Content” of the SAR in Part 1, and in Part 2 provides the “Standard Review Plan and Acceptance Criteria.” [1][b]

Based on previous practice, desirable outcomes, and/or the guidance in NUREG-1537, the requirements for demonstrating the minimum acceptable reactor safety are given below. Note that these requirements may dictate certain design features, for example: the use of burnable poisons to reduce power peaking; the speed of control element insertion to provide adequate shutdown and a withdrawal speed to limit a reactivity insertion accident; and pump characteristics that provide for adequate cooling during operation and during a flow coast-down.

[b] Note that NRC plans to publish a draft of a revised NUREG-1537 in 2025.

R2.1. The analysis of normal operation and transients expected during the life of the reactor must show that operational thermal limits are not exceeded with at least a 95% probability at a 95% confidence level.[c] The thermal limits to be considered are critical heat flux and onset of nucleate boiling; similar to the limits currently imposed on the plate fuel used in the NBSR.

R2.2. The analysis of design-basis accidents must show that no safety limit is exceeded with at least a 95% probability at a 95% confidence level. The technical specification safety limit basis for the NNS will be the temperature at which there is the probability of blistering; a blistering criterion also applies to the NBSR at present.. The same limit for the LEU plate fuel proposed for the NBSR has been considered for all NNS safety analyses.

R2.3. The analysis of a maximum credible accident[d] must show that the event leads to an exposure to a member of the public at the reactor boundary to be less than required by NRC (e.g., currently 100 mrem whole-body dose).

A theoretical loss-of-coolant accident (LOCA) assuming a consequential break in the primary cooling system is known to be a very low probability event in reactors operating at close to atmospheric pressure. Nevertheless, a reactor-in-pool design can essentially eliminate any serious consequences (and perhaps preclude any release of radioactivity to the environment) without hindering the other functions of the NNS.

R2.4. Reduce the risk from a LOCA by situating the reactor in a pool which will provide cooling if there is a pipe break in the primary cooling system.

For a non-power reactor, it is not necessary to have two independent rapid shutdown systems. Nevertheless, a backup means of assuring that the reactor can be brought to a shutdown state is necessary even if it is not a rapid system.

R2.5. The reactor should be designed with a backup shutdown system that uses instrumentation and operation independent of the normal shutdown system. For example, shutdown can be achieved by draining the reflector or some similar action that does not include introducing neutron poisons into the primary coolant or reflector.

Requirements for F3, Reactor Manufacturability

The NNS is expected to be an important contribution to science and technology for at least 60 years. The design of the NNS should follow well-established (state-of-the-art) approaches to research reactor design, that is, the design process should not be a research project and the

---

[c] The NRC does not have a numerical criterion for the acceptability of NPR thermal-hydraulic parameters.

[d] NUREG-1537 suggests the analysis of a maximum hypothetical accident (MHA) and explains what assumptions should be used for fission product release independent of the probability of an event leading to that release. An approach which takes into account improved methods for analyzing accidents (e.g., probabilistic risk analysis), since the concept of an MHA was introduced in NUREG-1537, is to define a maximum credible accident and augment it with defense-in-depth.

design should minimize the construction and lifetime cost of the project. While increasing the scientific productivity, the NNS operational and maintenance costs should be reduced compared to the existing NBSR reactor. The cost of fuel is determined by manufacturing cost and the cost of $^{235}U$. The expected annual cost of low-enriched uranium (LEU) fuel for the NNS should be comparable with that projected for the NBSR after conversion to using LEU (and not yet known).

R3.1. The fuel design (form and material) should already be qualified, that is, approved for use by the NRC, or enveloped by a qualified design. This requirement leads to the use of plates containing a fuel foil consisting of a U-10Mo fuel core with an interlayer of zirconium and cladding, the latter being an aluminum alloy. This fuel plate design is being developed by the Department of Energy to replace highly enriched uranium fuel in research reactors [2] and is expected to be qualified by the NRC within the next five years. An alternative, also being considered for use in research and test reactors, is a plate with dispersion fuel consisting of a uranium silicide and aluminum mixture. The fuel must contain uranium enriched in $^{235}U$ only up to 19.75 weight percent; the maximum enrichment allowed in the U.S. The NNS core should allow both fuel types (monolithic or dispersion) with minimal impact to cold neutron source brightness and thermal neutron beam performance.

R3.2. The fuel assembly and core design should be state-of-the-art, perhaps similar to existing designs. NCNR has had positive experience with a vendor providing fuel assemblies for the NBSR based on a square box design with slightly curved plates.

R3.3. The NBSR core design has fuel assemblies widely spaced and maximizes flux in the midplane gap. Most neutron sources are built with compact cores (without a midplane gap) to maximize the flux in the reflector region. This approach should be followed and recent expertise from foreign reactors should be considered. In particular, there is much to learn from the Argentine RA-10 [3] and the Australian OPAL reactor [4] designs.

R3.4. The fuel cycle should optimize the burnup of the fuel to minimize cost. The local burnup is limited by the allowable fission density determined through the fuel qualification effort at Idaho National Laboratory. Hence, in addition to concern over having power peaking too high so that thermal margins are too low, reduced power peaking allows for higher fuel assembly average burnup.

<u>Requirements for F4, Operational Reliability</u>

The design of the NNS must ensure a reliable source of neutrons is available to experimentalists for a repeatable operational period, that period being the length of the fuel cycle needed to run the reactor. Availability is as important to users as the neutron flux level at their instruments.

R4.1. The optimization of the fuel cycle should include the needs of the experimenters. This means that the fuel cycle length should be between 40 days and 50 days. It is assumed that the outage time between cycles will be 3-8 days as opposed to the NBSR outage time of 11 days;

hence, the capacity factor could be as high as 94%. The minimum capacity factor should be 83% (e.g., a 40-day fuel cycle and 8-day outage).

R4.2. A stable flux level is important to the users. The control system must be able to maintain a stable neutron source throughout the fuel cycle. Hence, reactivity control shims should be placed away from the periphery of the core where it is desirable for the flux to peak.

R4.3. To minimize outage time for maintenance, consideration should be given to having important components isolated so that work can be done while the reactor is operating. For example, having primary coolant pumps and heat exchangers in separate rooms would enable these components in one loop to be serviced during a reactor cycle when other loops are operational.

Requirements for F5, Adequacy of Balance-of-Plant

There are many structures, systems, and components that need to be considered in the future (e.g., spent fuel and fresh fuel storage, confinement, and radioactive waste). However, the only requirements at this stage are those that might impact the design of the reactor itself.

R5.1. The existing infrastructure at the NCNR should be used to the extent possible to limit cost and help assure availability. However, the ability of the NBSR to operate during the construction of the NNS must also be considered.

## 2.2 Design Down-Selection

Multiple options were considered for a future neutron source, and the experts concluded that a new fission reactor source is the most desirable and feasible to replace the NBSR [5]. As such, the NNS is designed as a fission-based research reactor.

Given that the NNS would be based on a fission reactor, a small effort began looking at potential designs in 2013. Although the functions and requirements for the NNS had not been codified at that time, the general path forward was clear: based on the experience of recent examples, it would be a light-water cooled and moderated reactor utilizing plate fuel and a heavy-water reflector housing the cold neutron sources and thermal beam guides. It would be located in a pool of water providing emergency cooling and it would be at the same 20 MW power level as the NBSR.

The 20 MW power level was felt to be an optimum choice because a) the licensing of a 20 MW reactor at NIST had already been done; b) it avoided technical issues at higher power such as higher heat loads on the cold neutron sources (CNSs) and possibly smaller safety margins and smaller cycle lengths; and c) designing a higher power reactor is a relatively inefficient means of generating the increased neutron fluxes needed to perform many types of scattering measurements on the forefront of condensed matter research. With respect to Item c) designing advanced cold sources, neutron guides and individual, specialized scattering

instruments can be far more effective than increasing power. Optimized cold sources and guide networks that are matched to state-of-the-art scattering instruments can improve performance over existing conventional scattering capabilities by orders of magnitude—an increase that simply cannot be achieved at a comparable cost by increasing reactor power alone (which can result only in proportional flux increases at best).

Advanced, high-performance instruments typically make use of a larger fraction of the available neutrons with a Maxwellian distribution by several means, such as through the employment of wavelength-dependent detectors, multiplexing, and imaging and focusing with mirror systems. Examples of such high-performance instruments currently operating at the NBSR include the inelastic scattering spectrometer MACS and the polychromatic beam reflectometer CANDOR. Nonetheless, a state-of-the-art, world class, advanced scattering instrument typically costs on the order of $15M. Thus, for a complement of 30 such instruments—appropriate for a major neutron scattering center—an investment of $500M is required, a sizable fraction of the overall facility cost.

The NBSR core design with well-spaced fuel elements and a gap at the axial midplane had worked well in the past to optimize the thermal flux for cold neutron sources and thermal beam tubes that face the unfueled midplane. However, it was recognized that designs with compact cores to optimize the thermal flux in the reflector could be more efficient and since the reactor would not be a “general purpose” reactor, there was no need for multiple in-core irradiation spaces.

Although no cores with midplane gaps in fuel were considered, one creative design was considered that mixed closely spaced fuel elements with horizontal separation of two core halves. The split core design enabled two large-volume CNSs to be placed close to the central flux trap [6]. This option, however, had reactor criticality control and stability issues due to the physical separation of the two halves and has not been considered further.

Different options considered are shown in Figure 2-1 with names and number of fuel elements (FEs) used as well as an idea of where a CNS might be located (in magenta). Most use box-like fuel elements. All use fuel plates (similar to what is used in NBSR) with LEU fuel enriched to the maximum allowed, 19.75 w/o $^{235}$U. The fuel was U-10Mo, the alloy being developed for research reactors to replace current highly-enriched uranium fuels. Light water cooling and moderation was used in the fuel elements with heavy water in the reflector (light blue) to provide thermal neutrons for the cold sources and beam tubes. The analysis with rectangular FEs all had the same fuel to simplify comparisons with respect to other features.

These studies were used to understand how different CNSs and beam tubes could be optimally integrated into the design of the reflector. The studies looked at the effect of fuel thickness in the plates, fuel length, and coolant channel width. It was seen that the peak neutron flux in the reflector was inversely correlated with the core volume and the fuel cycle length was positively correlated with core volume. The compromise selected for further study was the Box9 design with 21 plates in each fuel assembly.

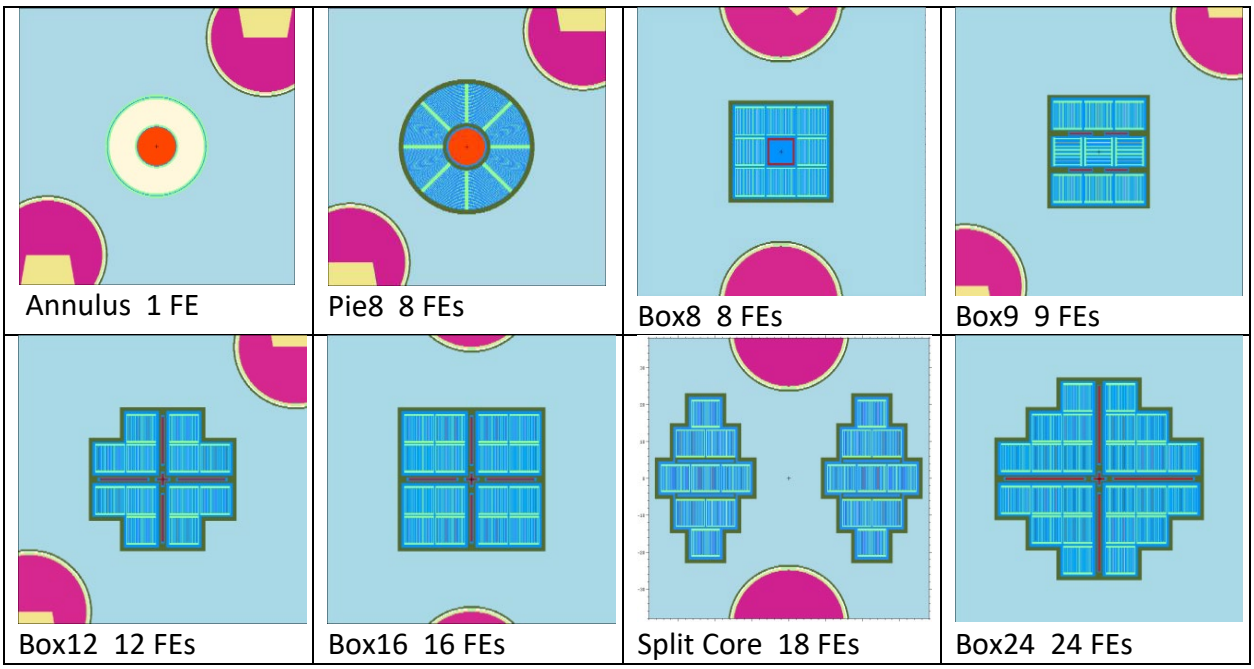



**Figure 2-1 Alternative Designs Considered with Varying number of Fuel Elements (FEs)**

## 2.3 References

[1] U.S. Nuclear Regulatory Commission, "Guidelines for Preparing and Reviewing Applications for the Licensing of Non-Power Reactors, NUREG/CR-1537, Part 1, Format and Content and Part 2, Standard Review Plan and Acceptance Criteria," U.S. Nuclear Regulatory Commission, NUREG 1537, 1996.

[2] B. Rabin, et al., "Preliminary Report on U-Mo Monolithic Fuel for Research Reactors," Idaho National Laboratory, INL EXT-17-40975. Revision 3, 2020.

[3] "Argentina's RA-10 research reactor nearing completion," *Nuclear Engineering International,* February 29, 2024.

[4] S.-J. Kim, "The OPAL (open pool Australian light-water) reactor in Australia," (in en), *Nuclear Engineering and Technology,* vol. 38, no. 9, pp. 443–448, 2006 2006.

[5] S. Wilson, M. Hore, and S. Kline, "Neutrons for the Future," National Institute of Standards and Technology, Gaithersburg, MD, NIST SP 2100-07, October 18-20, 2023, 2024, https://doi.org/10.6028/nist.sp.2100-07.

[6] Z. Wu, R. E. Williams, J. M. Rowe, T. H. Newton, and S. O'Kelly, "Neutronics and Safety Studies on a Research Reactor Concept for an Advanced Neutron Source," (in en), *Nuclear Technology,* vol. 199, no. 1, pp. 67-82, 2017-07-03 2017, doi: 10.1080/00295450.2017.1335146.

# 3 Reactor Design

## 3.1 Summary Description

The NNS pre-conceptual design was influenced by several reactors designed for neutron science and especially by the OPAL reactor design. The OPAL reactor specifications, published by the International Atomic Energy Agency (IAEA) as part of a Coordinated Research Project [1], were used extensively to ensure the use of realistic parameters for the NNS core and fuel assembly geometry.

NNS is a research reactor with a nominal power of 20 MW. It is composed of a light-water-cooled compact reactor core located inside a vertical channel (the "core chimney") that is surrounded by heavy-water in the reflector tank. These components/structures are located at the bottom of a reactor pool filled with demineralized light water. The reflector tank will contain the cold neutron sources and associated beam guides as well as thermal neutron beam tubes. The internals of the reflector tank with the reactor core at the center, two cold sources and beam tubes is shown in Figure 3-1.

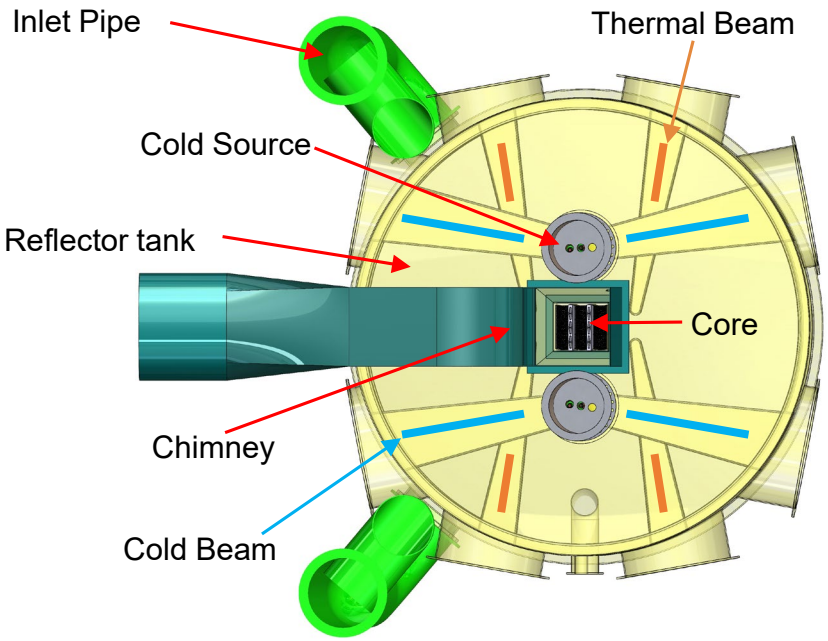



**Figure 3-1 Reflector Tank with Core, Cold Sources and Beam Tubes**

The core has nine fuel assemblies (FAs) in a compact three-by-three array and six control blades. The FAs are almost square in cross-sectional profile, and each contains 21 curved fuel plates consisting of fuel and cladding, the latter forming the first barrier to fission product release outside the reactor. The fuel is composed of a U-10Mo foil with a zirconium interlayer on each side. The six control blades contain hafnium as the neutron poison and are pushed upward out of the core by Zircaloy-4 follower rods.

The core is cooled by upward flow of demineralized light water, which also acts as a neutron moderator. The core chimney channels the coolant to where it is pumped away by the primary cooling system (PCS) for heat removal by the secondary cooling system. The PCS, including the water in the reactor pool, serves as the second barrier against any fission product release. The PCS has four centrifugal pumps and four heat exchangers each in separate rooms with three of each being used during operation. The fourth pump and heat exchanger can either be in standby mode or under maintenance.

The general layout of the reactor including the PCS is shown in the left side of Figure **3-2**. The right side of the figure shows the components inside the reactor pool. In Section 3.2 the core and reflector components are discussed, and the primary coolant system is discussed in Section 3.3.

Not shown in these figures is the system which provides cooling to the reactor pool and to the service pool (used primarily for storing fuel). This system is also important for providing shutdown and emergency cooling and it is described in Section 3.4.

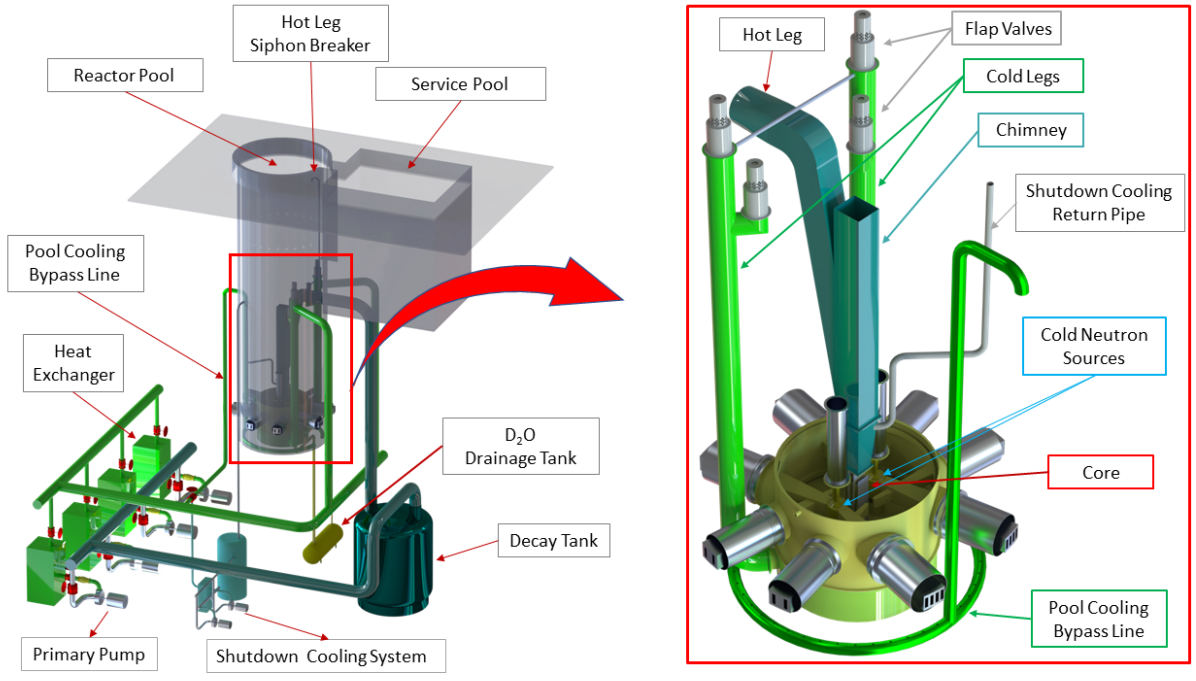



**Figure 3-2 Overview of NNS**

## 3.2 Reactor Core and Reflector Components

### 3.2.1 Core Assembly

The core consists of nine fuel assemblies and six control blades as shown in Figure 3-3. Fuel assemblies are arranged in a three-by-three array, with guide boxes for the control blades

separating each row. The FAs are all aligned with the curvature of the plates in the same direction. This requires the spacing from the end fuel plate to the chimney to be different on each side of the core and requires a mechanical design that prohibits the FAs from being loaded in another direction. The size of the core is 24.4 cm x 29.1 cm with a FA height of 96 cm (80 cm maximum plate length and 70 cm fueled length). A three-dimensional view of the core is shown in Figure 3-4.

The core is loaded as shown in Figure 3-5 during an equilibrium cycle with the control blades (not shown) between rows 1 and 2 and rows 2 and 3 on the figure. Three fresh assemblies (identified as A, B, and C and green in the figure) are loaded each cycle and then moved to another position (A', B', and C', yellow) in the next cycle and then in the third and last cycle moved to a final position (A", B", and C", red). The figure also uses row/column coordinates to locate the position of the assemblies.

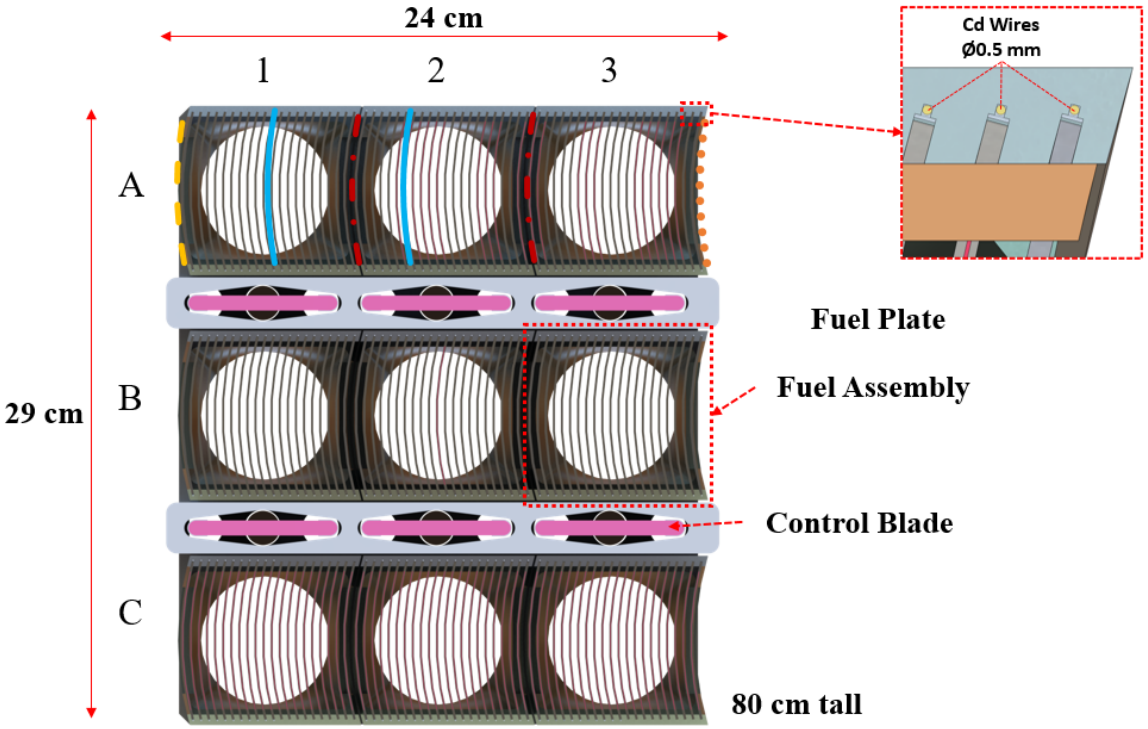



**Figure 3-3 Planar View of the Core**

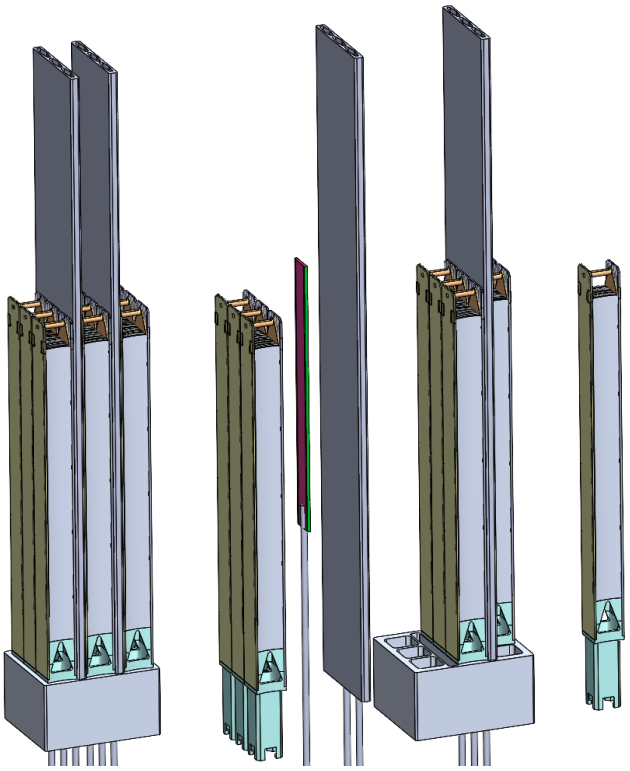


**Figure 3-4 Reactor Core; Exploded View on the Right Showing Assemblies, Guide Boxes and Control Blade**

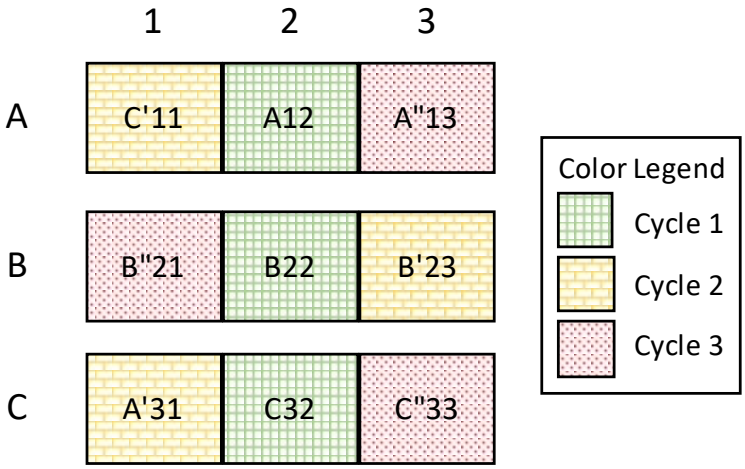



**Figure 3-5 Fuel Management Scheme**

### 3.2.2 Fuel Assemblies

The fuel assemblies are approximately 8 cm by 8 cm in cross-sectional profile, and each contain 21 curved fuel plates as seen in Figure **3-6**. The fueled region in each aluminum-clad curved plate is a U-10Mo foil with zirconium interlayer on each side. This type of fuel is currently undergoing qualification and demonstration testing at conditions relevant to the NNS. The fuel

core region of each fuel foil is 0.025 cm thick, the interlayer 0.0025 cm thick, the cladding 0.0415 cm thick, and the fuel extends 70 cm along the length of the plate. The uranium density is 15.4 g/cm$^3$ leading to a total of 728 g of $^{235}$U per fuel assembly. If this fuel type is unavailable, it is known that a dispersion fuel using $U_3Si_2$ may be a satisfactory alternative [2].

The fuel plates are assembled into two grooved side plates. The side plates contain cadmium wires with diameter of 0.05 cm next to each fuel plate along a 41 cm portion of the fuel height; the Cd burnable poison being used to control power peaking and reactivity in fresh fuel assemblies.

The outer fuel plates are slightly longer than the 19 internal plates to serve a structural function. The side plates are welded to the inlet nozzle at the bottom and connected to each other on the top by the lifting handle. The lifting handle also acts as a barrier in case of a loose connection between a fuel plate and the side plates. The inlet nozzle has a rectangular shape. Its upper part has two lateral passages to allow coolant flow to cool the outer channels formed between two fuel assemblies or between a fuel assembly and the chimney wall.

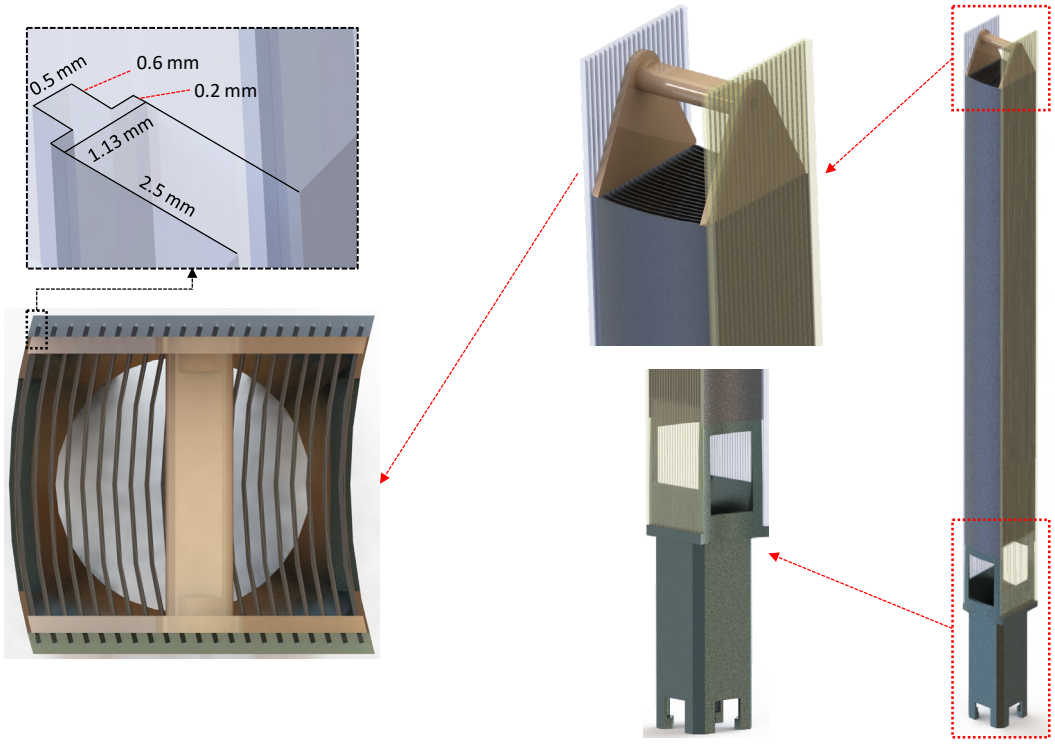



**Figure 3-6 Fuel Assembly with 21 Fuel Plates**

### 3.2.3 Control Blades

The primary reactivity control system is through six control blades organized in two rows in the core (see Figure 3-3 and Figure 3-4). Rapid insertion of the six control blades serves as the primary shutdown mechanism. The four control blades at the peripheral locations are designated as the safety or shutdown blades and are fully withdrawn from the core during reactor startup. The two interior control blades provide reactivity control during a fuel cycle to compensate for fuel burnup and temperature changes and are designated regulating blades.

The two types of blades are only differentiated by functionality; physically, all six control blades are identical (see Figure 3-7). Each blade is made of hafnium 700 mm long, 70 mm wide, and 7 mm thick. Along the blade surface, the two small flat sides are clad in a thin layer of Zircadyne, which prevents mechanical erosion of the hafnium while moving within the control blade guides. The bottom of each blade is welded to a Zircaloy-4 connecting rod which extends a few meters down to the operating piston in the lower room.

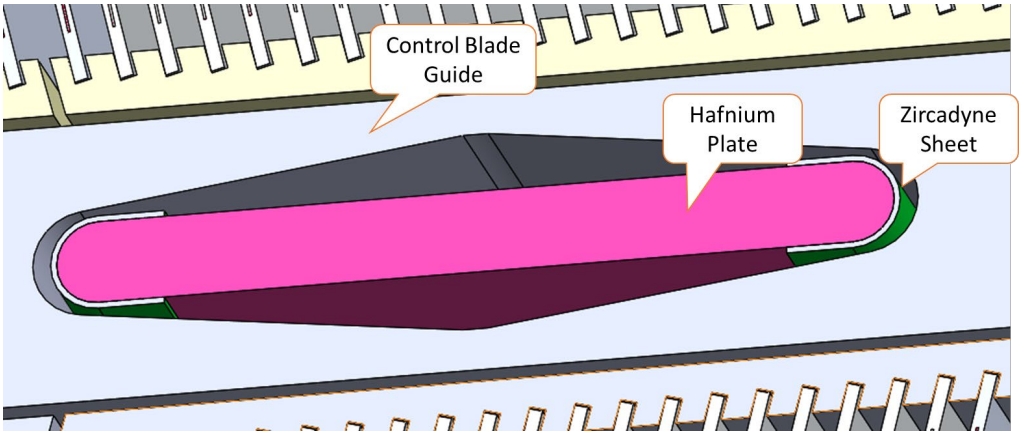



**Figure 3-7 Control Blade Inside Guide**

The control blades use passive fail-safe design features to ensure reactor safety. To achieve criticality, control blades are raised out of the core by operating rods electromagnetically coupled to drive motors. De-energization of the electromagnets naturally drops all control blades back in the core. This gravitational fail-safe system yields a rapid shutdown without electrical power or mechanical action. Faster shutdown time is achieved by rapid insertion of compressed air to the driving piston.

### 3.2.4 Reflector Tank

The reflector tank is made of Zircaloy-4 and has a cylindrical shape with two flat plates across the top and bottom. It is approximately 6 $m^3$ in volume. Along the vertical axis of the tank there is a hollow space with a square cross section in which the lower part of the core chimney and the core are located. The entire tank is watertight. A three-dimensional view is shown in Figure 3-8. The figure does not show cold neutron sources or piping to drain the tank as a backup

shutdown system or circulate water to a cooling system. It also does not show irradiation (rabbit) tubes that would be present for neutron activation analysis.

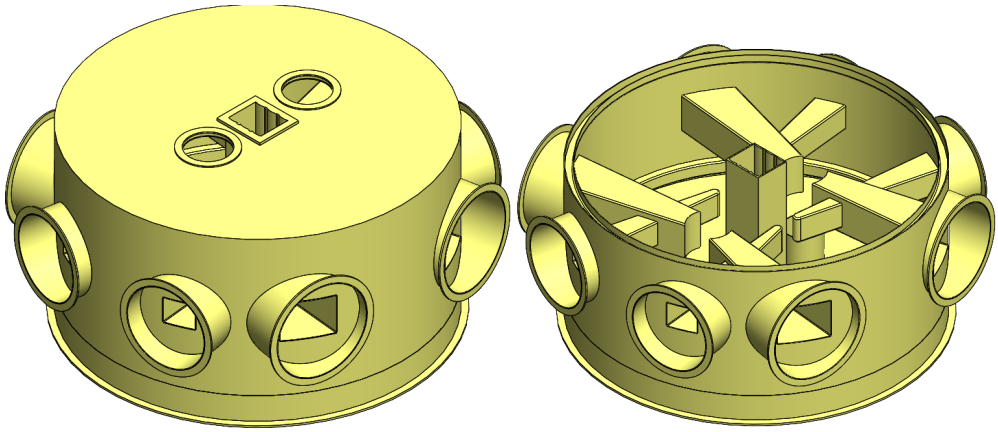


**Figure 3-8 Reflector Tank; Internal Beam Tubes Shown on the Right**

The inside of the tank contains heavy water, and the outer surface is in contact with de-mineralized light water. The heavy water and light water circuits are independent of each other. Fission chamber detectors for nuclear criticality control channels are also housed in the reflector tank (not shown here). They allow the active part of the detector to be at the edge of the core. The tank is filled with heavy water to almost full height. In the upper section, a thin layer of helium allows for expansion of the heavy water.

A view of the reflector tank showing the chimney with reactor core and two cold neutron sources with structures for cooling systems is shown in Figure 3-9. The cold neutron sources shown here and elsewhere in this report are conjectures. Eventually, they will be optimized based on the needs of the scientists using their beams. The beam tubes shown on the figure are of rectangular cross section with circular flanges at the exit. Four cold neutron beams and four thermal neutron beams are inside the reflector. The beams cross each other taking advantage of available space. The thermal beams are tangent to a side of the core, expanded eight degrees, with 20 cm height. The cold beams, with a height of 30 cm, point to the center of the cold sources and expanded to accommodate four guide splitters.

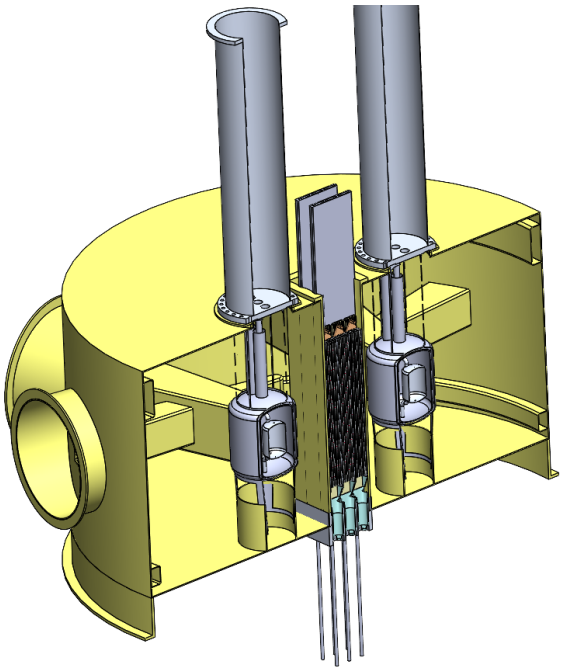


**Figure 3-9 Cutaway Showing Reflector Tank Internals**

The backup shutdown system is the partial dumping of heavy water contained in the reflector vessel. This system provides a completely independent means for reactor shutdown. It is triggered if less than four safety blades are inserted within the required time interval.

## 3.3 Primary Cooling System

The function of the Primary Cooling System is to remove heat from the core in operational and accident situations, thereby maintaining the core in a safe condition. Heat is extracted by the upward flow of cooling water through the core either by forced circulation when the reactor is at power, or by natural circulation when the reactor is in the shutdown or refueling state. Because the core is compact, the flow rate must be relatively high. The heat extracted from the core is transferred to the Secondary Cooling System, directly through the heat exchangers in the PCS, or indirectly through the Reactor and Service Pools Cooling System (RSPCS). Under abnormal conditions, or if the RSPCS is not available, the heat is transferred to the water of the reactor and service pools. Much like the OPAL reactor in Australia, low-carbon stainless steel (AISI 304L) is selected as the piping and reactor pool structure material due to its notable performance under the expected conditions of the reactor.

### 3.3.1 General description

A three-dimensional view of the primary coolant system is shown in Figure 3-2. Some of the components are inside and some components outside the reactor pool (not shown in all the figures). The PCS water flows upward through the core and then passes through the upper chimney. At the outlet pipe there is a pipeline connection for venting. This acts as a siphon-

breaker, preventing pool drainage in the event of a loss-of- coolant accident in the primary circuit. The siphon breaker is a passive component with no valves in the line. The coolant flows from the outlet pipe to a tank before completing the circuit to allow dissolved $^{16}N$, created in the core, to decay before the coolant moves further through the PCS.

From the decay tank the coolant enters three of four pump rooms each with a centrifugal pump and a heat exchanger (HX). The heat exchangers would be plate-type, like those used at the NBSR and at OPAL.

Three of the four pumps are used for normal operation allowing for one pump to be on standby or under maintenance. Maintenance is possible during operation as radiation protection is afforded by having the decay tank and thick-enough concrete walls separating the pump rooms. The pumps must have sufficient inertia via a flywheel to maintain the coolant flow rate through the core in the event of a loss of normal power supply. Each pump discharge pipeline directs the coolant through a check valve to its corresponding heat exchanger where the heat is transferred to the secondary cooling system.

The four branches of the primary side of the heat exchangers merge into the main pump discharge line. This main line splits into two branches, which pass through the reactor pool and discharge the cooling water into the lower plenum under the core. Water diffuses in the plenum before it flows into the fuel assembly inlet nozzles and enters the fuel assembly cooling channels.

In order to allow the establishment of natural circulation when the PCS pumps are not in operation, flap valves are in each of the lines returning to the pool. The flap valves remain closed during forced circulation due to the pressure provided by the PCS pumps. They open by gravity when the pumps stop due to either a failure or during a shutdown. The open position of these valves establishes a path within the reactor pool to remove the decay heat by natural circulation using the pool water. The primary cooling loop inside the pool consists of the pool itself plus the portion of the circuit between the flap valves in the pump discharge lines and the siphon breaker in the pump suction line.

The pump discharge line of the PCS has a connection to the RSPCS. This bypass diverts a fraction of the core cooling flow into the RSPCS. This fraction of flow returns to the bottom of the reactor pool through the pump discharge line of the RSPCS. This arrangement causes a downward flow into the upper chimney, equal to that flow rate diverted from the PCS (by mass balance). This flow can be regulated by a control valve. This branch contributes to the preservation of the hot water layer at the top of the pool. The reactor pool, and hence the PCS, is open to the atmosphere in the reactor building and there is evaporation from the surface of the reactor and service pools.

### 3.3.2 Pumps

Currently, single stage centrifugal pumps are recommended for the four primary pumps. Preliminary thermal-hydraulics analyses allow for the recommendation of pumps with 700 $m^3$/hr capacity and a total head of 75 m. Stainless steel casing and a mechanical shaft seal would be appropriate for any of the pumps based on OPAL's pumps. Each of the pumps should be equipped with inertial flywheels to ensure smooth and controlled transition to natural circulation in the event of an accident. The pumps should also be equipped with instrumentation to monitor the temperature and vibration of the pump, which could potentially be in the form of a thermocouple in the bearing housing and an accelerometer on the pump casing.

## 3.4 Reactor Pool and Service Pool Cooling System

The RSPCS, in addition to its function of removing heat from the pools during normal operation, is designed to remove decay heat from the core when none of the PCS pumps are in operation. The RSPCS also circulates water from the reactor and service pools to the reactor water purification system to maintain the purity of the demineralized water. The RSPCS removes residual core heat from the reactor pool and spent fuel decay heat from the service pool by forced circulation of demineralized water. The RSPCS transfers heat to the Secondary Cooling System (SCS) through the RSPCS heat exchanger.

The RSPCS consists of the circuit piping, a decay tank, two pool cooling pumps, a heat exchanger, associated instrumentation and pipe fitting components, valves including flap valves within the reactor pool, a toroidal distributor, siphon breakers in all suction and discharge lines and a two-way valve to allow transition to long term pool cooling mode.

During a reactor shutdown, it is possible to switch the water intake to the suction placed at the side of the upper chimney, immediately above the core. This, with the opening of the PCS flap valves, provides an additional means to remove decay heat from the core.

## 3.5 References

[1] G. Braoudakis, "OPAL Nuclear Reactor: Reactor Specification," *International Nuclear Information System,* vol. 46, no. 20, February 1, 2015 2015. [Online]. Available: http://inis.iaea.org/Search/search.aspx?orig_q=RN:46046717.

[2] O. S. Celikten, A. G. Weiss, and D. Sahin, "Comparison of $U_3Si_2$ and U-10Mo LEU-Fueled Reactor Cores for the Preconceptual NIST Neutron Source Design," presented at the 30th International Conference on Nuclear Engineering, ICONE 30, Kyoto, Japan, May 21-26, 2023.

# 4 Nuclear Design

## 4.1 Design-Basis

The nuclear design and related safety analyses provide credible support for the functional need of the NNS to provide neutrons to experimentalists in a safe and reliable manner. The design of the NNS, as described in Chapter 3, is a 20 MW thermal neutron spectrum reactor. To satisfy safety concerns it must have two diverse and independent shutdown systems with adequate shutdown margin and a negative power reactivity coefficient. Shutdown is initiated by primary control system instruments that sense anomalous behavior and initiate the insertion of safety blades into the core. The secondary shutdown system drains heavy water from the reflector. Excess reactivity of the core must be under specified limits during startup. The reactor must be designed for a fuel cycle of approximately 40 days; currently considered to be optimum for science applications and operations. The power distribution must be such that the maximum power density and maximum stripe power (axial integral of power along one-third of a fuel plate) do not lead to violations of any of the thermal limits (discussed in Chapter 5) either during normal operation or credible accidents.

In this chapter, the methodology used to determine the nuclear design is first summarized. Key nuclear parameters related to neutron flux and power distributions throughout an equilibrium fuel cycle and the reactivity of control blades, thermal feedback, and accidental reactivity changes are quantified. The nuclear reactor kinetics parameters used in the transient/accident analysis discussed in Chapter 7 are also listed in this section. More details on the nuclear design are found in reference [1].

## 4.2 Neutronic Steady-State and Burnup Model

A state-of-the-art neutronic model of the NNS reactor was developed based on the MCNP6.2 Monte Carlo code package [2] using cross section data from ENDF/B-VII.1 and ENDF/B-VIII.0 [3]. The code can perform depletion analysis (burnup) with the CINDER90 code [4] which is built into the package. This code package has been exhaustively validated for many applications including for analyzing the NBSR [5] [6] [7] which is similar to the NNS, both being thermal neutron spectrum reactors with curved fuel plate geometry.

A planar view of the geometry modeled in MCNP6.2 is given in part (a) of Figure 4-1 which expands to show the detail in different parts of the model. Hence, part (b) shows just the core and part of the reflector containing the cold neutron sources and cold and thermal neutron beam positions. Part (c) shows the entire core only and part (d) is a single fuel assembly and part (e) shows the detail within each assembly. The overall model shown in part (a) is shown enlarged in Figure 4-2 with components labeled. An elevation view is shown in Figure 4-3. Green or light blue coloring in these figures represents light water and yellow or slightly darker blue is heavy water. Light grey represents the concrete shielding outside the reactor. The detail of the model extends to explicitly representing the fuel within each plate as well as the

cadmium shim neutron absorber wires. The cold sources and crossing cold and thermal beam tubes are approximately represented. The control blades can be put at any axial position.

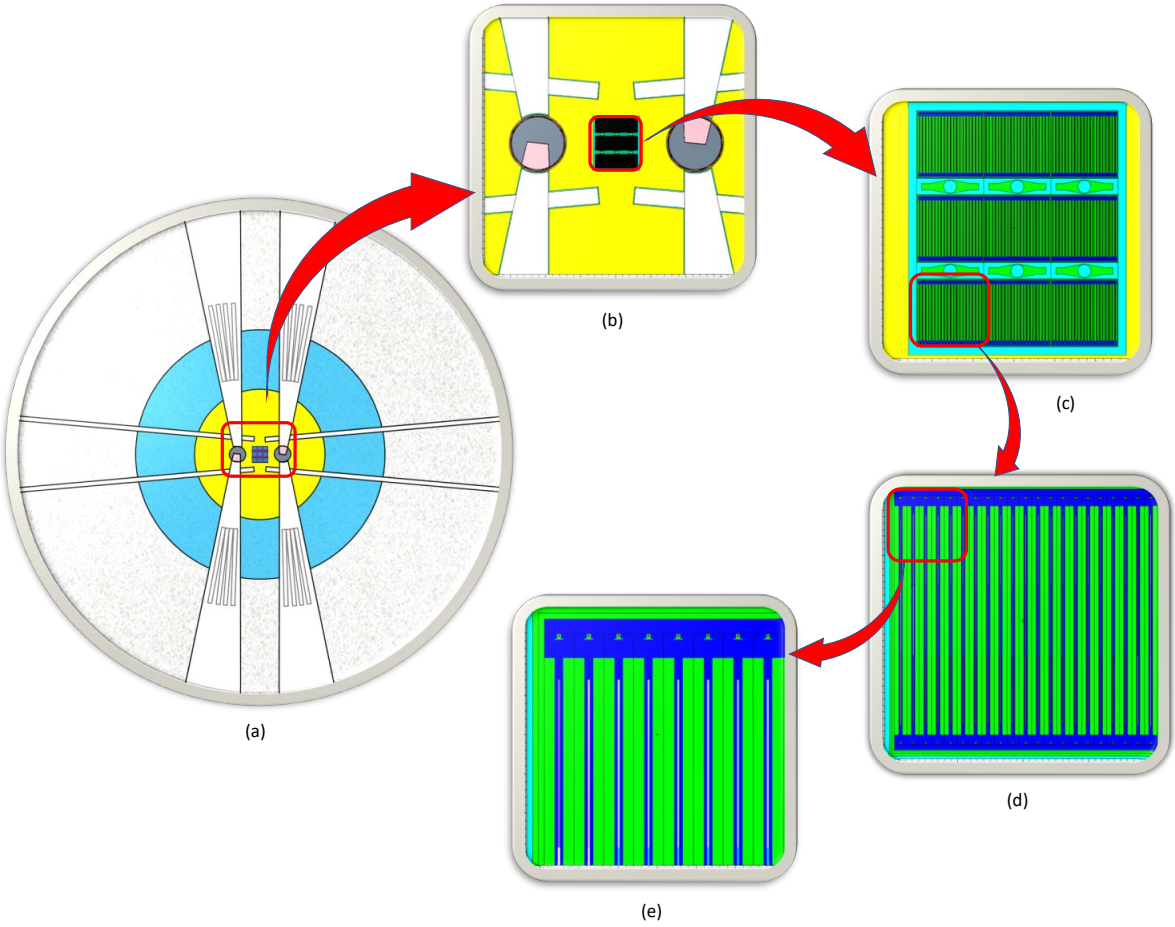



**Figure 4-1 Planar View of MCNP Model (a) with Details (b-e)**

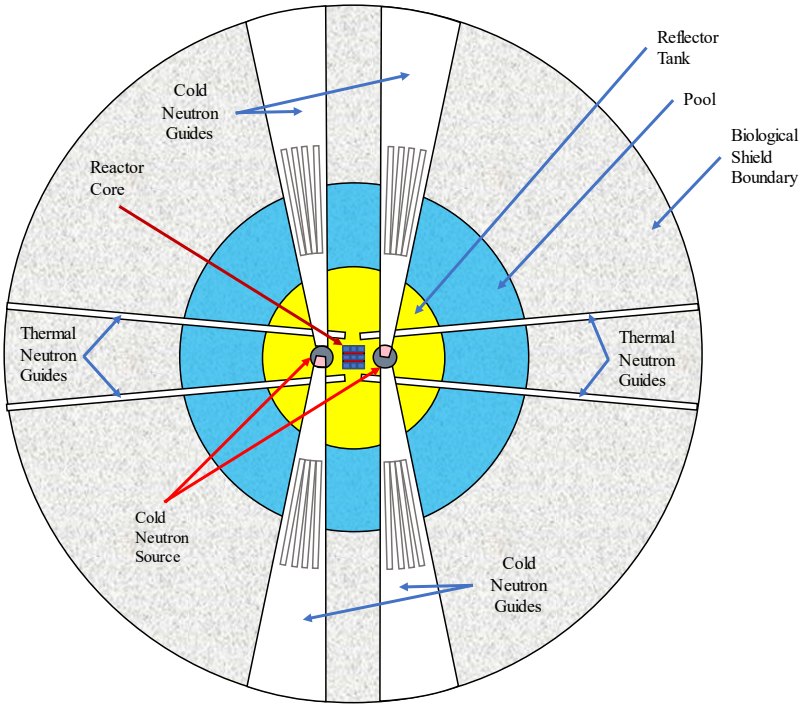



**Figure 4-2 Planar View of MCNP Model**

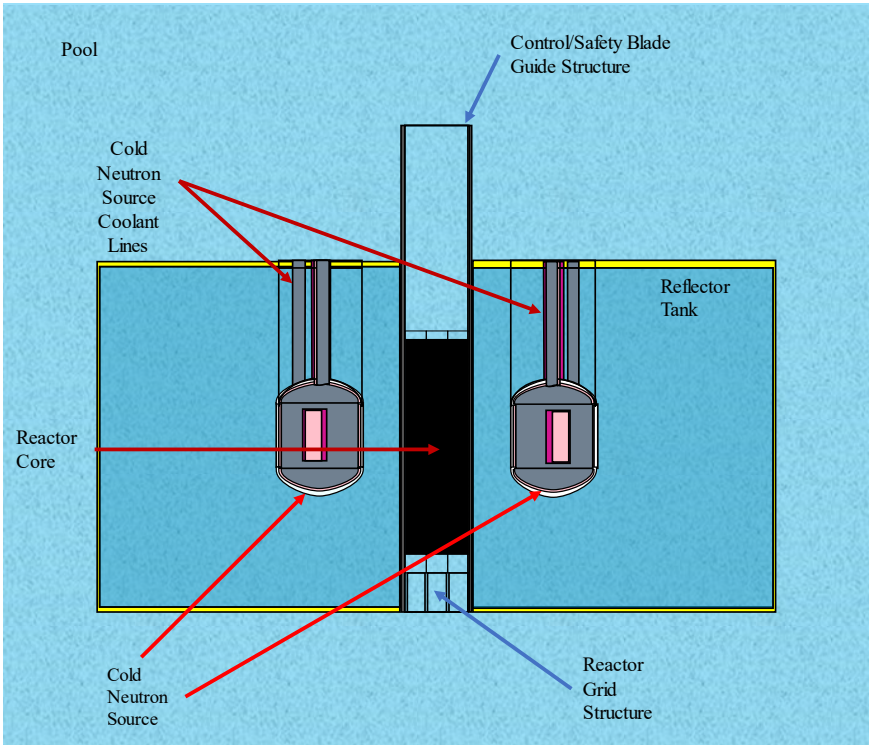



**Figure 4-3 Elevation View of MCNP Model**

The following lists key assumptions used in the modeling approach:

- The fuel plates are assumed to be flat whereas they will actually be curved (see Figure **3-6**). However, the water to fuel ratio for the flat representation is the same as with curved plates and hence, the difference is not expected to be significant [8].

- Cooling systems and in-reactor structures are not represented and will be a penalty in terms of reactivity when eventually they are part of the model. The detail in the reflector tank is limited as no piping, rabbit tubes, or instrumentation is modeled.

- The steady state reactor power used in the model to normalize the power distribution and determine burnup is 20.2 MW, one percent higher than the nominal reactor power of 20 MW. The 20 MW thermal power represents the heat being removed from the primary coolant system whereas it is known that some energy will be deposited outside the core. [Hence, the Reactor Pool and Service Pool Cooling System (Section 3.4).] Without further analysis to quantify this effect, the 1% increase in power used is assumed to be the same as for the NBSR where it is based on actual thermal shield and CNS heat load measurements.

- The spatial distribution of the fuel material composition in the nine assemblies is represented using 1350 different zones. The outer four plates (two on each side) in each assembly have 30 different compositions, three stripes along the transverse direction divided into ten axial zones for a total of 120 (4x3x10) zones. The 17 plates in the interior of each assembly all have the same composition distributed into 3x10 zones in a similar manner. Hence, there are 150 representative material composition zones in each fuel assembly.

- The spatial distribution of the burnable poison wire compositions in each assembly is divided into five axial zones with the 21 wires on one side of the assembly tracked separately from the wires on the other side. Hence, there are 90 (9x2x5) zones to track the Cd wire material compositions.

- The time between fuel cycles, shutdown, is assumed to be eight days, which is shorter than for the NBSR and considers that fewer moves will be needed to reload the core each cycle with only nine fuel assemblies for the NNS, as opposed to having to move 30 elements in the NBSR core.

The initial core can be loaded with all fresh assemblies because of the use of burnable poison wires. However, this kind of loading would require having the shutdown blades partially inserted. Subsequent cores get loaded as explained in Section 3.2.1 albeit it means removing fuel assemblies after the first two cycles that have not been burned for three cycles. Although the core in the third cycle contains fuel assemblies that are either fresh or burned once or twice, like in the equilibrium cycle, it still takes additional cycles to reach a true equilibrium fuel cycle.

In order to calculate the composition of the core in each cycle, the methodology shown in Figure 4-4 is used. The methodology is based on separating the fuel cycle into six state-points for accurate representation of core neutronics and burnup as seen in Figure **4-5**. The first is startup (SU), followed by beginning-of-cycle (BOC) which takes place 1.5 days after SU to allow for xenon and other short-lived fission products to build up. The remainder of the fuel cycle is divided into quarters so that the next three state-points are called quarter-two (Q2), middle-of-cycle (MOC), and quarter-four (Q4). Lastly, there is end-of-cycle (EOC).

Each burnup calculation (e.g., MOC to Q4) has the regulating control blades positioned so that the reactor is just critical at approximately the middle of that burnup. The insert in Figure 4-4 shows how the ancillary control blade calibration is done to determine the just-critical position, with the first cycle different because of the larger excess reactivity.

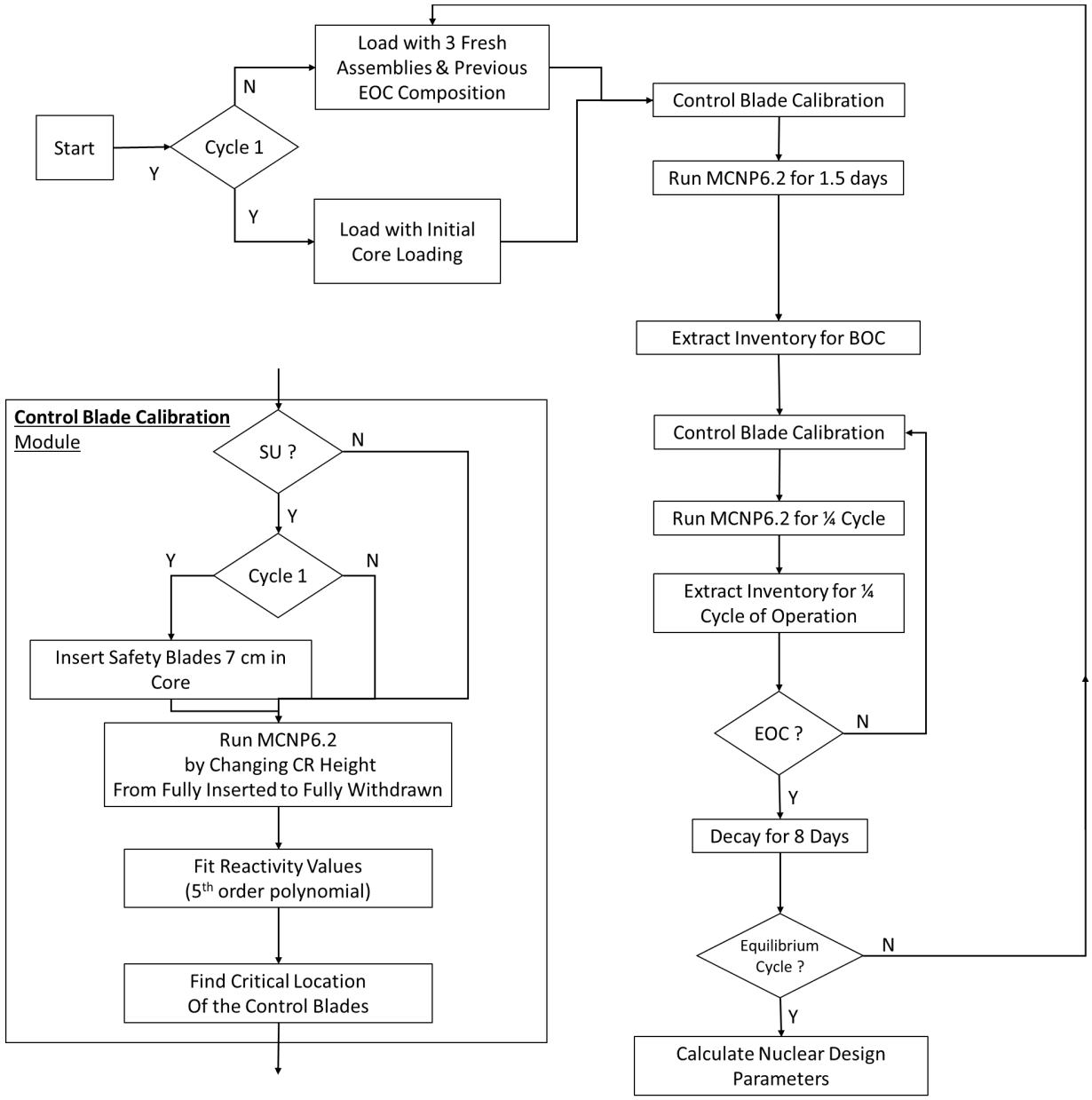



**Figure 4-4 Methodology for Calculating Each Fuel Cycle**

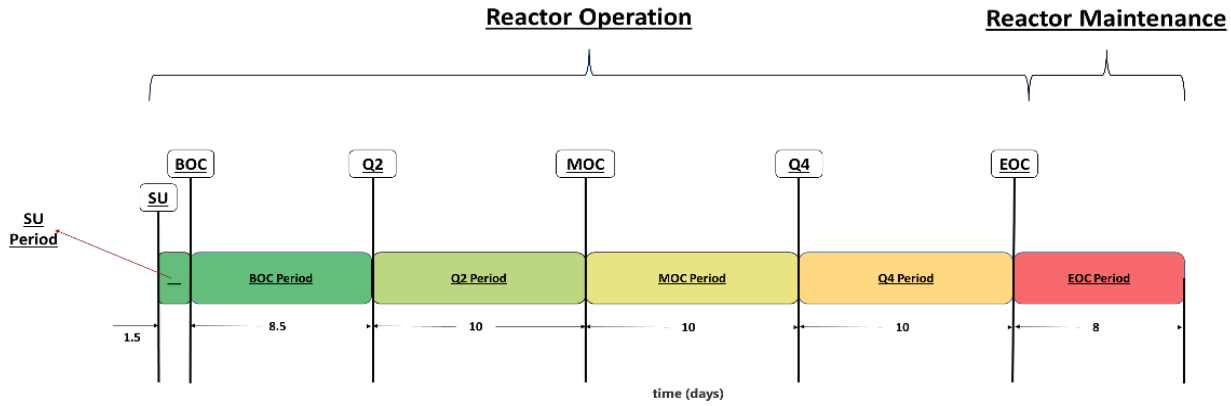



**Figure 4-5 Cycle States and Cycle Points**

## 4.3 Neutron Flux Distribution and Spectrum

To visualize the neutron flux distribution at full power, the neutron energy spectrum is divided into four groups: cold and thermal (<0.025 eV), epi-thermal (0.025 eV - 0.40 eV), resonance (0.40 eV – 100 keV), and fast (>100 keV). The neutron flux distribution for each group is given in Figure 4-6 from a planar perspective and Figure 4-7 from an elevation perspective.

The effectiveness of the nuclear design is demonstrated as the highest concentration of low-energy neutrons is in the cold sources, while fast neutrons are almost exclusively within the core, away from the cold neutron beams. The highest concentration of thermal neutrons is between the core and the cold neutron sources where they will be extracted into beam tubes shown on the figures. The maximum flux at the location of a cold source is ~$2.75 \times 10^{14}$ n/cm$^2$/s[e]. The design is not yet optimized and changes in location and orientation of the cold sources may be made in the future to maximize the cold neutrons delivered to beam tubes.

[e] Comparisons of flux at the CNS in the NNS and in the NBSR are given in Section 8.2.1.

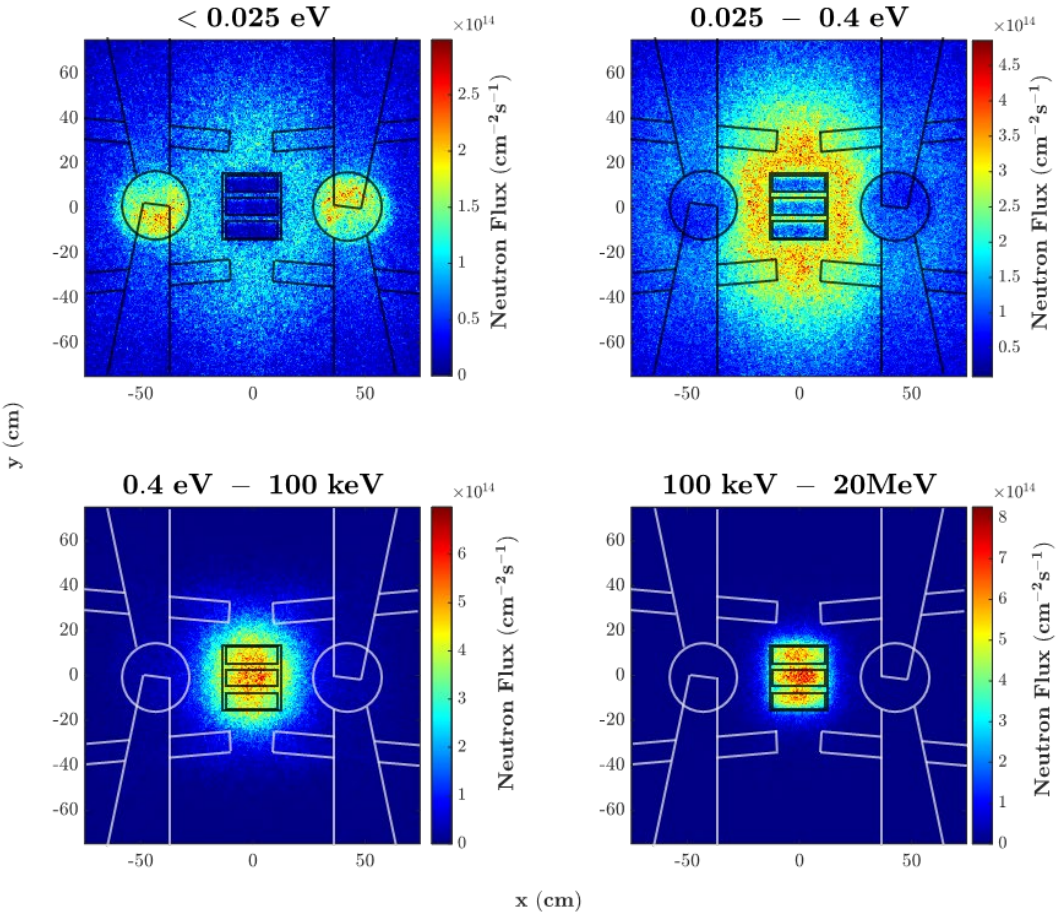



**Figure 4-6 Planar Views of Neutron Flux in Four Energy Groups at MOC**

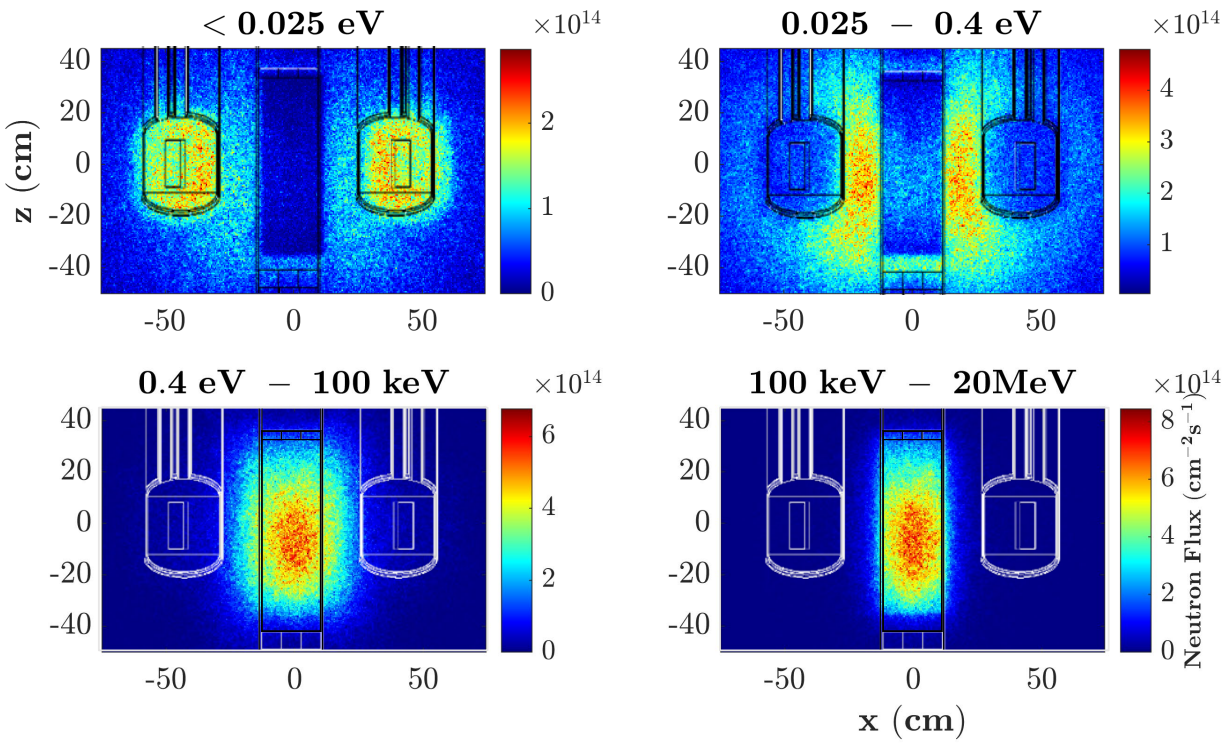



**Figure 4-7 Elevation Views of Neutron Flux in Four Energy Groups at MOC**

## 4.4 Power Density and Fission Density Distributions

Power distributions are computed using fission energy deposition tallies in the MCNP model, that is, the assumption is made that all fission energy is deposited within the fuel plate, a conservative assumption used for safety analysis. A high spatial resolution is obtained by discretizing each fuel plate into three transverse and 35 axial meshes yielding a total of (3x35x21x9) 19,845 mesh volumes of calculated W/cm$^3$.

Figure 4-8 shows the normalized fuel assembly power at four different points in the fuel cycle. At SU and BOC, the hottest fuel assemblies are in the second-cycle FAs[f] where the burnable poisons have mostly burned out. During the fuel cycle, the power shifts to the freshly loaded FAs as their burnable poisons are consumed. Hence, at MOC and EOC, the highest power is in the fresh fuel assemblies with the maximum normalized FA power at EOC being 1.12 in assembly B22 which has a total power of 2.49 MW.

Figure 4-9 shows the relative power in each of the three stripes (axially averaged) in each of the fuel plates in the core. It shows that the middle stripe always has the lowest power in a fuel plate and the stripes with the highest power are in the end plates (plates 1 and 21) closest to the chimney wall located in fuel assemblies in columns 1 and 3 where there is more water to

[f] For the location of FAs according to burnup, see Figure 3-5.

aid moderation relative to the inner plates. This includes not just the light water between the fuel plate and the chimney but also the heavy water in the surrounding reflector tank. The effect of the reflector tank can also be seen in contrasting the stripes along the edges next to the reflector tank with respect to those further in the interior of the core. The hottest stripes are at SU and BOC in the second-cycle fuel assemblies. At SU, the hottest stripe has a relative power of 1.75.

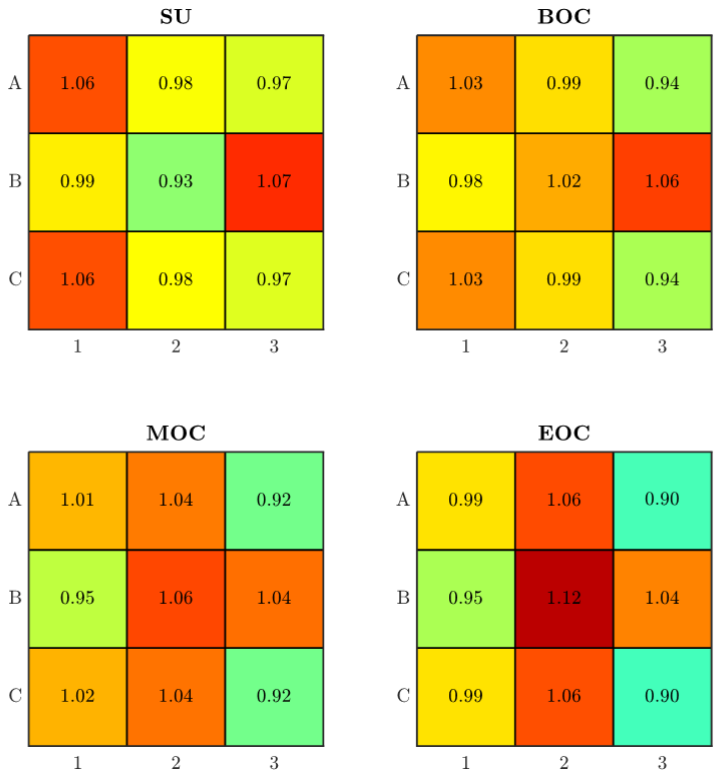



**Figure 4-8 Normalized Fuel Assembly Power During a Fuel Cycle**

The relative power as a function of axial position is shown graphically in Figure 4-10 for plates 1 and 21 separately, for the average of plates 2 through 20 , and for the fuel assembly average (plates 1 through 21), for the fuel assemblies with highest power. Plate 1, which is close to the chimney, has the highest plate power from SU through Q2 reaching ~1.89 around the midplane. For the remainder of the fuel cycle, plate 21, also next to the chimney, in row 2 has the maximum power. The effect on power distribution due to the burnable absorber Cd wires in fresh assemblies decreases with their depletion. This causes the location of the fuel assembly and fuel plate with maximum power generation to change around MOC for the remainder of the fuel cycle.

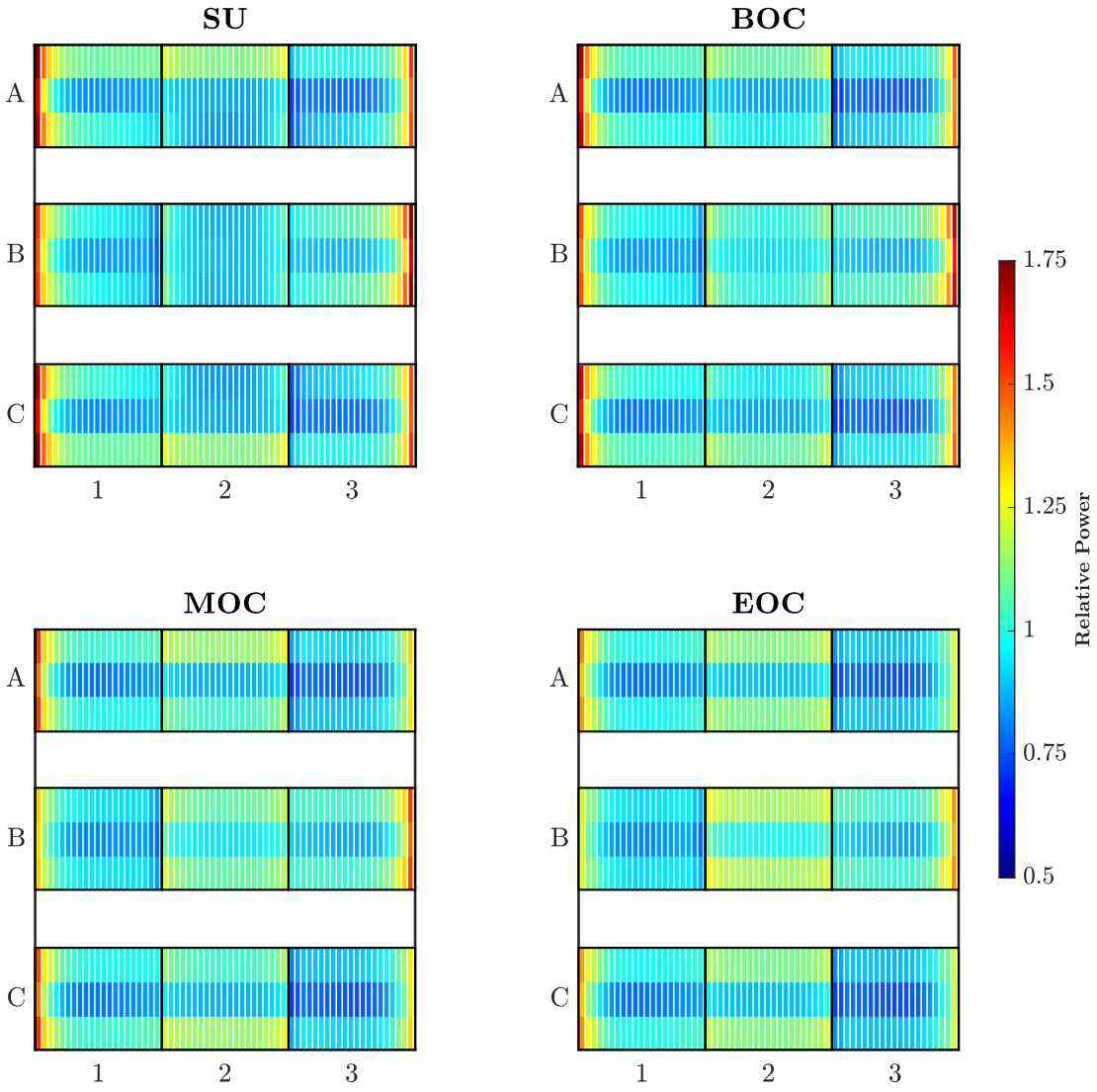



**Figure 4-9 Relative Power in Each Fuel Stripe**

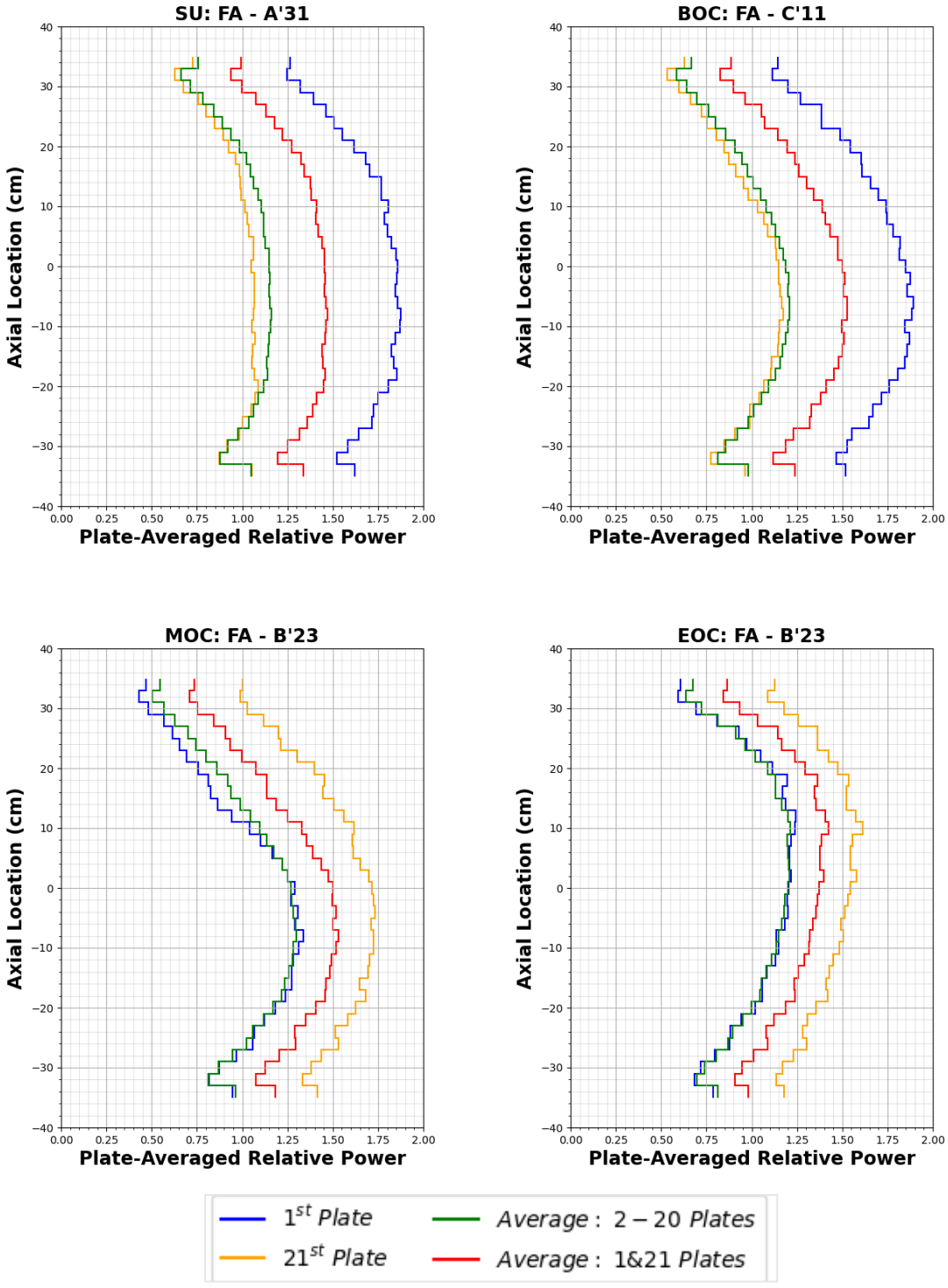



**Figure 4-10 Axial Power in Fuel Plates and for FA Average in FAs with Maximum Peaking**

The power density as a function of fission density is shown on Figure 4-11 for each mesh volume for six cycle states in the fuel cycle. The highest powers are at SU and BOC with the peak being ~18 kW/cm$^3$. The highest fission densities are obviously at EOC where the maximum is 4.5x10$^{21}$ fissions/cm$^3$.

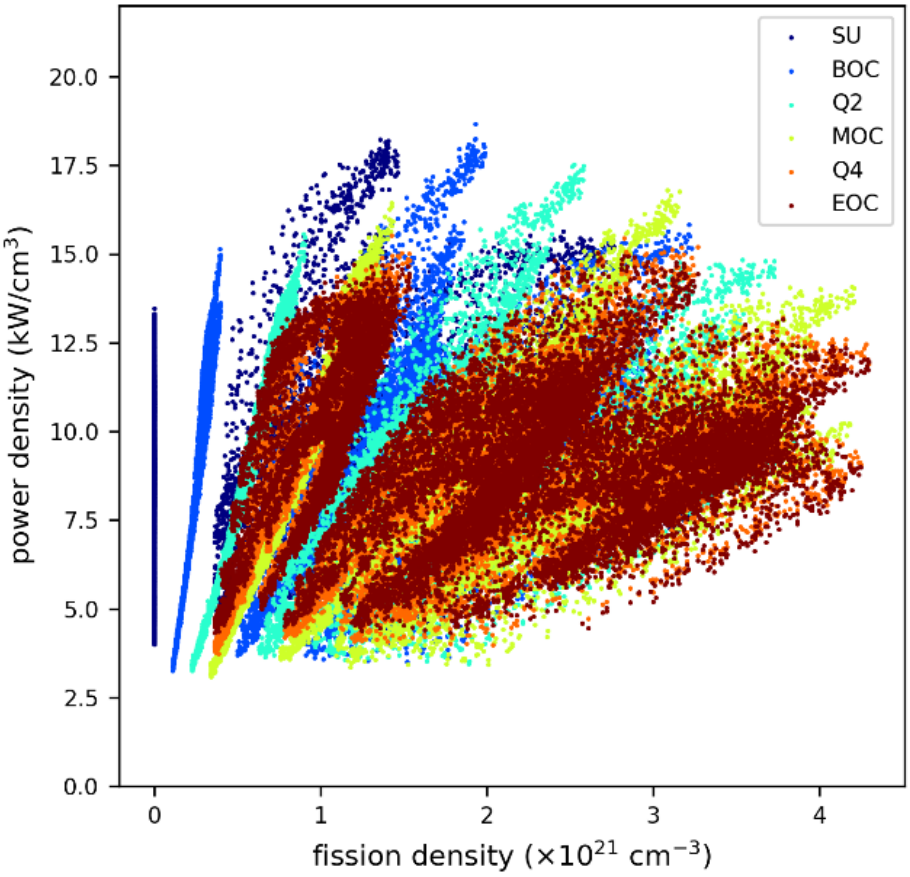



**Figure 4-11 Power Density versus Fission Density for Six Cycle States**

## 4.5 Reactivity of Control Blades

The control blades (described in Section 3.2.3) are shown in a top view of the core, Figure 4-12, where the safety/shutdown blades are numbered 1 through 4 and the regulating control blades are labeled A and B. Calculations to determine blade worth for different configurations are given in Table 4-1 at SU and EOC states. The results show the larger excess reactivity present in the SU core with respect to the EOC core. The excess reactivity at SU is less than 6 %Δρ.

The total worth of all blades (case 9 minus case 1) varies from 21.0 %Δρ to 24.1 %Δρ through the fuel cycle. The shutdown margin, with one safety blade stuck out and blades A and B also assumed to be out, is shown in cases 5, 6, 7, and 8. The smallest shutdown margin is above 4 %Δρ which is sufficient to assure complete shutdown. At this point, no consideration was given

for the burnup of the hafnium blades as they do not burn quickly, and they will perform for many cycles before their reactivity worth degrades.

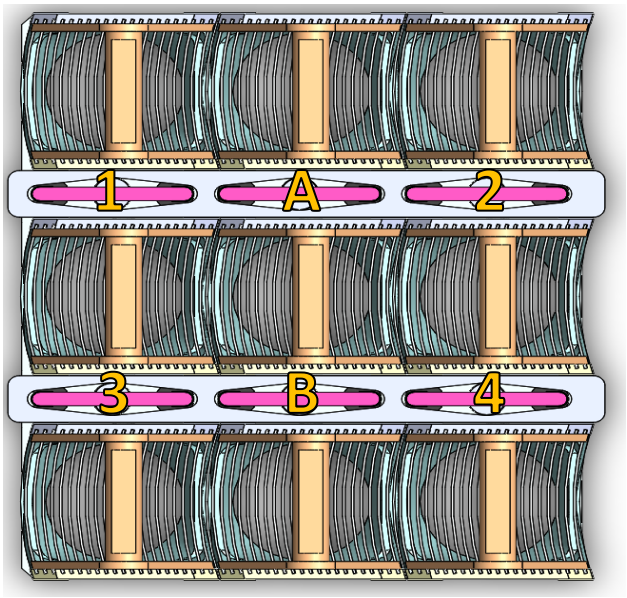



**Figure 4-12 Control Blade Positions in Core**

**Table 4-1 NNS Core Reactivity for Different Blade Configurations**

| | Blade Configuration | | $\%\Delta\rho$ | $\%\Delta\rho$ |
|---|---|---|---|---|
| **Case** | **Withdrawn** | **Inserted** | **SU** | **EOC** |
| **1** | 1, 2, 3, 4, A, B | -- | 5.66 | 4.22 |
| **2** | 1, 2, 3, 4, B | A | 2.39 | 0.01 |
| **3** | 1, 2, 3, 4, A | B | 2.31 | 0.04 |
| **4** | 1, 2, 3, 4 | A, B | -1.42 | -4.91 |
| **5** | A, B, 1 | 2, 3, 4 | -4.28 | -7.98 |
| **6** | A, B, 2 | 1, 3, 4 | -4.22 | -8.10 |
| **7** | A, B, 3 | 1, 2, 4 | -4.23 | -8.08 |
| **8** | A, B, 4 | 1, 2, 3 | -4.30 | -7.98 |
| **9** | -- | 1, 2, 3, 4, A, B | -15.30 | -19.88 |

The worth of the shutdown control blades as a function of position is given in Figure 4-13. The total worth of the safety blades (case 9 minus case 4) at SU is 13.9 %Δρ and at EOC it is 15.0 %Δρ. The corresponding curves for the regulating control blades are given in Figure 4-14. As shown in the figure, the total integral worth increases significantly as the cycle progresses. This is because these blades are next to the burnable poison wires, in the fresh fuel assemblies, which burn out during the cycle and cause an increase in the thermal flux at the location of the regulating control blades between assemblies A12 and B22 and between B22

and C32 (see Figure 4-12 and Figure 3-5). The total integral worth of the regulating control blades is approximately 7.1 %$\boldsymbol{\Delta\rho}$ at the fully withdrawn position at SU, and approximately 9.2 %$\boldsymbol{\Delta\rho}$ at EOC.

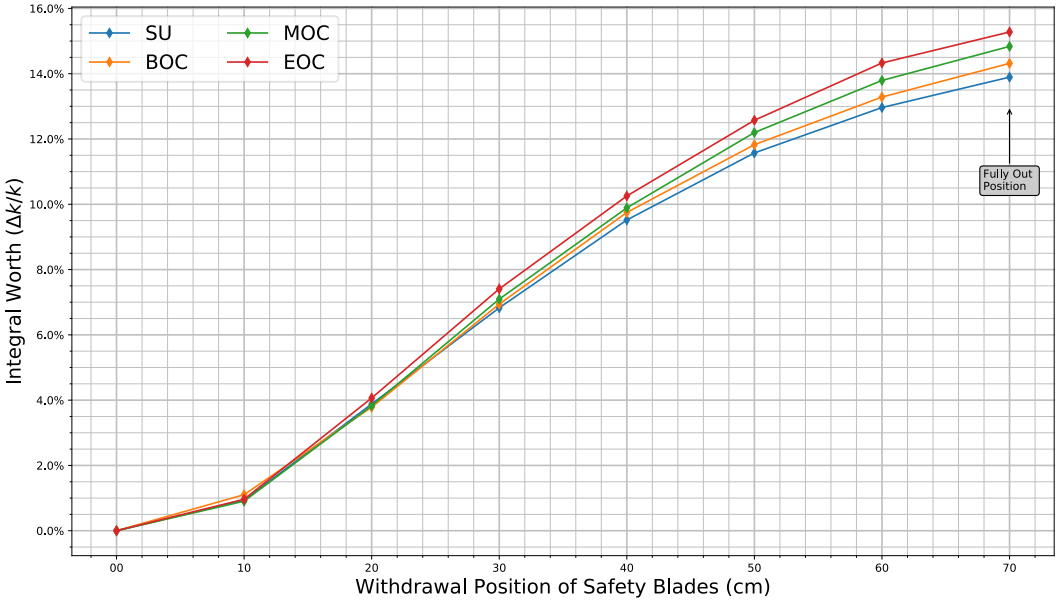



**Figure 4-13 Worth of Safety Blades at Different Fuel Cycle States**

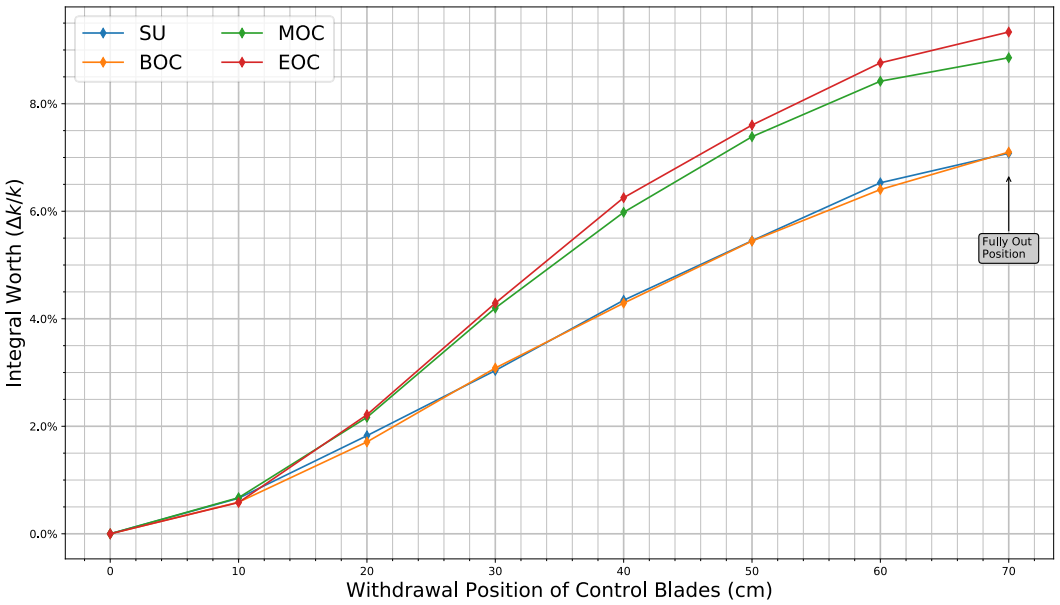



**Figure 4-14 Worth of Regulating Control Blades at Different Fuel Cycle States**

## 4.6 Reactivity Coefficients

Reactivity coefficients were calculated to show that feedback from increases in parameters that must remain within limits (e.g., temperatures, power) mitigates the effect; and to show that potential accidents (e.g., leakage of light or heavy water into different spaces) would not lead to increases in reactivity.

*Fuel Temperature Coefficient:* The Doppler reactivity effect in the NNS is anticipated to be smaller than in power reactors because of the minor temperature gradient across the very thin fuel layer, with an average calculated fuel temperature of approximately 75°C. Calculations indicate that the reactor's average reactivity decreases by 7 pcm for every degree Celsius increase in temperature. The total Doppler reactivity change from the cold state to the hot full-power state, resulting from the temperature rise in the fuel core, is calculated to be 385 pcm (0.39% Δρ).

*Moderator Temperature Coefficient:* The moderator is the light water coolant in the core. A change in temperature leads to both a change in density and a change in scattering properties. The latter was not supported in the code version being used so the analysis was done with the scattering kernel fixed for 20°C and only the density was changed. The moderator temperature coefficient was roughly constant over the range of 20°C to 90°C and averaged -0.017 %Δρ/°C at SU and -0.015 %Δρ/°C at EOC. The negative reactivity coefficient, meaning that the core is over-moderated, is necessary to ensure the safety of the reactor and is required by the NRC [9].

*Void Coefficient:* A negative void coefficient is considered necessary in case the water heats sufficiently to create voids or if gases enter the system. At SU it was calculated to be -0.25 %Δρ per % void and at EOC -0.23 % Δρ per % void for void fractions up to 10 %.

*Light/Heavy Water Mixing Coefficients:* In the unlikely leakage of heavy water from the reflector tank to the reactor pool, reactivity declines as seen on Figure 4-15 at both SU and EOC states. The calculation takes into account the change in density when the two liquids mix and assumes that the mixture is uniform throughout the component. The average effect over the range from zero to complete replacement in the pool is -0.23 %Δρ/at% at SU and -0.20 %Δρ/at% at EOC.

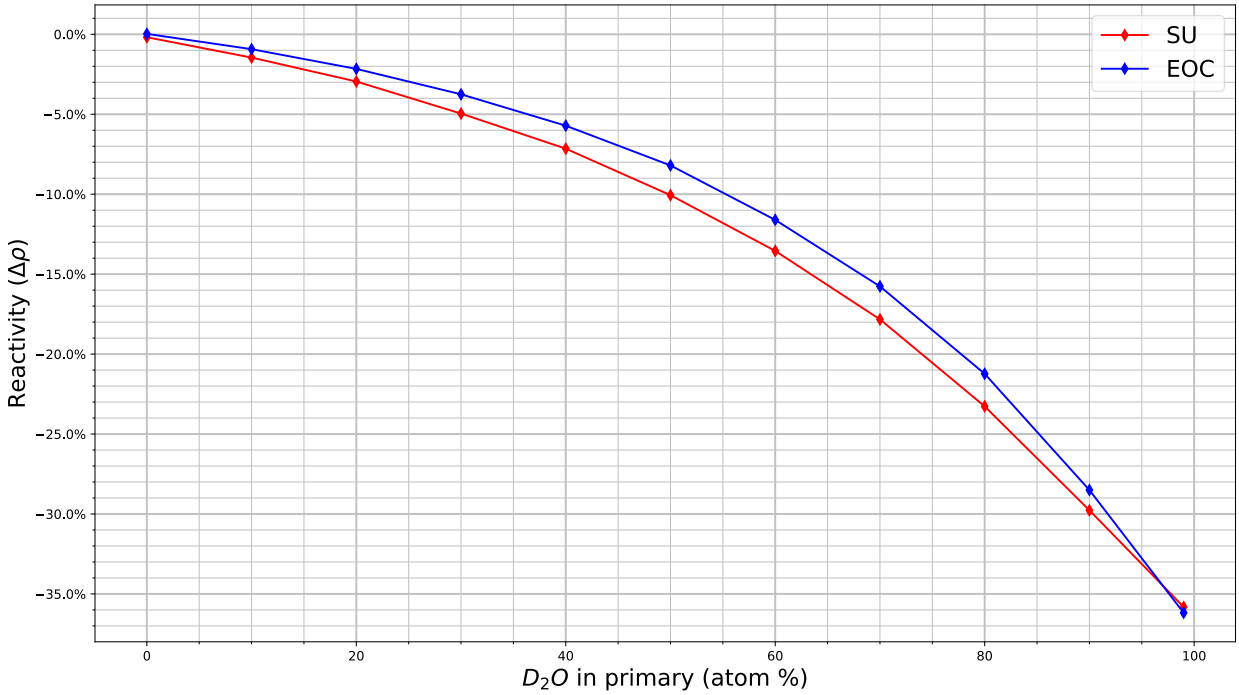



**Figure 4-15 Reactivity as a function of $D_2O$ in the Pool at SU and EOC**

When light water enters the reflector tank, it also decreases reactivity as seen in Figure 4-16 at both SU and EOC. In this situation all the water in the reflector tank can be replaced and the analysis is done up to having no heavy water. As can be seen the effect per unit change in atomic fraction is smaller at larger replacements. The average effect is -0.24 %Δρ/at% and -0.21 %Δρ/at% at SU and EOC, respectively.

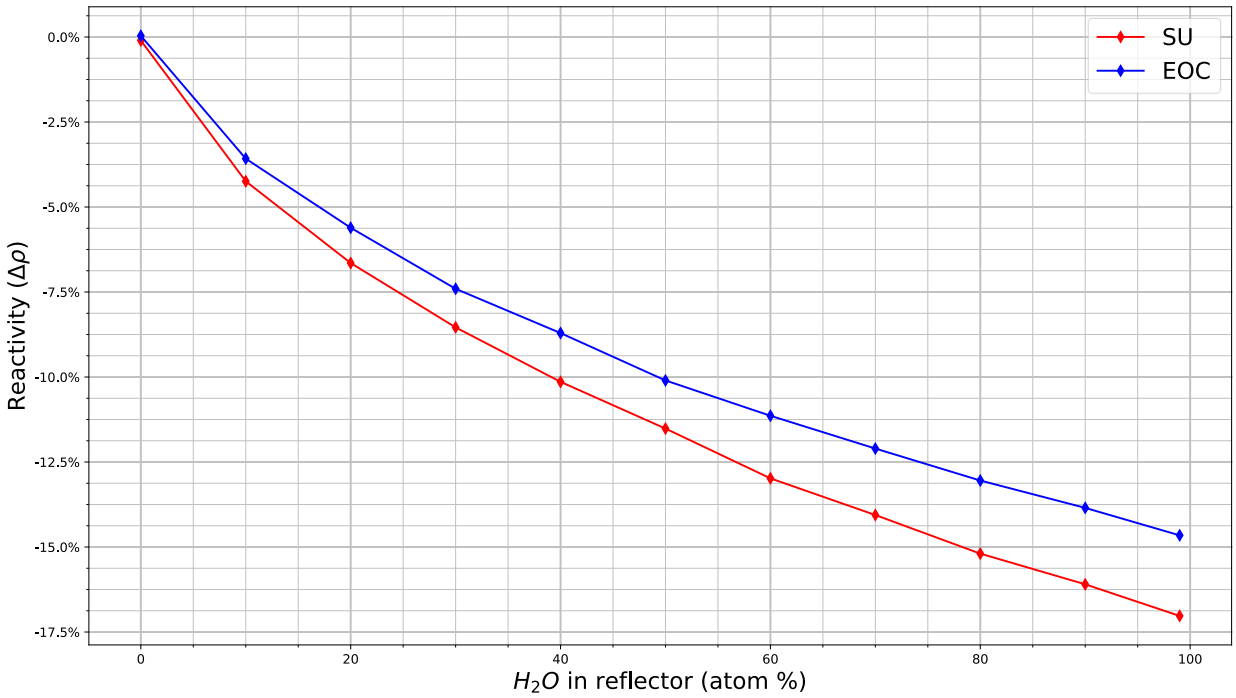



**Figure 4-16 Reactivity as a Function of $H_2O$ in Reflector at SU and EOC**

*Cold Neutron Source Boil-Off:* The two CNSs contain liquid deuterium ($LD_2$) and a failure of their refrigeration could lead to a boil-off. Their orientation in the reactor is shown in Figure 8-1 and more detail is provided in
Figure **8-7**. Calculations were done to see the effect of one or both of the CNSs with no $LD_2$. In both cases there was a negative effect on reactivity. Hence, no reactivity insertion would be possible under this accident condition.

## 4.7 Reflector Dump

A secondary shutdown system is a reflector dump mechanism. The reflector tank is filled with heavy water and is 1.30 m in height and radius. In a situation where normal shutdown by insertion of the safety blades is not functioning, the reflector tank can be drained. Figure 4-17 shows the effect on effective criticality constant ($k_{eff}$) while draining the tank at SU and EOC states. The curves show that the first 30 cm of draining does not have much of an effect but with the tank drained 50 cm the core is subcritical by more than 5 %Δρ.

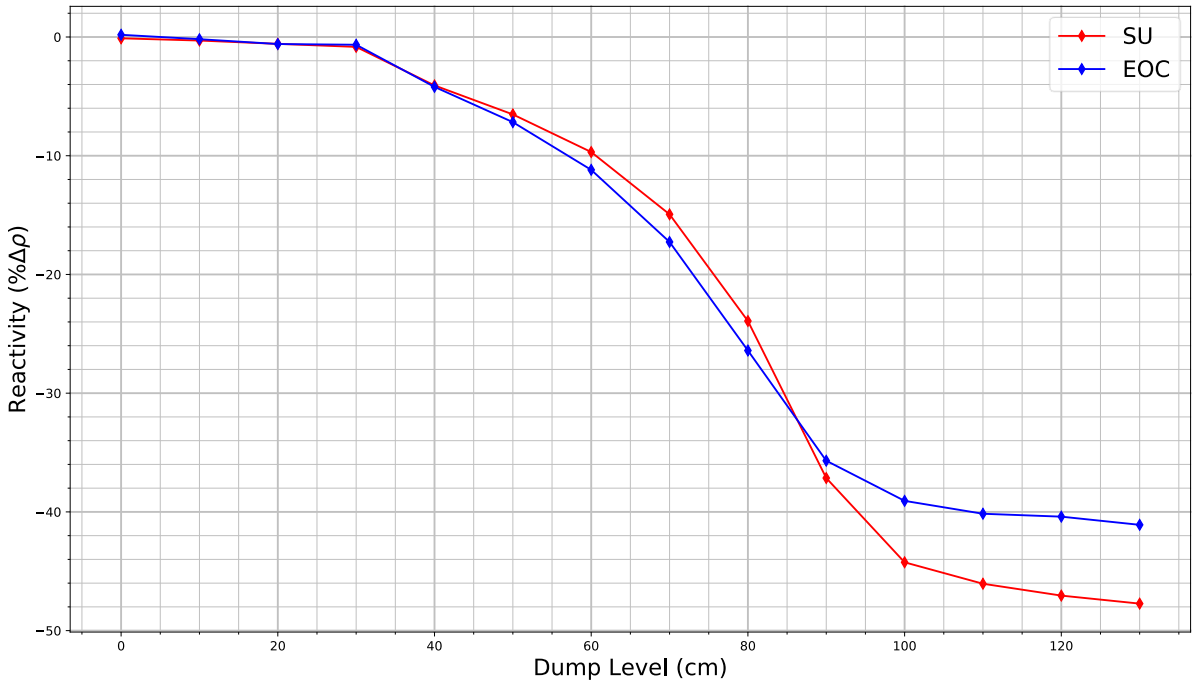



**Figure 4-17 Effective Multiplication Factor as a Function of Reflector Dump Level**

## 4.8 Kinetics Parameters

The kinetics parameters for delayed neutrons from fission products and from photoneutron events are needed for the transient analysis presented in Chapter 7. The photoneutrons are of interest in heavy water systems where the (γ,n) reaction on deuterium is possible. However, since the NNS has deuterium in the reflector and not in the core, it was found that their contribution could be neglected.

The delayed neutron parameters for fission products are calculated for each of six delayed neutron groups. They are the delayed neutron fraction ($\beta_i$) for each group, the corresponding decay constant ($\lambda_i$), and the prompt neutron lifetime ($l_p$). The latter is frequently given as the generation time $\Lambda$ equal to $l_p/k_{eff}$ and the two are obviously equal for a critical system. The neutron generation times are given in Table 4-2 for critical states throughout the fuel cycle. The statistical uncertainty in these numbers is less than 4%.

**Table 4-2 Neutron Generation Time for each Cycle State**

| Cycle state | Generation Time, $\Lambda$ (μs) |
|---|---|
| SU | 260 |
| MOC | 234 |
| EOC | 237 |

The delayed neutron fractions for both SU and EOC states are given in Table 4-3 along with the decay constants which do not change during the fuel cycle. The changes in delayed neutron fraction are seen in Table 4-3. An average $\beta_{eff}$ for the two cycle states of the fuel cycle is approximately 0.0064 ± 0.0004.

**Table 4-3 Delayed Neutron Fractions and Decay Constants**

| Group | $\beta_i$ at SU | $\beta_i$ at EOC | $\lambda_i(1/s)$ |
|---|---|---|---|
| 1 | 0.00035 | 0.00022 | 0.01334 |
| 2 | 0.00136 | 0.00089 | 0.03269 |
| 3 | 0.00088 | 0.00076 | 0.12073 |
| 4 | 0.00289 | 0.00279 | 0.30318 |
| 5 | 0.00059 | 0.00130 | 0.85177 |
| 6 | 0.00048 | 0.00036 | 2.86021 |
| $\beta_{eff} = \sum \beta_i$ | 0.00655 | 0.00632 | |

## 4.9 References

[1] O. Ş. Celikten, A. G. Weiss, and D. Şahin, "Pre-conceptual Design Activities of the NIST Neutron Source: Preliminary Neutronics Assessments," National Institute of Standards and Technology, Gaithersburg, MD, NIST TN 2316, November 2024, https://doi.org/10.6028/NIST.TN.2316.

[2] C. J. Werner *et al.*, "MCNP Users' Manual Code Version 6.2," Los Alamos National Laboratory, LA-UR-17-29981, 2017/09/27/ 2017. Accessed: 2021/07/07/07:57:01. [Online]. Available: https://mcnp.lanl.gov/pdf_files/la-ur-17-29981.pdf

[3] "LANL Distribution Site for Nuclear Data Libraries." Los Alamos National Laboratory. https://nucleardata.lanl.gov (accessed.

[4] M. L. Fensin, "Development of the MCNPX Depletion Capability: A Monte Carlo Linked Depletion Method That Automates the Coupling Between MCNPX and CINDER90 for High Fidelity Burnup Calculations ," Ph.D. dissertation, University of Florida, Gainsville, FL, 2008.," PhD, University of Florida, 2008. [Online]. Available: https://ufdc.ufl.edu/UFE0021946/00001

[5] R. D. Mosteller, "Validation Suites for MCNP," in *American Nuclear Society Radiation Protection and Shielding Division 12th Biennial Topical Meeting*, Sante Fe, NM, April 2002 2002: Los Alamos National Laboratory.

[6] P. Kohut, "Verification and Validation of the Monte Carlo Neutronic Code, MCNP-6.2," Brookhaven National Laboratory, Memo to Files August 18, 2020 2020.

[7] D. J. Diamond, "Validation of NBSR Neutronics Model," Brookhaven National Laboratory, Memo to Files 2020/05/01/ 2020. [Online]. Available: https://nistgov.sharepoint.com/sites/NIST_Neutron_Source/Shared%20Documents/Forms/AllItems.aspx?id=%2Fsites%2FNIST%5FNeutron%5FSource%2FShared%20Documents%2FReports%2FSupporting%20Documentation%2FCNS%5Frelated%2FNNS%5FCNS%5F

brightness%5Fv%5Fdiam%2Epdf&parent=%2Fsites%2FNIST%5FNeutron%5FSource%2FShared%20Documents%2FReports%2FSupporting%20Documentation%2FCNS%5Frelated

[8] A. C. C Lu, P Kohut, and L-Y Cheng, "Neutronic Simulation of Curved Fuel Plate with Flat Plate Geometry," in *RERTR 2022 – 42nd International Meeting on Reduced Enrichment for Research and Test Reactors*, Vienna, Austria, October 3-5, 2022.

[9] U.S. Nuclear Regulatory Commission, "Guidelines for Preparing and Reviewing Applications for the Licensing of Non-Power Reactors, NUREG/CR-1537, Part 1, Format and Content and Part 2, Standard Review Plan and Acceptance Criteria," U.S. Nuclear Regulatory Commission, NUREG 1537, 1996.

# 5 Core Thermal-Hydraulic Design

## 5.1 Design-basis

The thermal-hydraulic design-basis, to prevent the release of fission products, is assured by requiring that there shall be no fuel damage during normal operation or from any credible accident (credible and hypothetical accidents are discussed in Chapter 7 Safety Analysis). The design basis for non-power reactor fuel is given by the U.S. Nuclear Regulatory Commission (NRC) as no loss of fuel integrity for all anticipated operating conditions (Chapter 4.6 in [1]). A cladding temperature of 855 K, the solidus temperature for the aluminum alloy, would certainly cause the release of fission products. However, at the much lower temperature where blistering is possible fuel integrity might be challenged. Hence, herein, the blister temperature is considered as the acceptance criterion. Since the potential for blistering is a function of fission density, [2] the criterion codified as the Technical Specification Safety Limit could be a blister temperature as a function of the fission density distribution in the core. Instead, it is conservatively taken as the lowest temperature for blistering which is at the maximum fission density in the core. Based on the maximum fission density shown in Figure 4-11 the literature suggests a safety limit of 645 K [2].

Although cladding temperatures are calculated to assure that no fuel damage can take place, it is standard practice to be conservative and to assure that there is adequate margin during steady state operation to the critical heat flux, onset of flow instability, and the onset of nucleate boiling. Each of these margins consists of the ratio between a heat flux at which a certain level of boiling occurs and the local heat flux encountered by the flow in the analyzed condition.

## 5.2 Thermal-Hydraulic Methodology

### 5.2.1 System Model

The primary coolant system, as shown in
Figure 3-2, was modeled using the TRACE V5.0 Patch 5 code [3]. It incorporates models for reactor core kinetics, decay heat, heat transfer, fluid flow, and control logic. The code's robust modeling and proven track record in nuclear safety analysis allows it to be used for both normal steady state operation and the transient/accident analysis in Chapter 7. The overall model is shown in
Figure **5-1** and Table 5-1 provides some of the key hydraulic diameters. Each of the components in the model is summarized below; details are provided in reference [4].

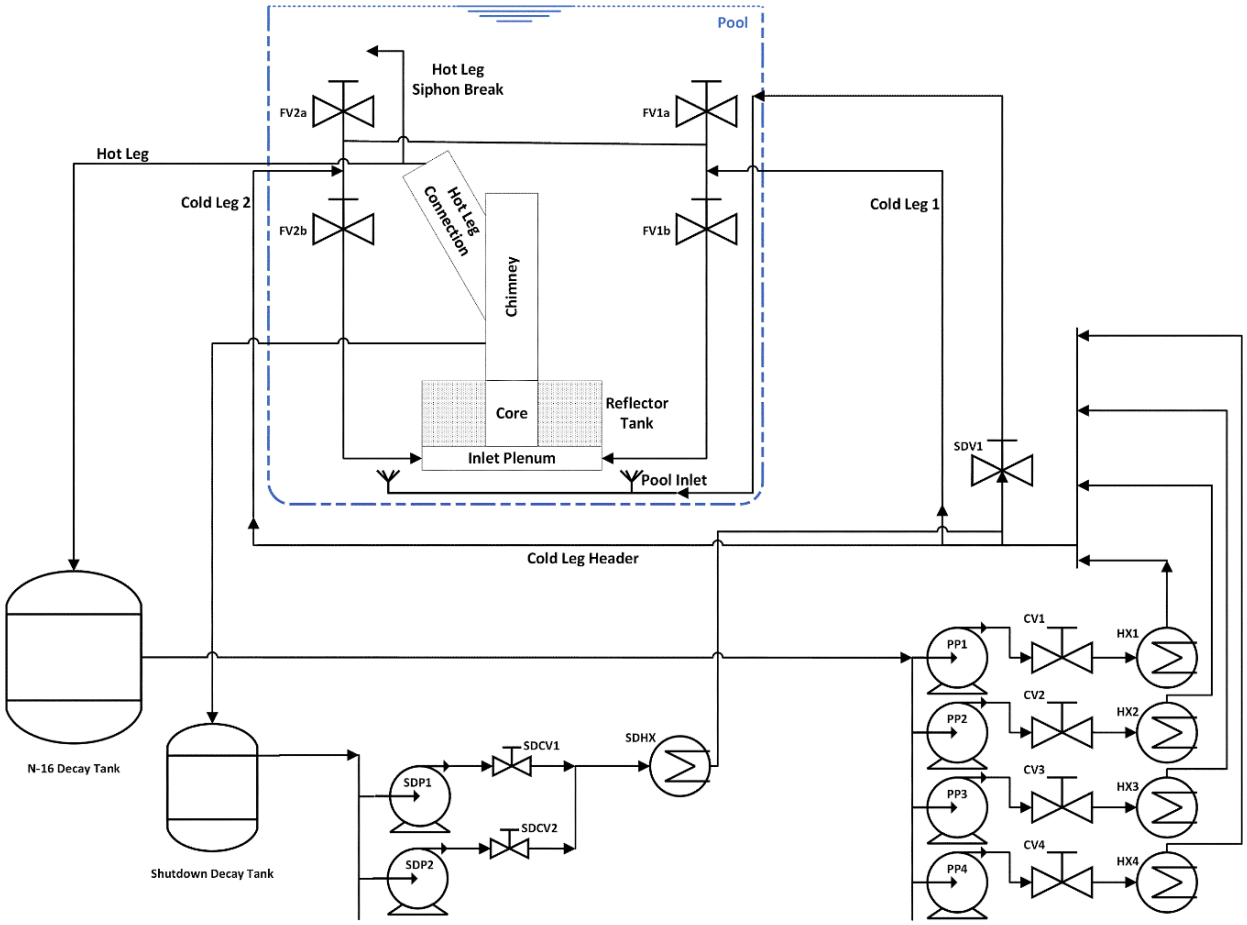



**Figure 5-1 Primary Coolant System Modeled in TRACE**

**Table 5-1 Hydraulic Diameters for Portions of the Primary System**

| Pipe | Hydraulic Diameter (m) |
|---|---|
| Pump Discharge Line | 0.478 |
| Cold Leg | 0.381 |
| Hot Leg | 0.597 |
| Chimney | 0.464 |
| Cold Leg Connector | 0.060 |
| Hot Leg Siphon Breaker | 0.060 |
| Pool Cooling Bypass Line | 0.203 |
| Pool Cooling System<br>(41 openings over 330° circumference) | 0.040<br>(For each opening) |
| Pool (15.3 m deep) | 4.5 (total)<br>1.612 (with reflector tank) |

### 5.2.2 Primary Coolant Pumps

Four primary pumps (PP1-PP4 in
Figure **5-1**) are included in the system, but only three are needed for operation. The fourth pump is designated as standby, ready to activate as necessary or being offline due to maintenance. Since the pump design for the NNS is not yet determined, the coolant pump characteristics of the NBSR are used to model the NNS pumps. TRACE models the pump head and torque using homologous curves, which represent the performance of the pump in a normalized format. However, the NNS pumps are expected to differ from the NBSR pumps by having a flywheel designed to maintain coolant flow to the core after reactor coolant pumps are shut down. The total moment of inertia of the pumps, including flywheels, is chosen to be 75 kg-$m^2$, which is compatible with the OPAL design [5].

In the NNS design, the pump discharge line has an interconnection with the reactor pool that diverts 10% of the total system coolant mass flow to the reactor pool. This flow creates a downward flow in the upper section of the chimney, preventing activated isotopes from reaching the top of the reactor pool. To achieve the 10% flow diversion, a valve is added to the TRACE model and the flow area of the valve is iteratively calibrated to provide the desired 10% flow diversion.

During normal operation, the coolant flow through the reactor coolant pumps is in one direction. However, in transient conditions, if one or two pumps are tripped, forced flow from the remaining energized pumps can create a backflow into the tripped pumps that may lead to reverse rotation of the impellers and result in damage to the pumps. To prevent backflow, NNS pumps are equipped with check valves at their discharge lines. In the TRACE model, the functionality of these check valves is represented by connecting valve components to the corresponding pipe components. The model is designed to reduce the flow area of the valve to zero whenever the liquid water velocity falls below 0.5 m/s at the interface between the valve and pump components. The control logic for the check valves is simulated using TRACE's control systems feature. When activated, this logic effectively reduces the flow area of the valve and isolates the pump from the coolant flow path. The closure time of the check valves is chosen to be one second to be compatible with the NBSR nozzle check valves, which close in ~0.7 s.

The nominal mass flow rate through the core is to be ~540 kg/s. Since 10% of the total system coolant mass flow is diverted to the reactor pool, the total system coolant mass flow rate is ~600 kg/s. Since three pumps are working in normal operation, each pump should deliver ~200 kg/s. To achieve the required mass flow rate, TRACE has an internal controller that modifies the pump impeller velocity. This controller is used to ensure that each primary pump delivers 200 kg/s.

### 5.2.3 Heat Exchangers

Each pump is connected to a separate plate-type heat exchanger (HX1-HX4 in

Figure **5-1**). TRACE models them with the same design as the NBSR heat exchangers. The heat exchangers have plates that are 1.83 m in length and collectively offer a total heat transfer area of 422 $m^2$ across the primary and secondary loops.

The secondary cooling loop is represented by a single mass flow rate source and pipes, rather than an explicitly detailed loop. Through iterations, the secondary coolant mass flow rate has been determined to be 900 kg/s, entering the heat exchangers at a temperature of 302 K. To ensure the system's operational parameters align with the desired reactor core inlet temperature, TRACE employs a steady-state controller. This controller adjusts the total heat transfer area of the heat exchanger, thus enabling the model to define and maintain steady-state conditions.

The TRACE internal controller is used to regulate the temperature of the reactor core inlet which is expected to be approximately 316 K. The TRACE internal controller adjusts the heat exchanger's heat transfer area until the defined core inlet temperature is achieved. This process involves iterative calculations, during which the secondary cooling system parameters are fixed, and the TRACE controller is used to match the reactor core inlet temperature of 316 K.

### 5.2.4 Flap Valves

A key feature of the NNS is having the reactor within a pool. This design ensures a substantial volume of coolant, which can function as a heat sink during certain abnormal conditions, and the NNS core can be cooled with natural circulation to remove decay heat. To establish a natural circulation path, the cold legs are equipped with two flap valves that connect the cold leg lines to the reactor pool. Both flap valves are above the upper edge of the chimney; the upper flap valve is located 195 cm above, and the lower flap valve is located 65 cm above. In the event of a loss of coolant where the water level of the reactor pool drops, the upper flap valves serve as siphon breakers and prevent the water level from dropping further below the upper flap valve. The lower flap valves will open, thus creating the natural circulation path. If the primary coolant pumps are stopped, both flap valves open due to the pressure loss in the system, and this establishes the natural circulation path. Both cold legs have separate sets of flap valves. The upper flap valves are connected to each other with a pipe to allow siphon breaking on both cold leg lines if one of the flap valves fails to open.

The flap valves are modeled in TRACE using built-in valve components with an actuation trip. The actuation trip is generated based on arithmetic computing blocks that calculate the hydrostatic and gravitational forces that act on the valve disc. In normal operation, the hydrostatic force is greater than the gravitational force because of the forced flow from the reactor coolant pumps. The flap valves are fully closed in this scenario. If the reactor coolant pumps are stopped, the gravitational force becomes greater than the hydrostatic force and the flap valves open in one second. The actuation trip is single-sided, meaning the flap valves are locked once they are open and they cannot be closed even if the hydrostatic force overcomes the gravitational force.

### 5.2.5 Shutdown Cooling System

Figure 5-1 includes the shutdown cooling system although it is neglected in the analysis of transients/accidents for conservatism. As with the NBSR design [6], the NNS has two centrifugal pumps (SDP1-SDP2 in the figure) that provide forced convection cooling to the reactor during shutdown periods with only one of the two pumps necessary to remove decay heat from the core. The shutdown pumps feed into a shutdown system heat exchanger (SDHX) and then to the pool cooling bypass line, maintaining cooling in the pool during shutdown periods. The shutdown system takes the hot coolant from the chimney, sends it to the shutdown decay tank (a smaller tank than the normal N-16 decay tank shown in Figure 5-1), which then offloads the hot coolant to the shutdown pumps and into the shutdown system heat exchanger. This allows the pool to remain relatively unaffected by the decay heat generated in the core during shutdown. The pool coolant bypass line allows some of the primary coolant to be directed towards the pool's cooling system via a shutdown valve (SDV1), which allows a minimal amount of coolant to be sent to the pool. During operation, it is expected that SDCV1-SDCV2 are closed. During shutdown, SDCV1 or SDCV2 is fully open and SDV1 is fully open.

### 5.2.6 Core Models

The reactor core contains nine fuel assemblies, arranged in three rows and three columns. The rows are isolated from each other by control blade housings (see Figure 3-3). This arrangement allows the treatment of each row as a grouped fuel assembly. For each row, the fuel plates near the reflector tank have the highest power peaking factors; therefore, these plates are explicitly modeled as single fuel plates. For each row, three fuel plates at each side are modeled separately, and the remaining 57 inner fuel plates are lumped into a single fuel plate by conserving the total power generation of fuel plates and total heated area.

The coolant channels are modeled following the fuel plate pattern. The lumped fuel plate is in a lumped coolant channel and the single fuel plates are connected to neighboring coolant channels. The openings of the control blade housing are lumped into a single bypass flow channel. The layout of the core model is shown in Figure 5-2 and the relevant dimensions are given in Table 5-2. The different coolant channels given in the table reflect the fact that some channels are between two fuel plates (FPs) and some channels are next to the chimney with the convex side of the FP next to the chimney on one side of the core and the concave side next to the chimney on the other side of the core. Although not represented in this TRACE model there are also unique coolant channels at the edge of a fuel assembly (FA) next to another fuel assembly.

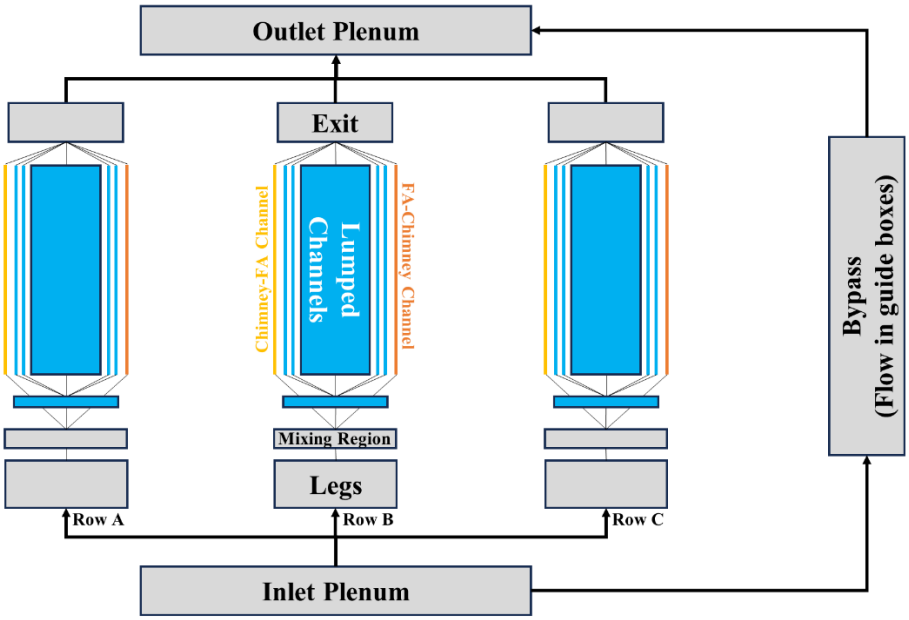
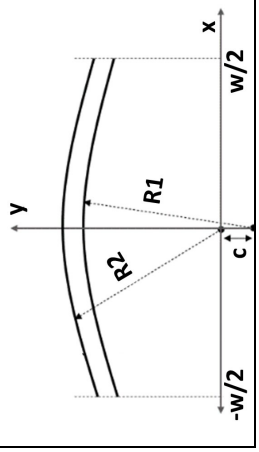



**Figure 5-2 Core Representation Used in the TRACE System Model**

**Table 5-2 Geometry for Core Coolant Channels**

| Parameter (mm) | Channel Type | | | | Curved Channels Guidance Graphic |
|---|---|---|---|---|---|
| | FP-FP | FA-FA | Chimney-FP | FP-Chimney | |
| **Inner chord length** | 69.757 | | | |  |
| **R1** | 141.13 | 141.13 | 140 | 141.13 | |
| **R2** | 140 | 140 | 140 | 141.13 | |
| **Arcs centers distance 'c'** | 3.874 | 5.39 | 4.024 | 4.024 | |
| **Channel width** | 69.757 | | | | |
| **Flow area ($A_{flow}$, mm²)** | 190.581 | 297.824 | 201.043 | 201.043 | |
| **Wetted perimeter ($P_{wet}$)** | 146.402 | 140.998 | 140.984 | 140.984 | |
| **Hydraulic diameter ($D_h$)** | 5.207 | 8.449 | 5.704 | 5.704 | |
| **Minimal gap** | 2.707 | 4.223 | 2.882 | 2.882 | |
| **Maximal gap** | 2.744 | 4.260 | 2.882 | 2.882 | |
| **Height** | 780 | 800 | 800 | 800 | |



The neutronics analysis, discussed in Chapter 4, provides the local power peaking and stripe (i.e., axially integrated power over a third of the fuel plate width) power peaking. Figure 5-3 shows power parameters at the startup (SU) state point. Fuel assembly average power is given as is the maximum and minimum local relative powers and their location. The fuel plate numbers (FP1-FP21) go from left to right relative to Figure 3-6 and the stripe numbers (S1-S3) go from left to right facing the concave side of the fuel plates. The axial location (Z) is in centimeters from the midplane. Although the neutronics analysis provides the power profile for

each fuel plate with 2 cm axial intervals, the TRACE model has each fuel plate divided into seven axial nodes each 10 cm long.

| | 1 | 2 | 3 |
|---|---|---|---|
| A | **Max : 1.95**<br>FP1 S3 Z: -8<br>**Avg : 1.06**<br>**Min : 0.48**<br>FP18 S2 Z: 32 | **Max : 1.44**<br>FP21 S3 Z: 0<br>**Avg : 0.98**<br>**Min : 0.42**<br>FP15 S1 Z: 32 | **Max : 1.68**<br>FP21 S3 Z: -6<br>**Avg : 0.97**<br>**Min : 0.45**<br>FP1 S1 Z: 32 |
| B | **Max : 1.69**<br>FP1 S3 Z: 10<br>**Avg : 0.99**<br>**Min : 0.46**<br>FP12 S2 Z: 32 | **Max : 1.37**<br>FP1 S1 Z: -22<br>**Avg : 0.93**<br>**Min : 0.43**<br>FP13 S1 Z: 32 | **Max : 1.93**<br>FP21 S3 Z: -8<br>**Avg : 1.07**<br>**Min : 0.48**<br>FP6 S2 Z: 32 |
| C | **Max : 1.96**<br>FP1 S3 Z: 2<br>**Avg : 1.06**<br>**Min : 0.49**<br>FP10 S2 Z: 32 | **Max : 1.46**<br>FP21 S1 Z: -8<br>**Avg : 0.98**<br>**Min : 0.43**<br>FP13 S3 Z: 32 | **Max : 1.67**<br>FP21 S3 Z: -10<br>**Avg : 0.97**<br>**Min : 0.45**<br>FP1 S3 Z: 32 |

**Figure 5-3 Power Parameters at Startup**

The simplification of fuel assemblies into lumped groups significantly reduces the computational cost of reactor simulations. To evaluate the impact of this simplification on accuracy, a separate detailed core model was constructed using TRACE with all 189 fuel plates and 192 coolant channels modeled. Each fuel plate in that model has 35 axial nodes to accommodate the power profile at two-centimeter nodes. **Figure 5-4** is a schematic of the detailed core model. This core model was used with boundary conditions from the TRACE simplified system model. The results at steady state, discussed below in Section 5.4, show the adequacy of the system model so that the simplified core model can be used in the analysis of normal and accident conditions.

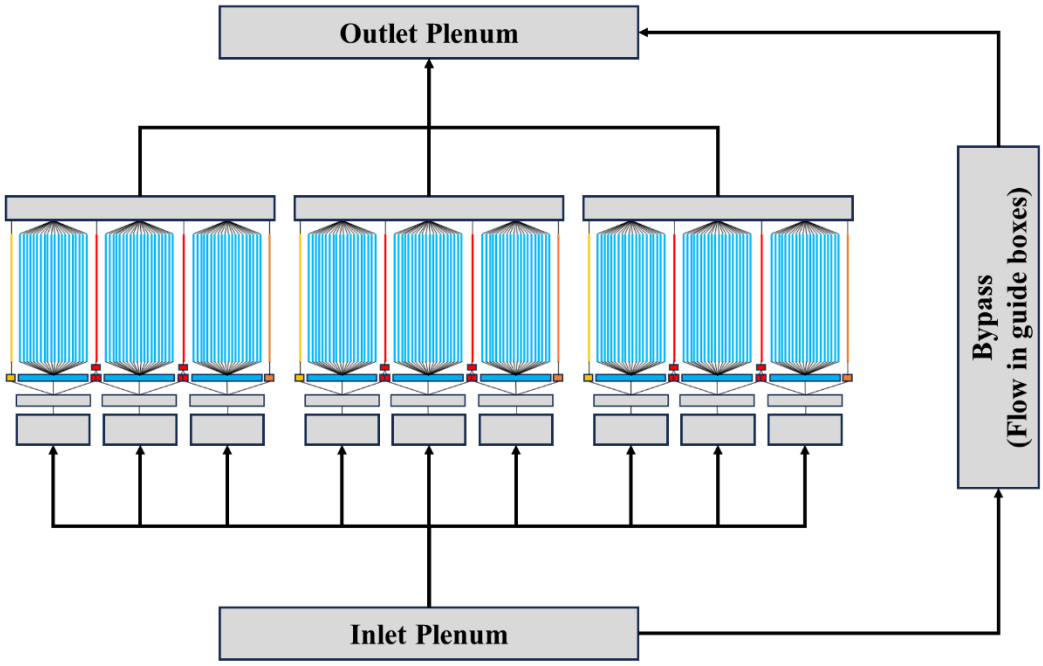



**Figure 5-4 Core Representation with Detailed Core Model**

The power distribution for the core comes from the neutronics model discussed in Chapter 4. All of the energy from fission is assumed to be deposited within the fuel plates. This is a conservative assumption when calculating thermal margins as some of the energy carried away by the coolant will be deposited directly into the coolant and control blade structures (e.g., some gamma and neutron energy deposition).

## 5.3 Computing Safety Margins

The thermal-hydraulic design basis is achieved by assuring the integrity of the fuel plates under normal and accident conditions. This is done by analyzing the minimums of the critical heat flux ratio (CHFR), the onset of flow instability ratio (OFIR), and the onset of nucleate boiling ratio (ONBR). Each of these ratios is the heat flux at which vapor generation is a concern divided by the actual heat flux. The ratios should be greater than unity to assure that any vapor generation would not increase temperatures and lead to fuel plate damage and the release of fission products.

At critical heat flux there is departure from nucleate boiling, and transition to film boiling which leads to burnout. Correlations due to Mirshak [7], and Sudo-Kaminaga [8] are used for the NNS as they have also been used for the NBSR [6] [9]. The Sudo-Kaminaga correlations were originally obtained for the Japan Research Reactor Unit 3 for rectangular coolant channels heated on both sides. They consider the effect of mass flux, inlet subcooling, outlet subcooling, flow direction, pressure, as well as the channel configuration. The Mirshak correlation is for rectangular channels heated on one side with upward flow and it has a smaller range of applicability. It is a function of flow velocity and temperature and pressure.

The most relevant flow instability for the NNS is the Ledinegg or static flow instability. This flow instability originates from the formation of two-phase flow in an otherwise single-phase flow channel. With increased pressure drop due to the two-phase condition, the channel flow would have to decrease to satisfy the imposed channel pressure drop. The onset of the Ledinegg instability is indicated by the sudden decrease in channel flow rate. A sudden decrease in flow rate has the potential consequence of a drastic reduction in the heat removal capability of the flow channel.

To monitor the onset of flow instability the Costa correlation [10] and the Saha-Zuber correlation [11] are used. Both of those correlations predict the heat flux at the point of onset of significant voiding (or at the similar point of net vapor generation), which can then be used to predict the onset of flow instability. The Saha-Zuber correlation has been used to assess the safety of the NBSR [6]. It depends on the Peclet number, the thermal conductivity of the coolant, channel geometry, and the coolant and saturation temperatures. It is limiting at low flow and low subcooling, where significant amounts of vapor are generated prior to achieving critical heat flux. Being a predictor of this onset of significant voiding makes it a conservative choice for the OFI. It is a function of the coolant velocity, and the saturation and bulk coolant temperatures.

The onset of nucleate boiling is the most limiting of the criteria used to assess the safety of the reactor. The Bergles-Rosenhow correlation [12] is used to determine the heat flux at this point. The correlation is based on experiments with water heated by stainless steel and nickel surfaces. It is a function of pressure and the outer cladding and saturation temperatures.

## 5.4 Steady-State Analysis

The TRACE models were used to calculate core conditions during normal operation at startup and the state point with the most limiting conditions as determined by the neutronics analysis. Results for the axial temperature distributions in the hot channel for each of the TRACE core models are shown in Figure 5-5. The coolant temperature ($T_{\infty}$), outer cladding temperature ($T_{c,o}$), and inner cladding temperature ($T_{c,i}$) are shown for the two channels that showed the highest temperatures in the two models, namely channel 2 in row A (aka row 1) in the detailed core model and channel 63 in row B (aka row2) in the system model. Although there is not much difference in temperatures in the two hot channels, the difference is likely due to the flow distribution between the channels being modeled with greater fidelity in the detailed core model, yielding differing pressure and flow profiles. The slightly higher temperatures in the system model results (found at all cycle states) makes it more conservative to use for safety analysis. Table 5-3 provides the maximum temperatures for the two models.

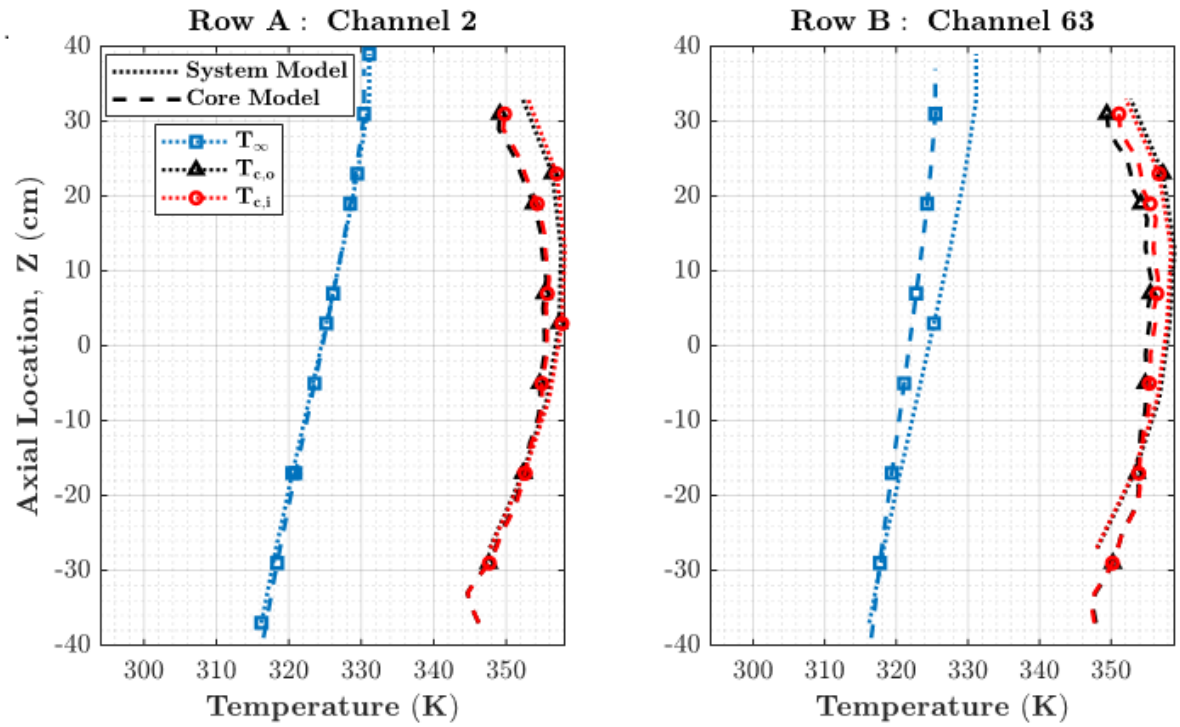



**Figure 5-5 Hot Channel Temperature Distributions for Both Core Models**

**Table 5-3 Maximum Hot Channel Temperatures and Location for Both Core Models**

| | | System Model | Detailed Core Model |
|---|---|---|---|
| **Hot Channel Location** | Row | B | A |
| | Channel # | 63 | 2 |
| **Maximum Temperature** | $\boldsymbol{T}_{\infty}$ (K) | 331 | 330 |
| | $\boldsymbol{T}_{c,o}$ (K) | 364 | 361 |
| | $\boldsymbol{T}_{c,i}$ (K) | 364 | 360 |

The pressure results from both models are shown in Figure 5-6 and Table 5-4. On average, both models predict a pressure drop ($\Delta \boldsymbol{P}$) of ~2.76 bar, but variations can be observed depending on the channel location and the model used to compute the pressure. For both models, the pressure varied depending on whether the channel is an outer channel (channel 1 or channel 64) or whether it is an inner channel (remaining channels) as these channels have different geometry at their inlet. At the outlet all channels feed into a single plenum. Referencing Table 5-2 and Figure 3-3, the pressure profiles for the FA-FA and FP-FP channels matched those of the inner channels, whereas the chimney-FP and FP-chimney channels matched those of the outer channels. Although the system model does not show variations between the FA columns, the core model predicts that column 2 has lower $\Delta \boldsymbol{P}$ (and lower flow rates) than columns 1 and 3.

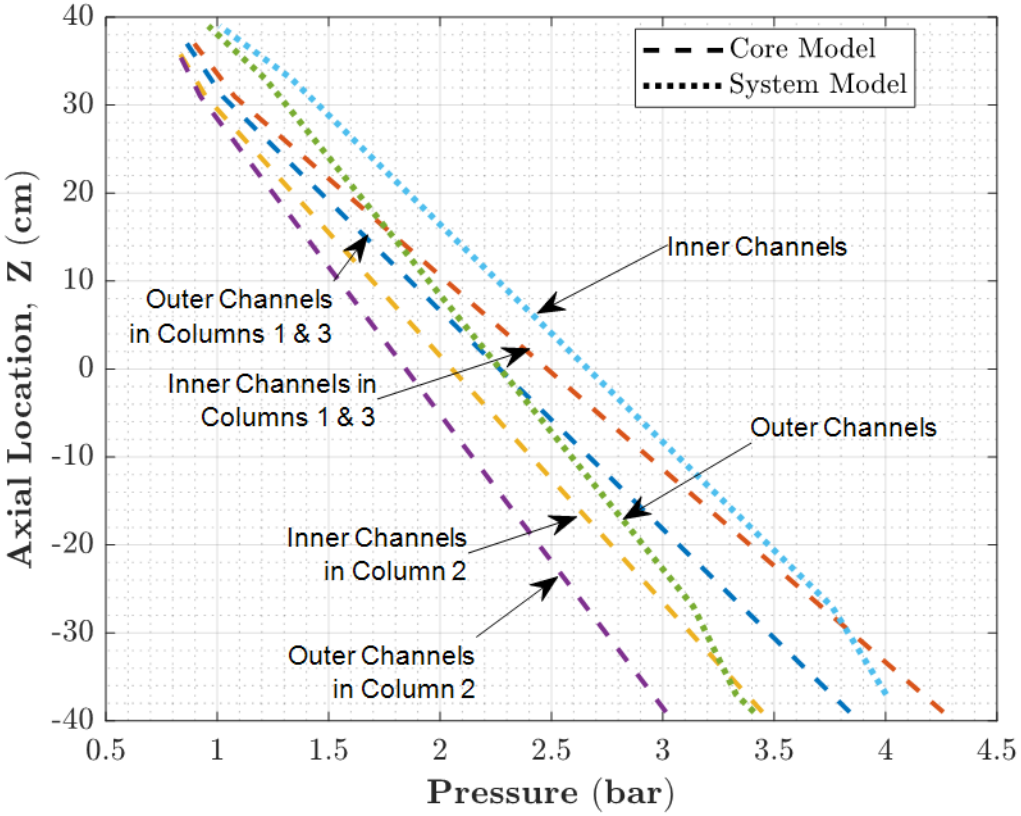



**Figure 5-6 Core Channel Axial Pressure Distributions**

**Table 5-4 Core Pressure Drop ($\Delta P$) for Both Steady State Models**

| | Location | $\Delta P$ (bar) | Average $\Delta P$ (bar) |
|---|---|---|---|
| **System Model** | Inner Channels | 2.99 | 2.72 |
| | Outer Channels | 2.45 | |
| **Core Model** | Inner Channels in Columns 1 & 3 | 2.98 | 2.80 |
| | Outer Channels in Columns 1 & 3 | 3.36 | |
| | Inner Channels in Column 2 | 2.64 | |
| | Outer Channels in Column 2 | 2.21 | |

The safety margins discussed in Section 5.3 were calculated at steady state conditions at startup for the system model and at all cycle statepoints for the detailed core model. Results for limiting (minimum) values are given in Table 5-5. In all cases there is a large margin to the point where a thermal limit might be challenged. In all cases, except for using the Costa correlation, the system model predicts a more conservative result than the detailed core model. In general, thermal margins increase through the cycle—another reason for using startup as the limiting point in the cycle for the transient/accident analysis discussed in Chapter 7.

**Table 5-5 Thermal Margins for Steady State Operation**

| Safety Criterion | Correlation | System Model | Core Model | | | | | |
|---|---|---|---|---|---|---|---|---|
| | | | SU | BOC | Q2 | MOC | Q4 | EOC |
| **MCHFR** | Mirshak | 3.03 | 3.09 | 3.08 | 3.24 | 3.42 | 3.72 | 3.74 |
| | Sudo-Kaminaga | 3.22 | 3.28 | 3.26 | 3.41 | 3.59 | 3.90 | 3.92 |
| **MOFIR** | Saha-Zuber | 7.17 | 7.22 | 7.25 | 7.71 | 8.20 | 9.17 | 9.31 |
| | Costa | 5.62 | 5.48 | 5.51 | 5.86 | 6.23 | 6.96 | 7.07 |
| **MONBR** | Bergles-Rosenhow | 1.96 | 2.15 | 2.23 | 2.31 | 2.42 | 2.39 | 2.38 |

## 5.5 References

[1] U.S. Nuclear Regulatory Commission, "Guidelines for Preparing and Reviewing Applications for the Licensing of Non-Power Reactors, Part 1 Format and Content," U.S. Nuclear Regulatory Commission, NUREG 1537, P01, 1996.

[2] L. Jamison *et al.*, "Review of the Technical Basis for Properties and Fuel Performance Data Used in HEU to LEU Conversion Analysis for U.S. High Performance Research Reactors," Argonne National Laboratory, ANL/RTR/TM-17/19 Rev. 2, 2022.

[3] U.S. Nuclear Regulatory Commission, "TRACE V5.0 Theory Manual: Field Equations, Solution Methods, and Physical Models," U.S. Nuclear Regulatory Commission, 2020.

[4] A. G. Weiss, A. Gurgen, E. R. Bures, and J. S. Shen, "Pre-conceptual Design Activities of the NIST Neutron Source - Preliminary Thermal-hydraulics Assessments," National Institute of Standards and Technology, Gaithersburg, MD, NIST TN 2323, February 2025, https://doi.org/10.6028/NIST.TN.2323.

[5] G. Braoudakis, "OPAL Nuclear Reactor: Reactor Specification," *International Nuclear Information System,* vol. 46, no. 20, February 1, 2015. [Online]. Available: http://inis.iaea.org/Search/search.aspx?orig_q=RN:46046717.

[6] NIST, "Safety Analysis Report (SAR) for License Renewal for the National Institute of Standards and Technology Reactor - NBSR; NBSR 14," ed: National Institute of Standards and Technology (NIST). 2023.

[7] S. Mirshak, W. S. Durant, and R. H. Towell, *Heat flux at burnout*. EI du Pont de Nemours & Company, Explosives Department, Atomic Energy …, 1959.

[8] M. Kaminaga, K. Yamamoto, and Y. Sudo, "Improvement of Critical Heat Flux Correlation for Research Reactors using Plate-Type Fuel," *Journal of Nuclear Science and Technology,* vol. 35, no. 12, pp. 943-951, 1998, doi: 10.1080/18811248.1998.9733966.

[9] D. Şahin *et al.*, "NBSR Alternative Fuel Management Schemes Analysis Procedure," NIST Center for Neutron Research, 2023.

[10] J. Costa, "Friction coefficient measurement in turbulent flow, simple phase with heat transfer, in a rectangular channel," France, Note CEA-N-1142, 1969. [Online]. Available: http://inis.iaea.org/search/search.aspx?orig_q=RN:49041845

[11] P. Saha and N. Zuber, "Point of Net Vapor Generation and Vapor Void Fraction in Subcooled Boiling," in *International Heat Transfer Conference 5*, 1974, Tokyo, Japan: Begellhouse, pp. 175-179, doi: 10.1615/IHTC5.430.

[12] A. E. Bergles and W. M. Rohsenow, "The Determination of Forced-Convection Surface-Boiling Heat Transfer," *J. Heat Transfer,* vol. 86, pp. 365-372, 1964.

# 6 Instrumentation and Control

## 6.1 Introduction

This chapter provides performance and design basics of the reactor instrumentation and control (I&C) systems and summarizes how they may be implemented. To achieve safe and efficient reactor operation, the important variables related to the reactor, its systems, and its environment are monitored, processed, controlled, and physically and digitally secured. There are four primary I&C systems, namely, reactor (nuclear) control system (RCS), plant process control system (PPCS), reactor protection system (RPS), and the radiation monitoring system (RMS). Other systems include post-accident monitoring system (emergency control station), condition monitoring system (CMS), plant documentation, and maintenance system. All of these I&C systems will be designed and implemented according to acceptable standards and guidelines.[g]

Operators interact with the nuclear reactor and plant processes via the PPCS panel, located in the main control room. PPCS consists of instrumentation displays, manual and digital controls, and annunciators. It is the primary human machine interface (HMI) for control of the reactor and secondary processes.

The reactor control and protection systems can generate protective actions such as reactor trip signals and reactor rundown signals after receiving inputs from the nuclear and process instrumentation. The setpoints for automatic actions are determined to be sufficiently lower than the Limiting Safety System Settings derived from safety analyses as described in Chapter 7, Safety Analysis.

The radiation monitoring system measures radiation levels at different locations throughout the facility, process piping, and building exhaust air. Monitoring of liquid releases and mixing are to be described in later design documentation; no reactor safety issues are associated with liquid releases.

The functionality of the RCS, RPS and RMS overlap where these systems interact through signals or data communications. For instance, RCS includes the drive mechanism for the six control blades—the clutches which can be released with reactor trip signals from the RPS. The reactor will not have a fully digital reactor control and safety system. In fact, the RPS, RCS, and RMS compose a “digital hybrid” system, where RPS is equipped with analog signals connected to hard wired safety relays.

---

[g] Examples of standards and guidelines that will be followed are: IEEE STD 7-4.3.2-2003 IEEE Standard Criteria for Digital Computers in Safety Systems of Nuclear Power Generating Stations, and IAEA NP-T-1.4 Implementing Digital Instrumentation and Control Systems in the Modernization of Nuclear Power Plants

## 6.2 Design Philosophy

The following are the design criteria for all NNS I&C systems.

- Robust
  - architecture based on digital recorders, digital meters, and industrial HMIs
  - minimized number of components

- Reliable
  - simple design, isolated systems, where a failure of one system does not disable others
  - the RPS actuations of the emergency systems do not require operator interaction
  - when possible, the I&C system is designed as fail-safe

- Redundant
  - HMI screen failure will not result in operational problems; digital recorder and digital meters will be available
  - critical safety variables on isolated digital meter displays
  - trend and mimic displays operate simultaneously
  - a single failure will not prevent a safe shutdown of the reactor

- Simple
  - simplified network and data flow
  - minimal custom coding
  - low maintenance requirement
  - modular approach for easy repair and replacement
  - detailed configuration management plan

- Secure
  - physical network barrier (data diode) to outside network
  - robust protocols for modification and access to digital components
  - physical security of all components
  - allow isolated continuous network security monitoring

Robust and Reliable: The hardware used for data acquisition and display should have sufficient meantime between failures.

Redundant: Process information would be displayed on multiple interfaces. Each device shall employ a separate, isolated input/output unit to acquire readings. Digital meters use internal input/output circuitry to gather readings.

Secure: Network layers within the RCS, RMS and RPS are isolated and segmented through industrial firewalls. There are network security monitoring taps at each choke point to

continuously monitor network traffic for intrusion analysis for both egress and incoming communications. Configuration changes are monitored by system monitors and for critical components create warnings to the operators and analysts. Within the supervisory network layer, industrial zero trust architecture concepts are followed to the extent possible while ensuring continuous operation. This includes but is not limited to variable trust, credential rotation, password policies, managed service accounts, secure transmission protocols and domain isolation.

In addition to the above design criteria, the following are important to consider.

Diverse: Digital components with different firmware/manufacturer are interchangeably used in the system. Hardware used in reactor control and protection systems provides functional software and equipment diversity for displaying sensor information and actuating associated alarms.

Defense-in-Depth: Process parameters are displayed on a mimic screen and a trend screen both provided by two independent systems. Digital recorders, industrial HMIs and digital meters shall be based on different technologies. The digital meters and digital recorders are isolated from each other preventing single point common cause failures. In other words, any of them failing does not affect others for signal, power, or relay actuation.

Modular and Straightforward: Configuration files for the simple digital components, recorders, industrial HMIs and meters, are saved on a secondary system. The components can be easily replaced with minimal impact and testing. When possible, connections to the process are made by plug-and-play type terminals.

## 6.3 Reactor Control System (RCS)

The control system for the reactor will be based on a digital hybrid concept, where most of the human machine interface will utilize digital infrastructure and the safety related system actions will utilize hard wired analog relay circuitry.

Of all the parameters that are measured and controlled, the thermal neutron flux levels, primary cooling parameters, and radiation levels are the primary quantities that are measured for reactor operation and safety. The nuclear instruments will be placed in the reflector vessel and able to detect distorted power distributions as well as power level. These sensors are capable of monitoring neutron flux in the core for the whole operational range, including startup after long shutdowns, where the neutron density in the core is minimal. There is minimum of one decade overlap between the channels, covering from source range level to greater than full power for monitoring unlikely power spikes.

During normal operation, after withdrawal of the safety blades, the reactor is controlled with the regulating control blades (see Section 3.2.3). The control system shall be designed to ensure

reliable operation and minimize inadvertent reactor shutdown. The potential for false reactor trips (scrams) is minimized using redundant analog circuitry and coincidence (voting) logic.

Since the NNS is defined as a research reactor, and not required to provide power during emergencies, it is shut down during adverse conditions such as severe weather phenomena, a seismic event, or fire. The reactor would be shut down should any of these events occur. The reactor I&C system, however, is required to remain operable and provide minimum functionality to ensure safety of the reactor and confinement.

## 6.4 Reactor Protection System (RPS)

The reactor protection system receives signals from nuclear, radiation and process instrumentation. The RPS monitors conditions that are important to safety including reactor parameters and parameters outside the reactor. Actuation of the RPS generates a reactor trip, driving the safety blades in and making the reactor subcritical. In emergencies that have a defined release of radioactive material, actuation of the system generates a major scram, which includes closure of the confinement building.

Two diverse systems will initiate and actuate actions for automatic reactor scram and shutdown. Built using analog circuitry and relays, the primary shutdown system inserts all control blades at maximum speed into the core whenever a system process parameter exceeds safe operation limits. A digital secondary shutdown system lowers the heavy water level in the reflector vessel to shut down the reactor whenever a monitored process parameter exceeds safe operation limits and signals from the primary shutdown system indicate a problem with that system.

The primary parameters of concern in the reactor are core power level (or neutron flux level), the reactor period, the reactor pool and reflector vessel levels, and the primary coolant flow and temperatures. Other significant parameters include radiation levels in the confinement air and the exhaust stack. In addition to initiating a reactor trip, the radiation parameters automatically activate equipment to prevent activity in the air from escaping the confinement.

There is a large margin between the setpoints at which RPS actions occur and the limiting safety system settings calculated via safety analysis as shown in Section 7. Limiting safety settings are chosen conservatively based on safety analysis results, namely safety limits. This conservative approach provides further assurance that the actual safety limit will not be exceeded. For example, the normal licensed operating power level is 20 MW and reactor trip can be set at 125% of this level (25 MW), while the limiting safety system setting may be 150% (30 MW). These setpoints ensure that the reactor safety limit is not violated.

Table 6-1 and Table 6-2 list some basic inputs for reactor scram and rundown, respectively. These signals provide minimum process and nuclear instrumentation inputs for safe reactor operation. Several rows are marked as N/A (not available) in Table 6-1 and Table 6-2 due to lack of design basis information at this stage of the project.

**Table 6-1: Reactor Trip Inputs**

| Scram Signal | Source | Trip Setting |
|---|---|---|
| Manual scram | Two scram pushbuttons | |
| Neutron flux high | Nuclear instrument channels | 125% (25 MW) |
| Period scram high | Nuclear instrument channels | 5 seconds |
| Nuclear instrument power off | Nuclear instrument channels | |
| Gaseous monitor high | Gaseous monitor system | |
| Core outlet flow low | N/A | 370 kg/s |
| Core inlet flow low | N/A | 370 kg/s |
| Core temperature difference high | N/A | 13 K |
| Core outlet temperature high | N/A | 338 K |
| Pool Level low | N/A | 1 m below top of pool |
| Core pressure drop high | N/A | 5 bar |
| Core pressure drop low | N/A | 4 bar |

**Table 6-2: Reactor Rundown Inputs**

| Rundown Signal | Source | Rundown Setting |
|---|---|---|
| Log/linear channel period rundown | Nuclear instrument channels | 10 seconds |
| High flux rundown | Nuclear instrument channels | 115% |
| Reactor outlet temperature high | N/A | |
| Startup prohibit | N/A | |
| Safety Blades on Test | N/A | |
| Safety blades not seated | N/A | |

## 6.5 Radiation Monitoring System (RMS)

The Radiation Monitoring System consists of area monitors, duct monitors, and effluent monitors located throughout the facility to show any release of radioactive isotopes of activity greater than limits established for those isotopes or monitor potential release to the environment. Gamma radiation monitoring instruments are in and above the reactor pool and in the stack ventilation system. Stack monitoring is accomplished by gaseous monitors to provide continuous indication of the radioactivity in the air, either gaseous or particulate. If radioactivity thresholds are exceeded for the gaseous monitors, a scram signal would be generated, and two Engineered Safety Feature systems would be activated: the confinement building penetrations would close, and the emergency ventilation system would start. All area radiation monitors, and gaseous radiation monitors would also indicate alarms in the control room.

Additional area monitors would be positioned at locations where either experimental work is performed or where work involving radioactive material is likely to be undertaken. As a result, personnel in those areas can be warned by the alarms associated with the monitors of any

unanticipated changes or hazards. Secondary coolant is normally continuously monitored for beta-gamma radiation and sewer discharge is sampled periodically for beta-gamma radiation.

## 6.6 Condition Monitoring System (CMS)

Safety of the reactor is ensured by the RPS, which generates a reactor scram when the setpoints of certain reactor parameters are exceeded. Unanticipated changes due to malfunctions in the NNS systems may also actuate RPS to generate a reactor scram. However, minor changes, specifically long-term drifts or increased noise in system parameters can be unnoticed because the RCS can compensate for these changes. Eventually, some minor changes may propagate to challenge the safe operation of the reactor or cause malfunctioning equipment. Hence, a Condition Monitoring System (CMS) would continuously collect real-time sensor measurements and analyze the measurements to determine changes in the NNS systems. The CMS would identify abnormal occurrences and warn the operators. The CMS consists of plant state condition monitoring, sensor condition monitoring, and system component condition monitoring.

Plant state condition monitoring aims to distinguish between normal plant states and abnormal states. While most of reactor life is spent in a normal state, abnormal states do take a small part; therefore, abnormal state data can be characterized by sparse distribution. CMS analyzes the sensory data and identifies the abnormal state if the sensor measurements are significantly different from the normal state.

Sensor condition monitoring aims to identify sensors that need recalibration. Successful operation of CMS, RPS, and RCS are dependent on the sensor measurements. To catch errors in sensor measurements, CMS reconstructs the sensors based on sensor measurements. Deviations between the measured and reconstructed signals identify sensors that need evaluation. There are two additional benefits of sensor condition monitoring. First, drifting sensors would be replaced before causing unintended interruptions. Second, sensor condition monitoring would allow cross calibration of sensors to increase required physical calibration intervals, reducing maintenance requirements.

System component condition monitoring aims to determine the degradation of individual rotating/moving components, such as safety and control blades, pumps, valves, cooling fans, etc. CMS collects the system parameter measurements and health indicators of these individual components. Health indicators can be external measurements such as electrical power, acoustic or vibration sensor data. CMS forecasts the degradation of components to identify maintenance requirements.

CMS utilizes Digital Twin (DT) of the NNS. DT is a digital representation of a physical object or a system. With advanced data processing and analytics techniques, computer models can produce a virtual version that mimics the characteristics of the physical version of the system. DT is a simulation-informed, data/knowledge-driven virtual environment in which all the data and related information about the actual NNS are stored and processed to guide the operation.

DT would employ a real operational data collector, high-fidelity computational physics-based models, and advanced data analytics tools. The CMS provides the forecast of the health and performance of the NNS based on the DT. DT system also allows prediction of future plant states for given internal or external system perturbations. For instance, to guide operator decision, future states of the secondary cooling systems can be predicted based on cooling tower doors, fan speed or outdoor temperature, etc.

## 6.7 Emergency Control Station (ECS)

The Emergency Control Station, or Post Accident Monitoring System, is utilized when evacuation of the control room is necessary during and after an accident. The ECS provides essential reactor information, such as ventilation, radiation monitoring, critical plant process information, such as primary coolant flow rate, reactor inlet and outlet temperatures, confinement ventilation system, nuclear instrumentation, and radiation monitoring systems. ECS further allows control of the emergency ventilation system, and shutdown systems. The ECS would be located outside of the confinement building.

ECS allows operators to ensure that the reactor is shut down, and safety systems are online while engineered safety features are effective (the confinement building penetrations would close, and the emergency ventilation system would start). Additionally, the ECS monitors potential radiation release into the confinement and/or the environment. The information allows operators to take further actions when necessary. ECS systems are directly hard-wired in parallel to the main control room, process instrumentation and radiation sensors.

# 7 Safety Analysis

## 7.1 Safety Philosophy

The health and safety of the public and NIST workers would be protected in the event of an NNS accident. This protection results from the facility design features, the Technical Specifications that would be in place [e.g., Safety Limits, Limiting Safety System Settings (LSSS), and Limiting Conditions for Operation (LCOs)], and the well-qualified and trained staff of NCNR. This holistic approach ensures that no credible accident could lead to unacceptable consequences to the public, workers, or the environment. This chapter presents analyses to help show why this is true. It is not meant to provide a rigorous safety analysis, which would be premature at this point, but rather to understand how the NNS reacts to accident conditions.

The accident scenarios that will need to be considered in an NNS Preliminary Safety Analysis Report (PSAR) are identical to those considered in the Safety Analysis Report [1] for the NBSR with highly-enriched uranium fuel; namely,

- loss of normal power accident
- loss of heat sink accident
- loss-of-flow accidents
- reactivity insertion accidents
- loss-of-coolant accidents
- misloaded fuel assemblies
- flow blockage in one fuel assembly
- external events
- experiment malfunctions
- natural circulation cooling at low power operation

However, several events (the last four in the list) are not considered at this stage of the design and as stated above, the events that are calculated are to show general characteristics and are not evaluated as rigorously as those in an actual PSAR.

The flow blockage of one fuel assembly leading to fission product release, which might be considered the maximum hypothetical (i.e., not credible) accident is one of the accidents not considered. Currently there is insufficient design information about the balance-of-plant (e.g., confinement design) to assess radiological consequences to staff or the public. Damage to the core from external events, such as tornados, hurricanes, floods and earthquakes is also not considered herein. Assuming that the NNS is built at the NIST site, these events will not be credible as a result of design features, administrative controls and the seismological and climatological characteristics of the site as discussed for the NBSR [1].

Experiment malfunctions are not considered as the current design does not have any in-core or near-core irradiation sites for experiments. Natural circulation will be considered in the

future when it will be necessary to define a Technical Specification with the allowable power level without forced circulation.

For a given initiating event, the analyses discussed below include credible assumptions expected to lead to maximum consequences. The progression of each accident is analyzed to the extent necessary to determine the degree of potential hazard. For most events it is clear that there is margin to reaching critical heat flux, onset of flow instability, and onset of nucleate boiling and for loss-of-coolant accidents sufficient margin to the assumed safety limit. For the sake of brevity all the criteria discussed for normal operation in Section 5.4 are not used. For the critical heat flux the Sudo-Kaminaga correlation is used, for onset of flow instability the Costa correlation is used, and for onset of nucleate boiling, the Bergles-Rosenhow correlation is used.

## 7.2 Methodology

For time dependent events, the TRACE systems analysis code [2] described in Chapter 5 is used with additional modeling. The model calculates the time dependent reactor power level and the thermal hydraulics for the primary coolant system piping with pumps and heat exchangers and coolant channels within the fuel assemblies. Initial conditions (e.g., power, flows, and temperatures) are assumed to be at nominal conditions rather than at limiting (i.e., conservative) conditions.

TRACE calculates the time dependence of reactor power using point kinetics with no thermal-hydraulic feedback. As shown in Section 4.6 moderator and fuel temperature increases lead to negative reactivity feedback and their neglect adds to the conservatism of the model. For decay heat the American Nuclear Society standard [3] is used.

The detailed neutronics model used to calculate physics parameters for use in the accident analysis is discussed in Chapter 4. These parameters are the steady state power distribution, neutron kinetics parameters, and the reactivity worth of the regulating and safety blades. The backup shutdown system wherein $D_2O$ is drained from the reflector tank is also modeled although for the analysis herein only the primary shutdown system is used. The neutronics model includes a plate-by-plate representation of each fuel assembly, control blades, coolant channels, the reflector with beam tubes and cold neutron sources, and other structures internal to the reactor. The power distribution used for transient/accident analysis is assumed to be independent of time and for the startup state point since, as discussed in Section 4.4, the peak local power density during operation is calculated to be at startup and beginning-of-cycle.

The reactor protection system (RPS) logic described in Chapter 6 was modeled and initiated reactor trip via the insertion of the safety blades upon reaching a setpoint and after a conservative instrumentation response delay of 0.50 s. Table 6-1 provides the trip setpoints that are modeled. No credit is given for the insertion of the regulating blades that would also take place. The safety blades are completely withdrawn during normal operation and the reactivity insertion is not sensitive to the time in the cycle as seen in Figure 4-13. The figure also

shows the total worth of the safety blades is smallest at SU, albeit not significantly. The safety blades are assumed to be inserted with the assistance of a pneumatic system as is the case in the OPAL reactor [4] and hence, the assumption is that it only takes 0.9 s for complete insertion. The SU statepoint has the lowest integral worth for the safety blades and hence is used to be conservative. Based on uniform speed and reactivity vs position for the blades (see Figure 4-13), the reactivity inserted as a function of time is shown in Table 7-1.

**Table 7-1 Safety Blades Reactivity vs Time After Reactor Trip**

| Time (s) | Reactivity (Δρ) | Time (s) | Reactivity (Δρ) |
|---|---|---|---|
| **0.0** | 0.0 | 1.0 | -0.0677 |
| **0.5** | 0.0 | 1.1 | -0.0903 |
| **0.6** | -0.0072 | 1.2 | -0.1132 |
| **0.7** | -0.0170 | 1.3 | -0.1317 |
| **0.8** | -0.0301 | 1.4 | -0.1389 |
| **0.9** | -0.0468 | | |

## 7.3 Loss of Power Accident (LOPA)

This event assumes the loss of all electrical power to the NNS. The de-energization of the control rod electromagnets causes the safety blades to drop into the core immediately without any signal from the reactor protection system. Hence, the power in the fuel plates is decay heat from approximately one second into the event.

The pumps in both the primary and secondary cooling systems also trip immediately. The secondary cooling system pumps stop within one second, however, the primary pumps stop slowly due to their flywheels. This is seen inFigure 7-1 which shows the mass flow rate in the hot channel ($\dot{m}$) during the event with a dashed line showing the initial value. At approximately 100 seconds the pumps have stopped, and the flow continues due to natural circulation only.

The reduced flow rate is insufficient to keep the fuel and coolant temperatures from rising, however, when the natural circulation flow rate increases, the temperatures are again moderated. This is seen in Figure 7-2 which shows the clad inner ($T_{c,i}$) and outer ($T_{c,o}$) temperatures, the coolant temperature ($T_\infty$), and the saturation temperature in the hot channel at an elevation 23 cm above the fuel midplane where the hot spot during the event is located. The hot channel is in the second cycle fuel assembly in row B column 3 in the last channel between two fuel plates (channel 63) at the edge next to the reflector. Since the clad thickness is small, the inner and outer clad temperatures are always very close. They rise almost 60 K and the coolant temperature follows closely. At 100 seconds the decay heat is approximately 3% of initial power and decreasing. After 110 seconds the flow rate (Figure 7-1) is 1% of the initial flow rate but increasing sufficiently to reduce the temperatures.

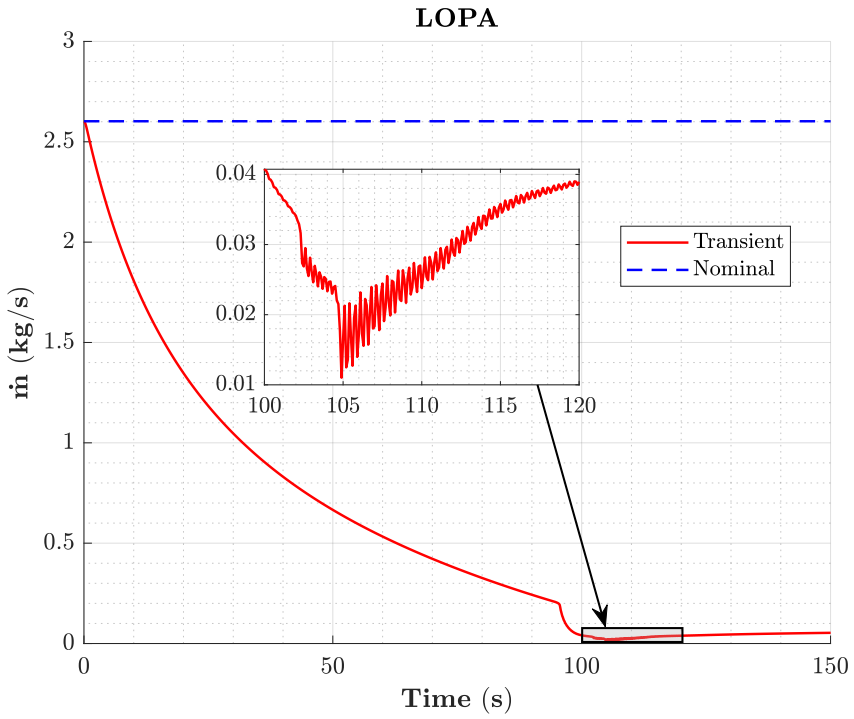



**Figure 7-1 Hot Channel Coolant Flow Rate During a Loss of Power Accident**

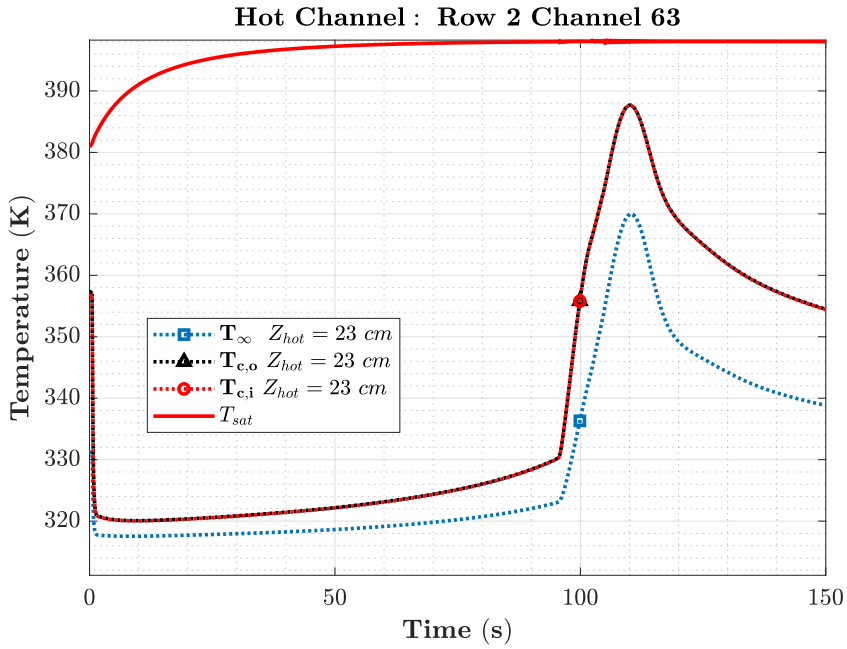



**Figure 7-2 Temperatures During a Loss of Power Accident.**

The results for the thermal limits during the LOPA are acceptable. The minimum values occur at ~110 seconds when the temperatures are highest, and the flow rate is lowest. The evolution of the mCHFR is seen in Figure 7-3 and for the mOFIR in Figure 7-4. The former reaches a

minimum of 2.70 and the latter 2.72. The minimum ONBR is 1.34. These ratios increase immediately after reactor trip due to the decrease in power and begin to decrease when the decrease in flow rate becomes more important. With the flow rate very small and undergoing oscillations after 100 seconds (Figure 7-1) the ratios show oscillatory behavior and reach their minimum.

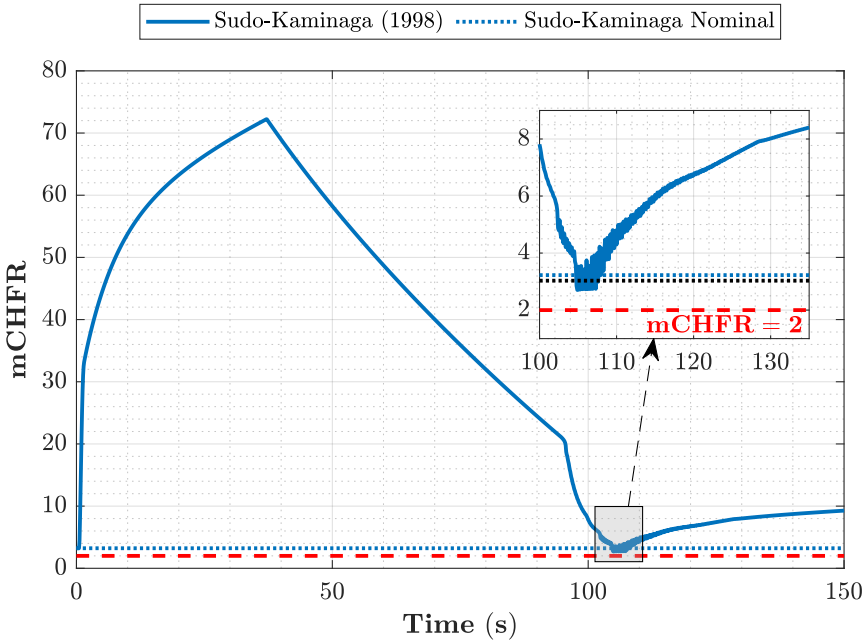



**Figure 7-3 Minimum CHFR During a Loss of Power Accident**

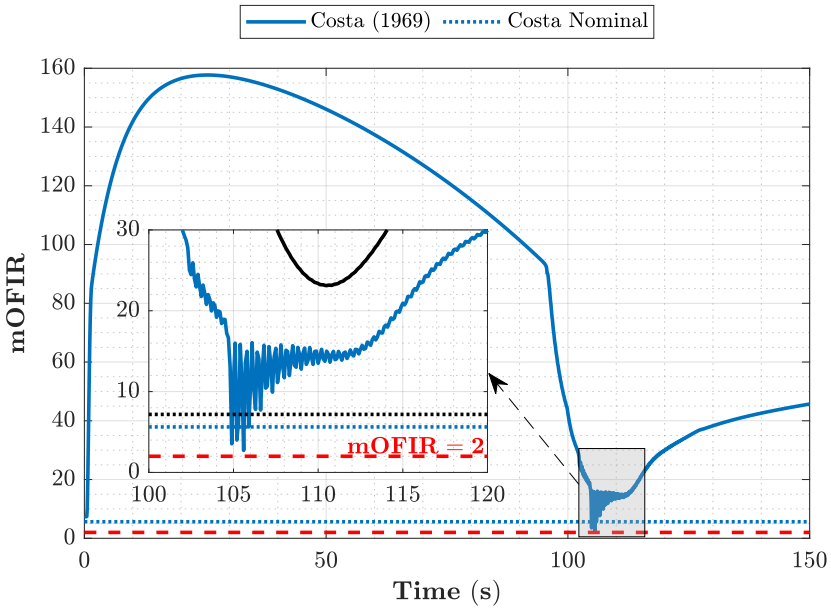



**Figure 7-4 Minimum OFIR During Loss of Power Accident**

## 7.4 Loss of Heat Sink Accident

In this event there is a complete loss of cooling capability in the secondary loop. The accident is initiated by the unexpected trip of the secondary pumps. Coolant flow stops in one second in the secondary loop, rendering the heat exchangers non-functional. It is assumed that the reactor protection system or an operator does not trip the reactor. Hence, the reactor stays at full power and coolant temperature continues to rise until a reactor trip is caused by the setpoint for the outlet temperature at approximately 240 seconds. The primary cooling pumps continue to operate at their normal capacity during the entire event.

Figure **7-5** shows the temperatures in the hot channel increasing with time. As with other accidents, the hot channel is the end channel within the fuel assembly (channel 63) in row B. The precipitous drop at approximately 240 seconds is caused by the reactor trip. Since the coolant temperature does not increase significantly during this event (12 K increase in the hot channel), the minimum CHFR only goes down from 3.22 during normal operation to 3.12 before reactor trip. Similarly, the minimum OFIR goes from 5.62 during normal operation to 4.04 before reactor trip. The change in the minimum ONBR is from 1.96 to 1.81.

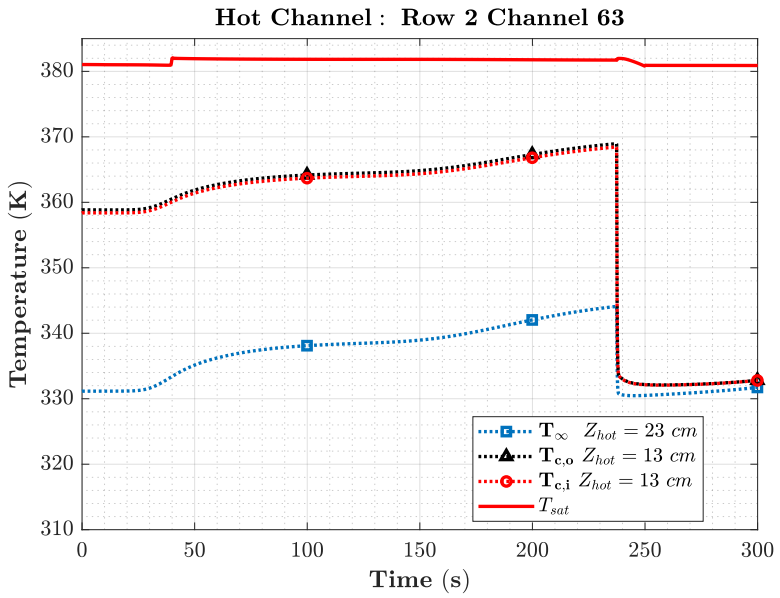



**Figure 7-5 Temperatures in Hot Channel During a Loss of Heat Sink Accident**

## 7.5 Loss of Flow Accident (LOFA)

Two loss of flow accidents were analyzed. The first assumes a single primary pump shaft seizure which immediately stops flow in that circuit and the second assumes that two pumps trip at the same time. The secondary circuit continues to remove heat during both events. Both transients are initiated at 1.0 s.

The flow rate in the pump seizure event is shown in Figure 7-6 for the hot channel. Although the flow rate drops precipitously, since two pumps continue at normal capacity, the flow rate stabilizes at ~75% of full capacity. However, the initial drop in the core flow rate at around one second is sufficient to cause reactor trip via the pressure drop signal.

When the flow rate decreases, the coolant temperature starts to rise. However, reactor trip quickly causes the temperature to decrease. Temperatures in the hot channel are shown in Figure 7-7 and the corresponding power is shown in Figure 7-8. The rapid decrease in power due to the fast acting safety blades is the same in all events with reactor trip.

Since the increases in temperature are minimal, the minimum CHFR only decreases to 3.21, the minimum OFIR to 5.58, and the minimum ONBR to 1.68 during the event. This occurs when the temperatures reach a maximum just before reactor trip.

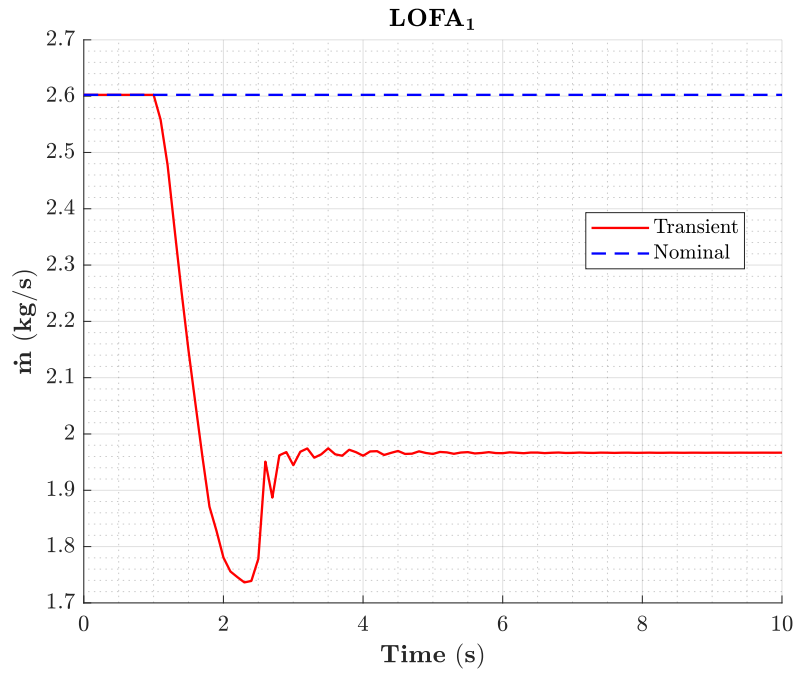



**Figure 7-6 Hot Channel Flow Rate During Loss of Flow Accident (Pump Seizure)**

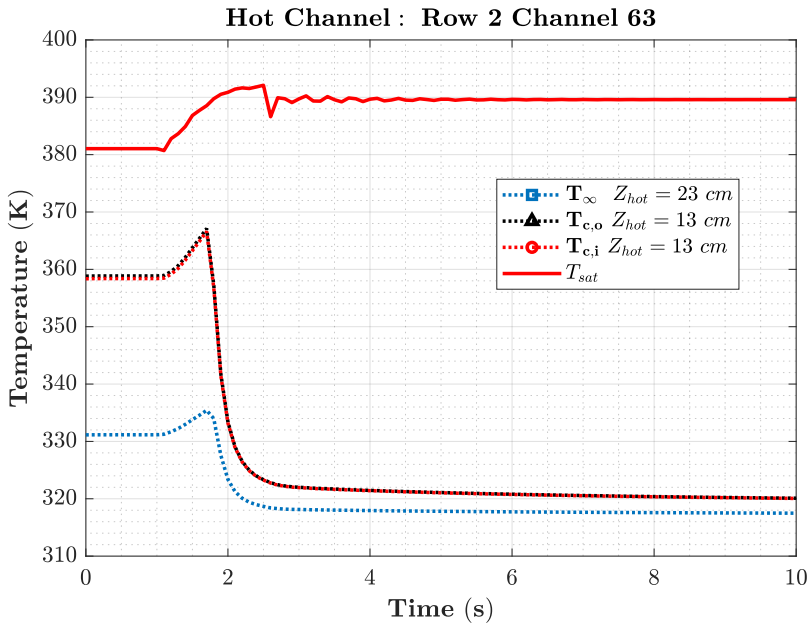



**Figure 7-7 Temperatures in Hot Channel During LOFA (Pump Seizure)**

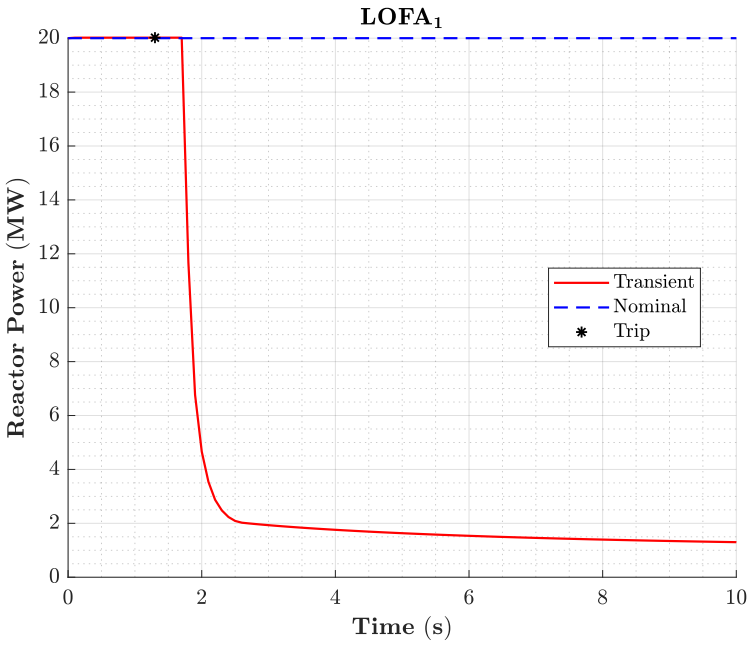



**Figure 7-8 Reactor Power During Loss of Flow Accident (Pump Seizure)**

The other LOFA analyzed assumes that there is a trip of two of the three primary pumps. This results in a gradual decrease in coolant flow rate as the flywheels slow down for the two impacted pumps while the third pump is still operating at full capacity. Figure 7-9 shows the hot channel flow rate during the event. The decrease in pressure drop results in reactor trip at approximately 3.3 seconds. The reduced flow rate causes the coolant temperature to rise and at 3.7 seconds reactor power is reduced to decay heat and temperatures decrease.

The temperatures in the hot channel are shown in Figure 7-10. Since the increases in temperature are minimal, the minimum CHFR only decreases to 3.23, the minimum OFIR to 5.63, and the minimum ONBR to 1.89 during the event. These minima occur when the temperatures reach a maximum just before reactor trip.

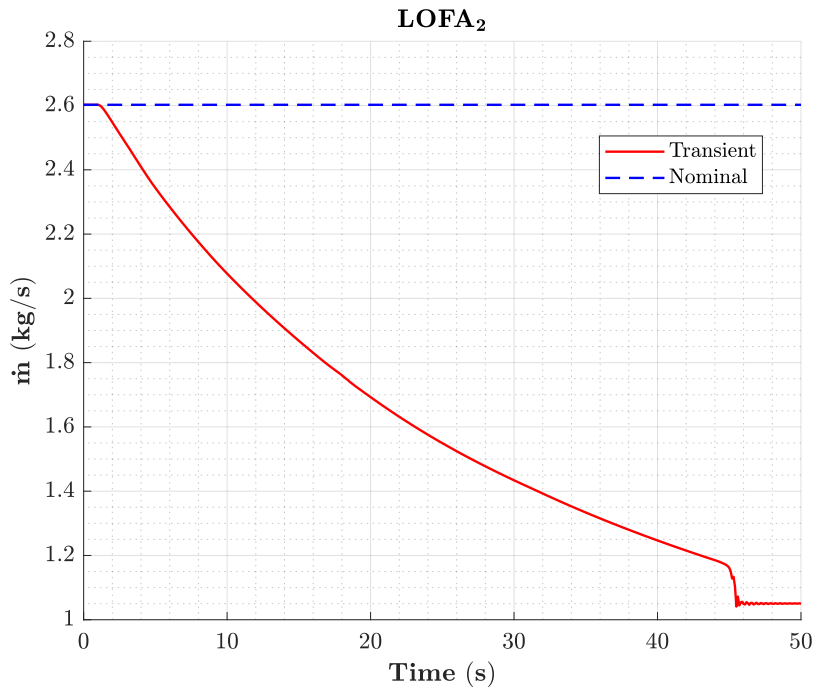



**Figure 7-9 Hot Channel Flow Rate During LOFA (Trip of Two Pumps)**

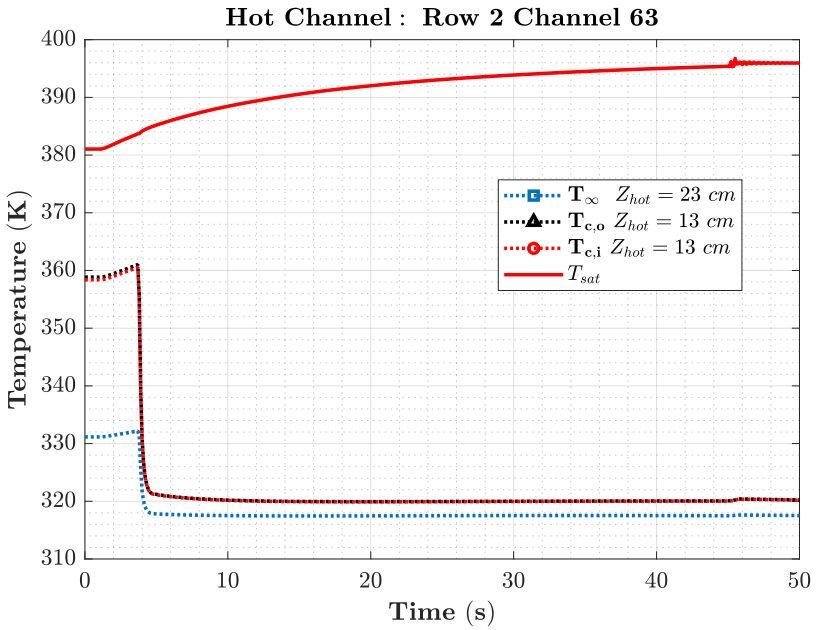



**Figure 7-10 Temperatures in Hot Channel During LOFA (Trip of Two Pumps)**

## 7.6 Reactivity Insertion Accident (RIA)

At this point in the design of the NNS, the only source of an accidental insertion of positive reactivity during normal operation is the uncontrolled withdrawal of the two regulating blades.

Assuming similar mechanical design as in the OPAL reactor, the blades would move at their maximum feasible velocity of 3.5 mm/s [4]. The assumption is made that the differential worth added is the maximum value seen in Figure 4-14 for SU and BOC, namely, 0.10 %Δρ/cm and hence 0.035 %Δρ/s is added uniformly during the RIA. Other statepoints may have larger reactivity insertion rates and will be considered in future, more detailed, safety analyses.

The power increases as shown in Figure 7-11 until the trip setpoint at 125% of normal power is reached at three seconds. It is assumed that there is no trip on reactor period which would have come sooner. With the reactor shut down, and the pumps still operational, the increases in temperatures shown in Figure 7-12 quickly turn around and there is no threat to the fuel. The minimum CHFR (2.36), OFIR (3.62) and ONBR (1.49) occur when the temperature peaks.

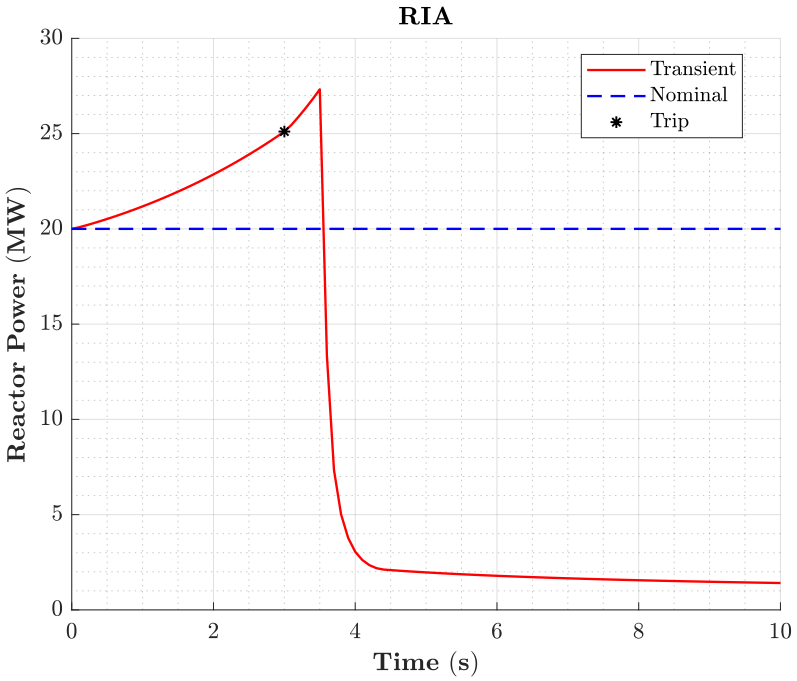



**Figure 7-11 Reactor Power During Reactivity Insertion Accident**

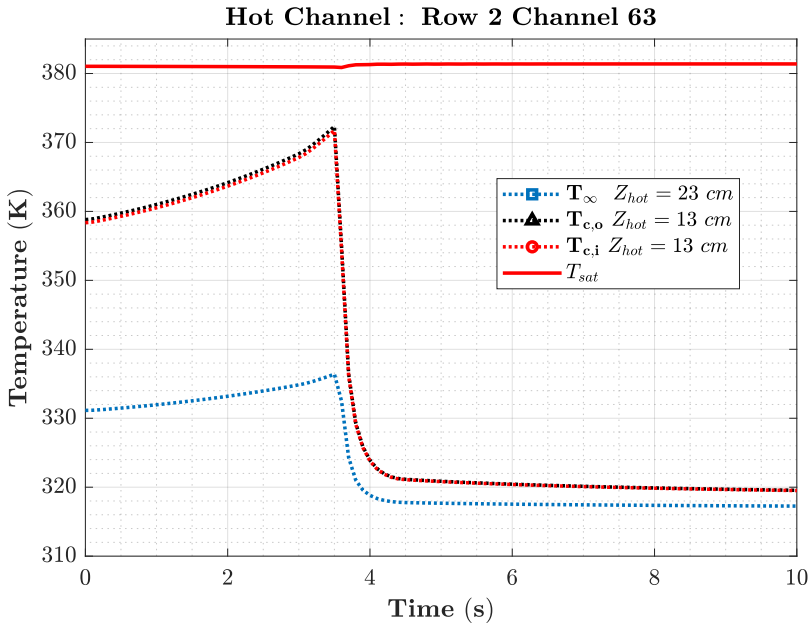



**Figure 7-12 Temperatures in Hot Channel During Reactivity Insertion Accident**

## 7.7 Loss of Coolant Accident (LOCA)

When the initiating event is a pipe break, some of the primary coolant flows out of the system and there is the potential for overheating of the fuel. However, the low probability of this event is recognized in the same way it has been recognized for the NBSR, namely [1], "the main piping [would be] is located in protected areas, system pressures are low, and flow rates are small so that wear is not an issue." Therefore, a sudden loss of primary coolant from the NNS due to a guillotine break is not credible. For the NNS, the positioning of the reactor within a pool provides emergency cooling. Two events were considered starting at 1.0 s.

One loss of coolant accident analyzed assumes a small pipe break resulting in an opening of 78.5 $cm^2$ in the discharge line of the primary coolant pumps; the line having a flow area of 3.14 $m^2$. This causes an immediate drop in system pressure causing a reactor trip. The assumption is made that some LOCA trip signal will be designed to trip the primary pumps at this time. The primary pumps take about 100 seconds to fully stop. The secondary loop remains operational, and the issue is whether there is sufficient cooling in the primary for the decay heat.

Figure 7-13 shows the temperatures in the hot channel during the event. For this event the hot spot is located below the fuel centerline—as opposed to it being above the centerline in all other events analyzed. The clad temperature goes above the saturation temperature at 94 seconds but only briefly. The minimum CHFR at that point is 1.09, however, the peak cladding temperature is only 405 K which is much less than the assumed safety limit of 645 K (see Section 5.1) . The cladding temperature is only a few degrees different than fuel temperature which is the basis for concluding that temperatures remain much lower than the safety limit.

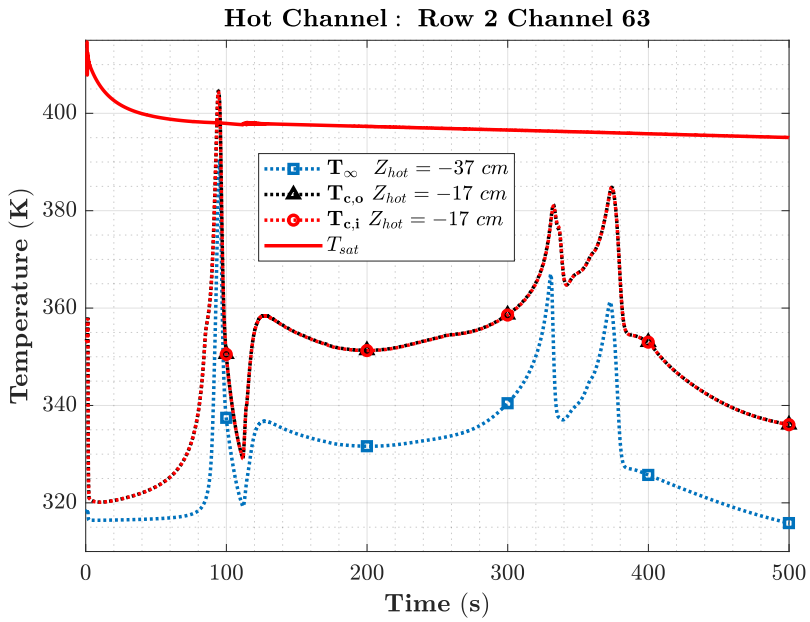



**Figure 7-13 Temperatures in Hot Channel During LOCA (78.5 cm$^2$ Break)**

The reason for the peaking of temperature relates to how the flow rate in the core is impacted by the pipe break. Figure 7-14 shows the mass flow rate ($\dot{m}$) in the core as well as the minimum CHFR. The flow becomes stagnant at around 94 seconds (the coastdown period on the graph) after the flywheels are essentially stopped and this causes the temperatures to peak. Temperatures drop again because the flow starts to increase—albeit in the opposite direction. This can be seen in the insert in Figure 7-14 showing what happens when the flow is stagnant. Changes in the direction of flow when the flow is close to being stagnant cause the temperatures to change rapidly, for example immediately after 100 seconds and during the period from 325 s to 375 s. An insert also shows results when the flow has stabilized to natural circulation due to the water coming from the pool.

The minimum CHFR on Figure 7-14 follows the expected behavior as the temperature of the fuel increases and decreases. Hence, it becomes very low (1.09) at 94 seconds at the start of the stagnant period and then again when the flow changes from downflow to upflow and natural circulation is calculated to begin. The minimum OFIR follows similar qualitative behavior and like the mCHFR, reaches its lowest value, 0.74, at the beginning of the stagnant period (at 90 seconds). These low values last a few seconds only.

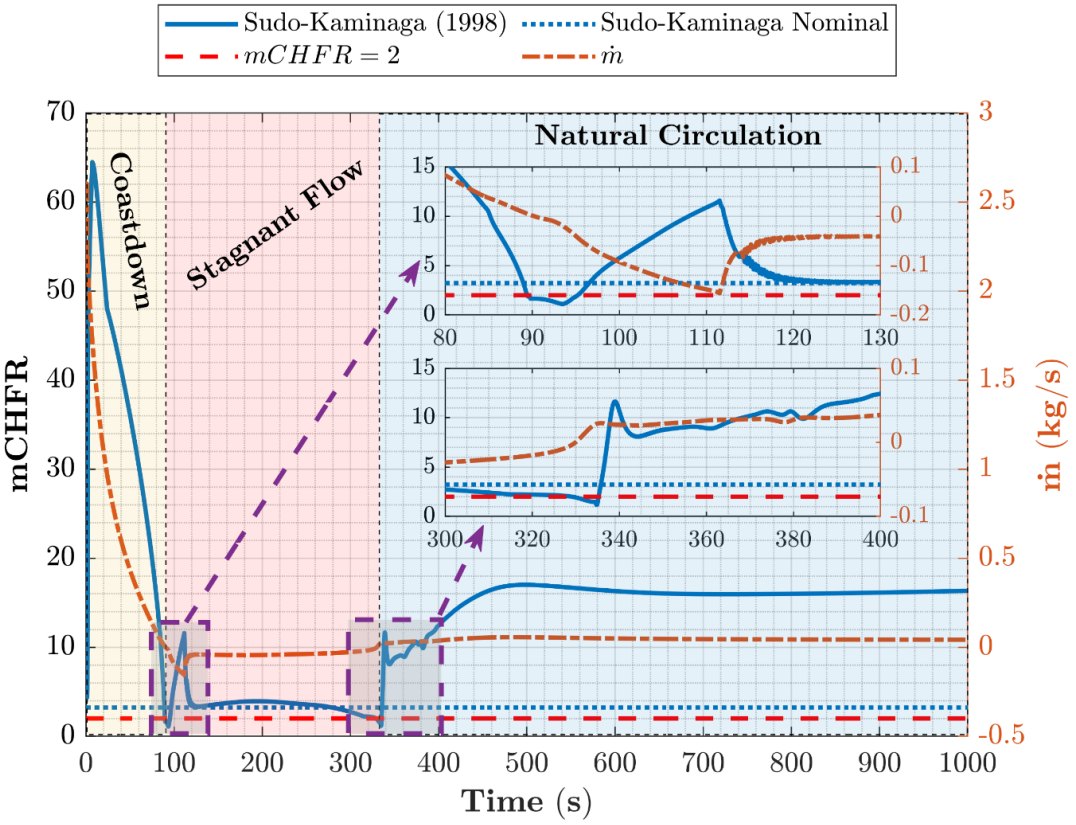



**Figure 7-14 Mass Flow Rate and Minimum CHFR During LOCA (78.5 cm$^2$ Break)**

A second LOCA was analyzed assuming a larger break with an area of 314 cm$^2$. Again, reactor trip occurs quickly due to a low-pressure signal and in turn the assumption is made that the primary pumps trip. The temperatures in the hot channel for this LOCA are shown in Figure 7-15. As usual, the hot channel is channel 63 in row B. In this LOCA the hottest temperatures are above the centerline. In this case the hottest temperatures are reached immediately after reactor trip at the start of the accident (1.6 s).

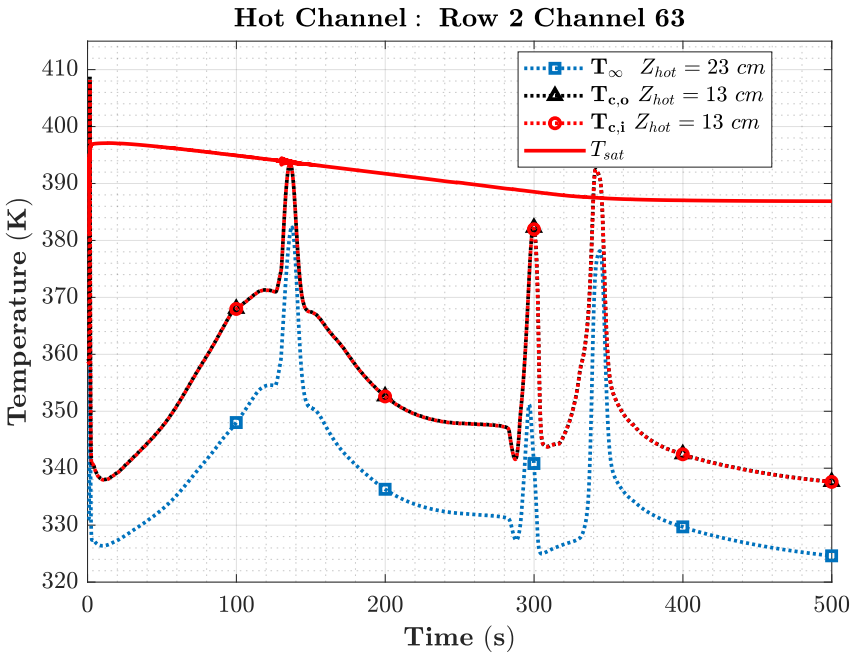



**Figure 7-15 Temperatures in Hot Channel During LOCA (314 cm$^2$ Break)**

The maximum clad temperature at 1.6 s is 409 K, again much less than the assumed safety limit. As with the smaller break, there are additional peaks in the clad and coolant temperatures due to the flow becoming stagnant as it switches direction. Although the bulk coolant temperature never exceeds the saturation temperature, that does not mean that nucleate boiling does not occur. The core flow (and minimum CHFR) are shown in Figure 7-16 where the inserts show the very low flow rates and changes in direction. For each of the peaks in temperature there is a corresponding decrease in the mCHFR as shown on the figure. The lowest value for mCHFR is 1.18 at 301 s. The mOFIR follows similar qualitative behavior and is lowest, 0.37, at 340 s.

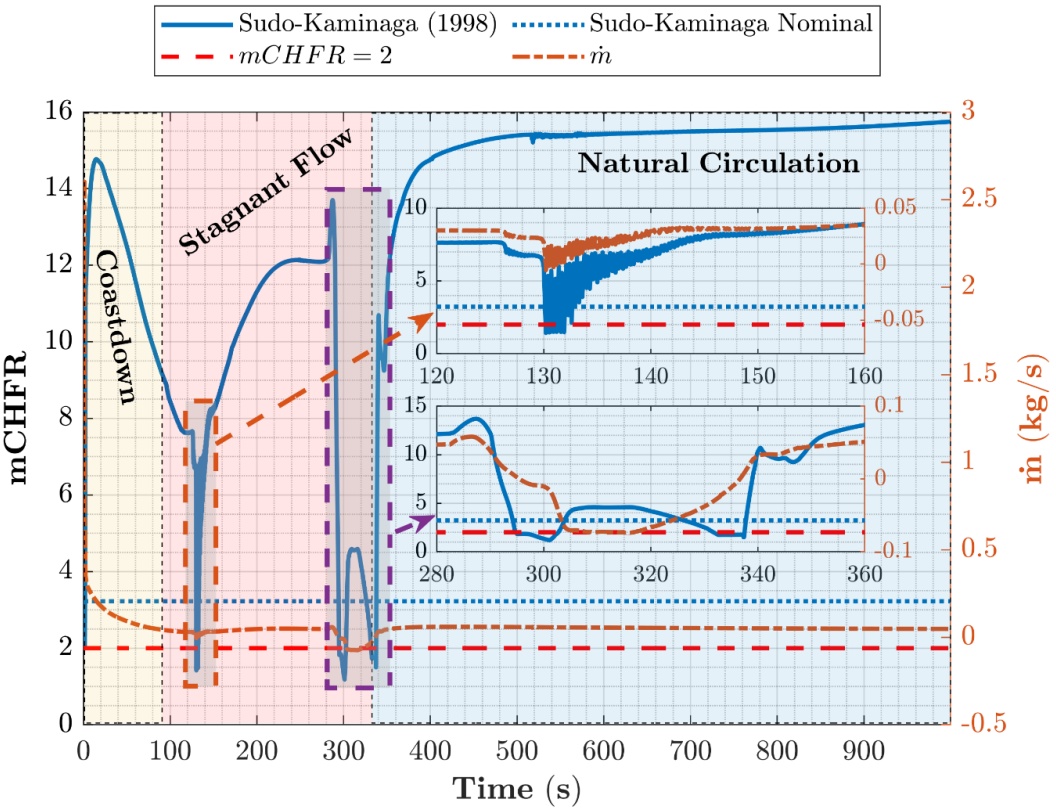



**Figure 7-16 Mass Flow Rate and Minimum CHFR During LOCA (314 cm$^2$ Break)**

## 7.8 Misloaded Fuel Assembly

Fuel assemblies are keyed so that they can only be placed with the plates aligned as shown in Figure 3-3. Strict adherence to procedures reduces the probability that any FA can be misloaded. However, to see what the consequences of such a misloading might be, it is assumed that the locations of two assemblies are interchanged. Figure 3-5 shows the normal loading. Taking into consideration the symmetry in the core leads to a need to consider 18 different situations with two fuel assemblies interchanged. Calculations are done for the entire fuel cycle with the misloading to see if the changes in power peaking might be excessive.

The misloaded fuel assemblies that lead to the largest (albeit small) increase in power peaking move the cycle 2 FA in column 3 row B to column 1 row B where it is between two other cycle 2 FAs in that column. The increase is because cycle 2 FAs are the most reactive. The fuel assembly relative powers for this case are shown in Figure 7-17, which shows small differences relative to the nominal situation shown in Figure 4-8. Indeed, the increase in local power density is less than one percent.

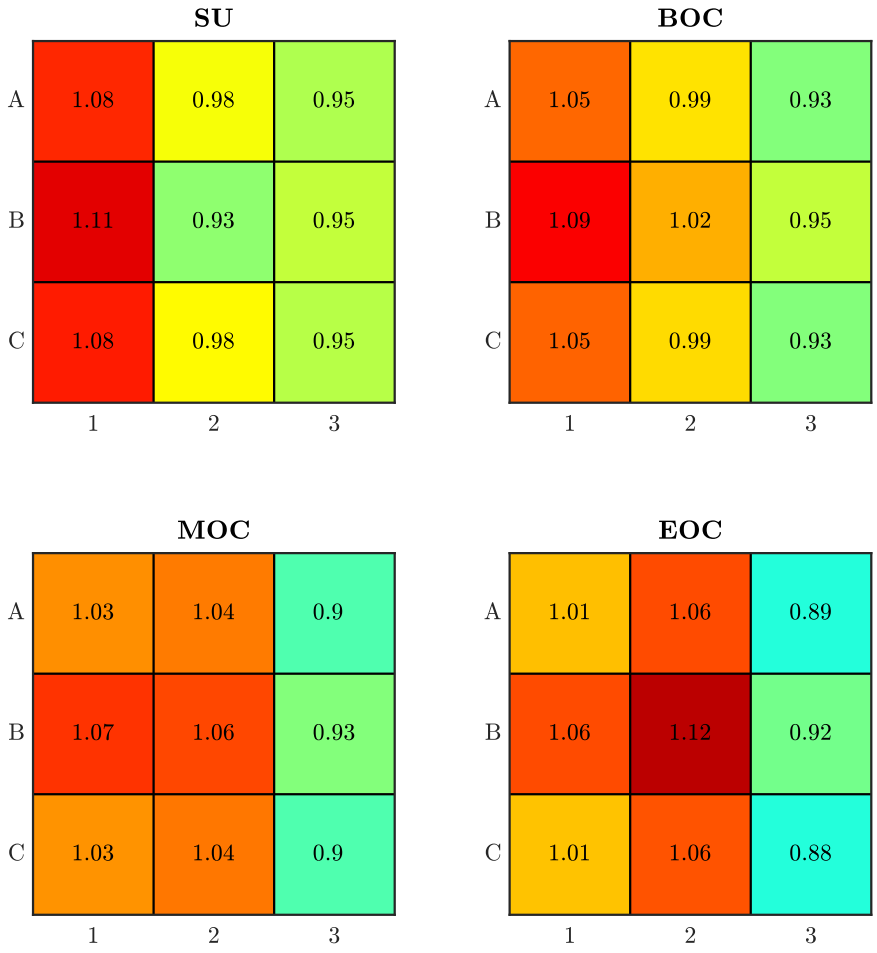



**Figure 7-17 Normalized Fuel Assembly Power with Misloaded Fuel Assembly**

## 7.9 References

[1] NIST, "Safety Analysis Report (SAR) for License Renewal for the National Institute of Standards and Technology Reactor - NBSR; NBSR 14," ed: National Institute of Standards and Technology (NIST). 2023.

[2] U.S. Nuclear Regulatory Commission, "TRACE V5.0 Theory Manual: Field Equations, Solution Methods, and Physical Models," U.S. Nuclear Regulatory Commission, 2020.

[3] *Decay Heat Power in Light-Water Reactors*, ANSI/ANS-5.1-1994 (R2023), A. N. Society, 2023.

[4] G. Braoudakis, "OPAL Nuclear Reactor: Reactor Specification," *International Nuclear Information System,* vol. 46, no. 20, February 1, 2015. [Online]. Available: http://inis.iaea.org/Search/search.aspx?orig_q=RN:46046717.

# 8 Cold and Thermal Neutron Beam Production

## 8.1 Cold and Thermal Neutrons

The unique properties of thermal and cold neutrons for scientific applications have been enumerated in Chapter 1. Thermal neutrons are typically characterized by a room-temperature Maxwellian energy distribution, while cold neutrons may be characterized by Maxwellians with lower effective temperatures, sometimes in the tens of Kelvin range. There are diverse definitions of what constitutes an upper energy limit for cold neutrons but an early definition, adopted by Webb [1], has cold neutrons having energies less than 0.005 eV or neutron wavelengths, $\lambda$, greater than about 4 Å. This definition is adopted herein since cold neutron instruments largely exploit neutrons with wavelengths greater than 4 Å. Note that published work associated with cold neutron production at the OPAL reactor [2] refers to cold neutron energies less than 10 meV ($\lambda$ > 2.9 Å), necessitating caution when comparing published cold neutron flux values between facilities. Hence, the latter definition would inflate brightness values.

In this chapter, the cold and thermal neutron delivery systems, beams, and guides are summarized. More details are available in references [3], [4], [5], and [6]. The scientific employment of these beams is discussed in Chapter 9, Neutron Science Facilities.

## 8.2 CNS Design and Performance

Production of cold neutrons requires a dedicated Cold Neutron Source (CNS) and the resulting cold neutron beams must have minimal epithermal and fast neutron contamination. The CNS usually comprises a localized region of cryogenically cooled moderator placed in or near the peak of the unperturbed thermal neutron flux in the moderator/reflector of a research reactor (or near the target/moderator of a pulsed neutron source). Its objective is to shift the thermal Maxwellian neutron flux distribution towards lower energies (lower temperatures), in this case, energies less than 0.005 eV.

Currently, the NNS pre-conceptual design has two identical cylindrical liquid deuterium ($LD_2$) sources with 30 cm diameters, although the possibility of having dissimilar CNSs, optimized for diverse instrument requirements is not excluded. A fixed-diameter CNS thimble may be employed with residual space surrounding a smaller-diameter CNS filled with a $D_2O$ reflector.

The CNS design will be simplified to achieve the highest operational reliability and stability. In the following, the parameters that impact cold neutron brightness and a comparison with the current beams at NCNR are given.

### 8.2.1 Liquid Deuterium CNS Cold Neutron Brightness

#### *8.2.1.1 Effect of CNS Location*

The cold neutron brightness was evaluated at the proposed neutron guide entrances (assumed 1.5 m distant from the CNS center). It was concluded that placing the CNS vertical axis at (*x*=45 cm, *y*=0 cm) with respect to the center of the core (see Figure 8-1 and reference [4]) offers a good compromise between cold neutron gain, lower fast neutron contamination of the beam, and lower heat load. This and the mirrored (-45, 0) location for the second CNS are the origins of the CNS vertical axes in the reactor core model.

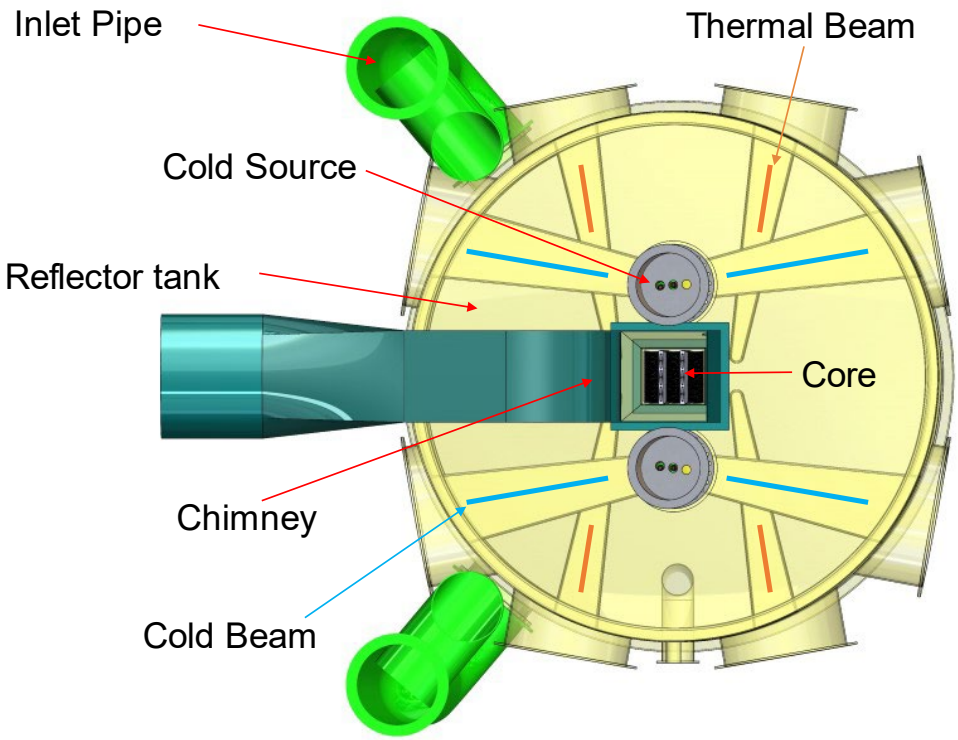



**Figure 8-1 Schematic Showing Access to the Two Cold Neutron Sources and Thermal Beam Tubes**

#### *8.2.1.2 CNS Brightness Gains with Respect to NBSR*

MCNP simulations of the CNS cold neutron brightness were compared with those for the NBSR Unit 2 ($LH_2$) and Unit 3 ($LD_2$) models [3], [4]. The brightness was evaluated along the beam direction within the solid angle range of acceptance of high-performance neutron guides [4]. The results are shown in Figure 8-2. Corresponding total and cold neutron spectrum integrals are summarized in Table 8-1, indicating cold neutron brightness gains of about 3.48 and 2.64 with respect to the present NBSR $LH_2$ Unit 2 and the future $LD_2$ Unit 3 CNS, respectively.

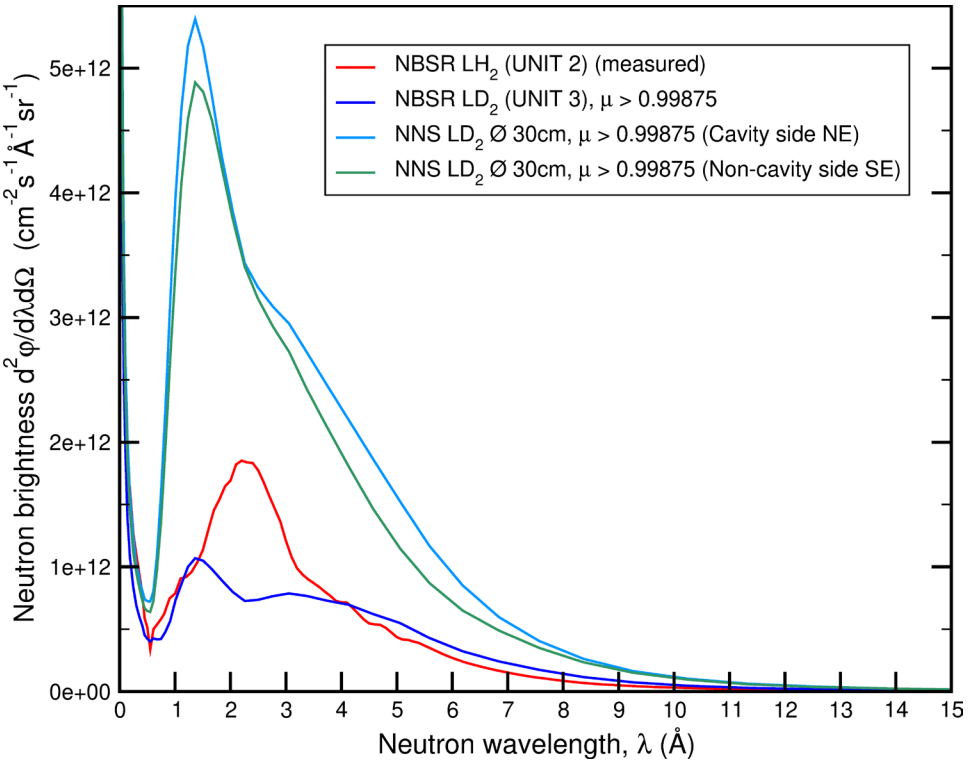



**Figure 8-2 Brightness Spectrum of the NBSR and NNS**

**Table 8-1 Integrals of Neutron Brightness in Figure 8-2 for All Wavelengths and for $\lambda \geq 4$ Å**

| Brightness Integrals for CNS ($cm^{-2}s^{-1}sr^{-1}$) ($m > 0.99875$ at guide entrance) | | | | | |
|---|---|---|---|---|---|
| **Wavelength Range (Å)** | **NBSR Unit 2 $LH_2$** | **NBSR Unit 3 $LD_2$** | **NNS $LD_2$ Cavity Side)** | **Ratio NNS/NBSR Unit 2 $LH_2$** | **Ratio NNS/NBSR Unit 3 $LD_2$** |
| 0→60 | $6.99\times10^{12}$ | $5.65\times10^{12}$ | $1.81\times10^{13}$ | 2.59 | 3.20 |
| 4→60 | $1.44\times10^{12}$ | $1.90\times10^{12}$ | $5.01\times10^{12}$ | 3.48 | 2.64 |

The simulated brightness gains in Table 8-1 (for equivalent 20 MW operating power) are better understood from an examination of the core thermal flux distributions (Figure 8-3). The compact core of the NNS produces a peak thermal neutron flux in the reflector outside of the fuel region, whereas the NBSR thermal flux peaks at the center of the fuel which is inaccessible to thermal beam and cold neutron source thimbles. The thermal flux distribution of the NNS alone allows the thimbles to be placed much more optimally in the thermal flux peak. The NNS core will produce a minimum peak unperturbed thermal neutron flux in the reflector of about $5\times10^{14}$ $cm^{-2}s^{-1}$ at 20 MW. For the NBSR the beam thimbles are located at a radius where the unperturbed thermal neutron flux has fallen to about $2\times10^{14}$ $cm^{-2}s^{-1}$ at 20 MW power.

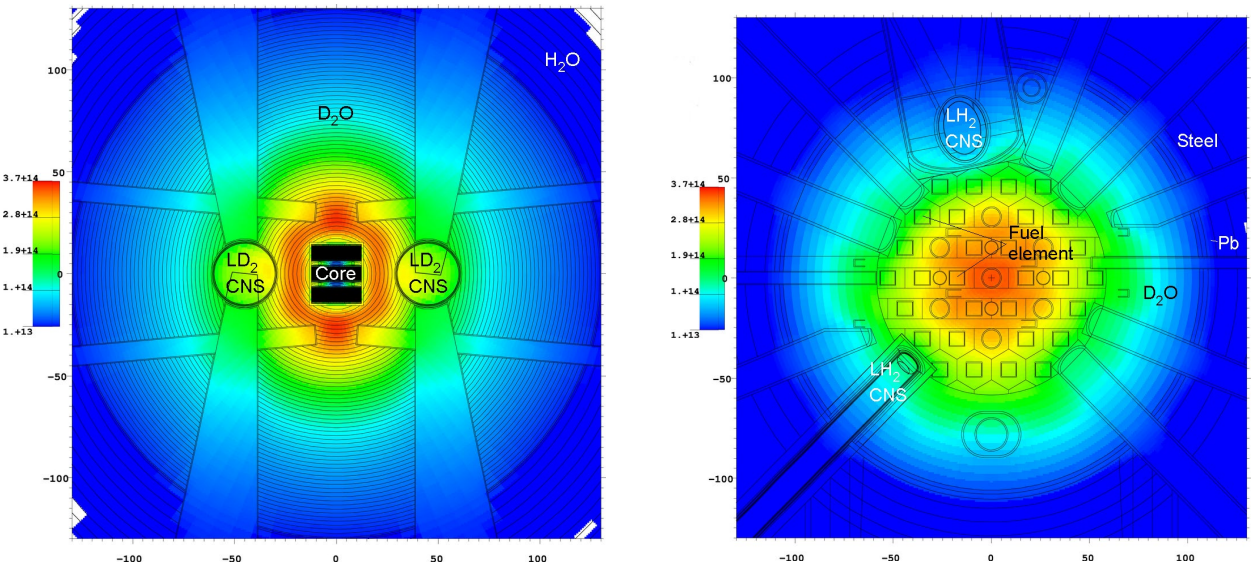



**Figure 8-3 Comparison of the Core Thermal Flux Distributions of the NBSR and NNS**

Because of the current uncertain instrument configuration, a figure-of-merit for the potential cold neutron gain at the instruments is the total cold neutron currents within a usable divergence range at the combined guide *entrances*. The rationale is fully described in reference [4]. Thus, the figure-of-merit is the ratio of these total currents for the NNS compared with the NBSR. The currents were evaluated for the 12 NBSR guide entrances for both the Unit 2 and Unit 3 cold neutron sources and for the NNS configuration of 16 equal area guide entrances placed 1.5 m from the CNS center. The NNS results (for 6 cm × 15 cm guide entrances) with respect to the NBSR Unit 2 and Unit 3 CNS are summarized in Table 8-2 and Table 8-4, respectively. The corresponding values for 6 cm × 20 cm NNS cold neutron guide entrances are given in Table 8-3 and Table 8-5, respectively.

**Table 8-2 Transmittable Neutron Currents Entering the Cold Neutron Guide Networks for the NBSR Unit 2 CNS ($LH_2$) versus the NNS CNS with 6 cm × 15 cm Guide Entrances**

| Cold Source | $J_{tot}$ (all λ) ($s^{-1}$) | $J_{tot}$ (cold neutrons λ ≥ 0.4 nm) ($s^{-1}$) |
|---|---|---|
| NBSR $LH_2$ Unit 2 (all cold guides) | $3.0\times10^{13}$ | $6.3\times10^{12}$ |
| NNS (6 cm × 15 cm) (16 equivalent guide entrances) | $2.3\times10^{14}$ | $5.8\times10^{13}$ |
| Gain NNS/NBSR Unit 2 | 7.5 | 9.2 |

**Table 8-3 Transmittable Neutron Currents Entering the Cold Neutron Guide Networks for the NBSR Unit 2 CNS ($LH_2$) versus the NNS CNS with 6 cm × 20 cm Guide Entrances**

| Cold Source | $J_{tot}$ (all λ) ($s^{-1}$) | $J_{tot}$ (cold neutrons λ ≥ 0.4 nm) ($s^{-1}$) |
|---|---|---|
| NBSR $LH_2$ Unit 2 (all cold guides) | $3.0\times10^{13}$ | $6.3\times10^{12}$ |
| NNS (6 cm × 20 cm) (16 equivalent guide entrances) | $2.8\times10^{14}$ | $7.0\times10^{13}$ |
| Gain NNS/NBSR Unit 2 | 9.1 | 11.1 |

**Table 8-4 Transmittable Neutron Currents Entering the Cold Neutron Guide Networks for the NBSR Unit 3 CNS ($LD_2$) versus the NNS CNS with 6 cm × 15 cm Guide Entrances**

| Cold Source | $J_{tot}$ (all λ) ($s^{-1}$) | $J_{tot}$ (cold neutrons λ ≥ 0.4 nm) ($s^{-1}$) |
|---|---|---|
| NBSR $LD_2$ Unit 3 (all cold guides) | $4.0\times10^{13}$ | $1.4\times10^{13}$ |
| NNS (6 cm × 15 cm) (16 equivalent guide entrances) | $2.3\times10^{14}$ | $5.8\times10^{13}$ |
| Gain NNS/NBSR Unit 3 | 5.7 | 4.2 |

**Table 8-5 Transmittable Neutron Currents Entering the Cold Neutron Guide Networks for the NBSR Unit 3 CNS ($LD_2$) versus the NNS CNS with 6 cm × 20 cm Guide Entrances**

| Cold Source | $J_{tot}$ (all λ) ($s^{-1}$) | $J_{tot}$ (cold neutrons λ ≥ 0.4 nm) ($s^{-1}$) |
|---|---|---|
| NBSR $LD_2$ Unit 3 (all cold guides) | $4.0\times10^{13}$ | $1.4\times10^{13}$ |
| NNS (6 cm × 20 cm) (16 equivalent guide entrances) | $2.8\times10^{14}$ | $7.0\times10^{13}$ |
| Gain NNS/NBSR Unit 3 | 7.0 | 5.2 |

Overall, the gains in usable cold neutron current are about a factor 10 with respect to the existing Unit 2 CNS and about 5 with respect to the future Unit 3 CNS. Potentially higher gains are possible with larger CNS diameters (Section 8.2.1.3)

*8.2.1.3 Effect of CNS Diameter on CNS Brightness*

MCNP simulations [4] indicate that moderate increases in the NNS $LD_2$ vessel diameter at the same axial position may lead to enhanced cold neutron brightness for wavelengths greater than about 3 Å, but with diminishing returns as the diameter approaches 40 cm. The results for several CNS diameters are compared with the NBSR Unit 2 and Unit 3 CNS in Figure 8-4. The

corresponding brightness ratios are shown in Figure 8-5 and Figure 8-6, respectively. Note that increasing the vessel diameter without reducing the height is at the expense of increased CNS heat load and $LD_2$ inventory, so the CNS neutronic performance gain will be weighed against such disadvantages as the design evolves.

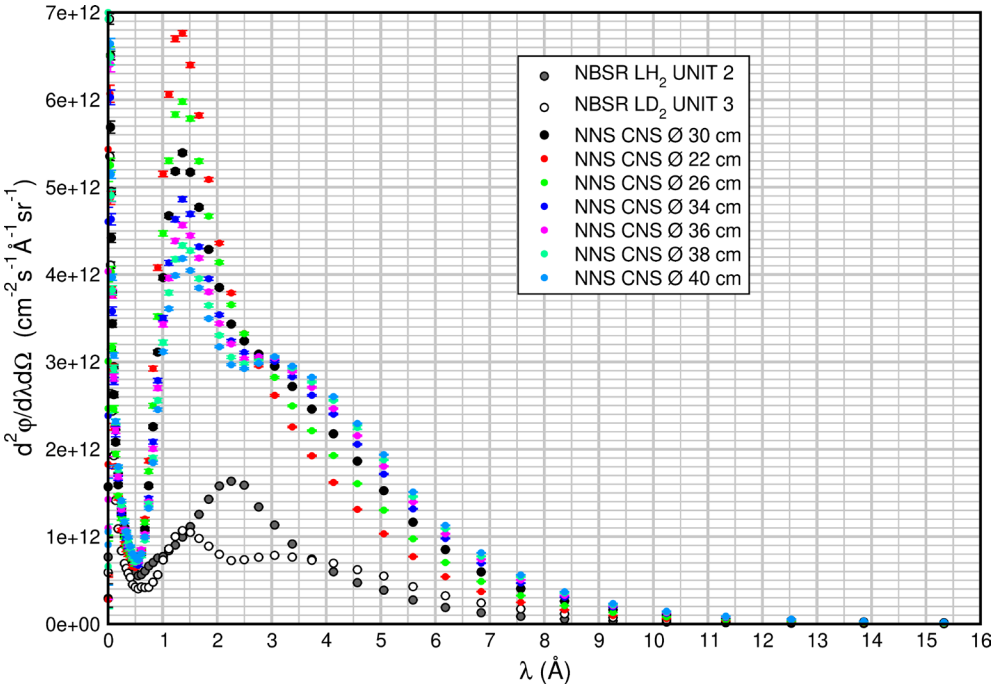



**Figure 8-4 Brightness for the NNS with Various $LD_2$ Vessel Diameters and for the NBSR $LD_2$ Unit 3 CNS**

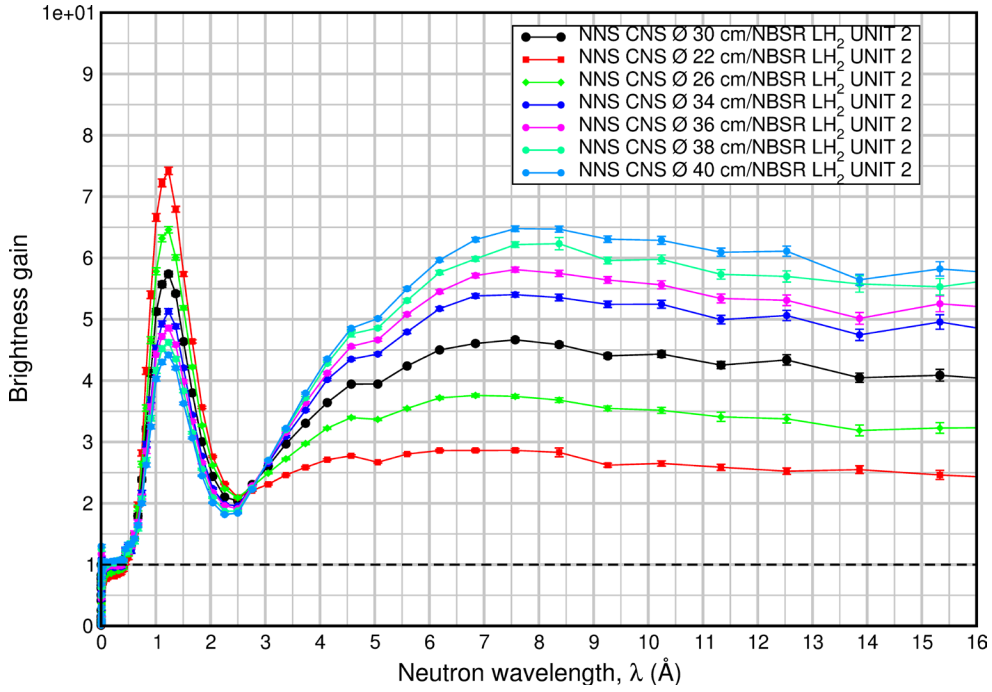



**Figure 8-5 Brightness Ratios with Respect to the Present NBSR $LH_2$ Unit 2 CNS for Different NNS $LD_2$ Vessel Diameters**

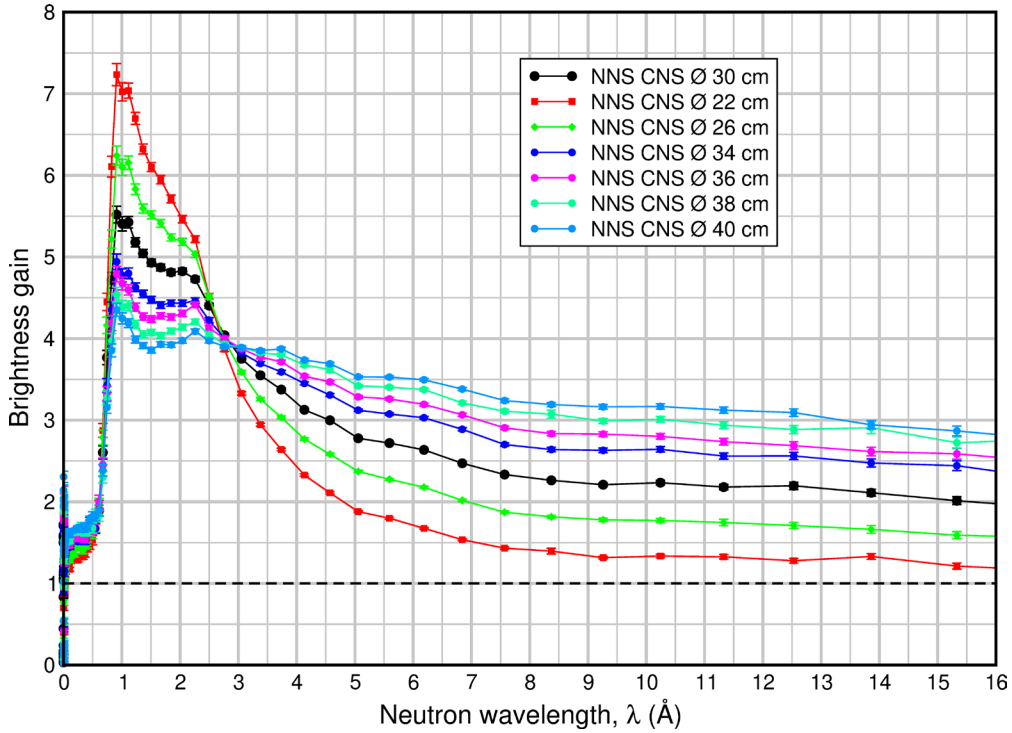



**Figure 8-6 Brightness Ratios with Respect to the Future NBSR $LD_2$ Unit 3 CNS for Different CNS $LD_2$ Vessel Diameters**

*8.2.1.4 Influence of a CNS Cavity (Re-Entrant Hole) on the CNS brightness in the beam direction*

The introduction of a cavity (non-cryogen-filled space) into the CNS volume may enhance the cold neutron flux in the beam direction [4]. In the OPAL CNS design, this was accomplished by placing a He-filled displacer inside the $LD_2$ vessel. The NNS MCNP CNS model with the cavity is illustrated in plan view through the center of the CNS in Figure 8-7.

The present model gives the wavelength-dependent cold neutron gains (ratio of light blue to dark green curves in Figure 8-2) shown in Figure 8-8. Further optimization of the cavity arrangement of the NNS CNS, including introducing a more symmetrical, shallower, or reshaped dual-cavity arrangement will be explored following the pre-conceptual design phase, with consideration of the heat load and engineering implications.

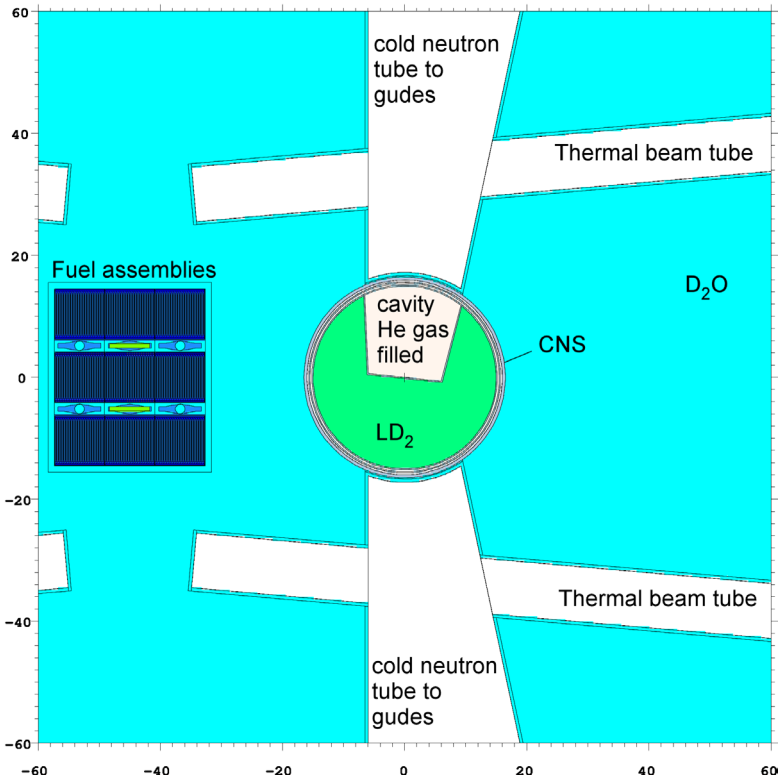



**Figure 8-7 Planar View of the CNS with One Cavity**

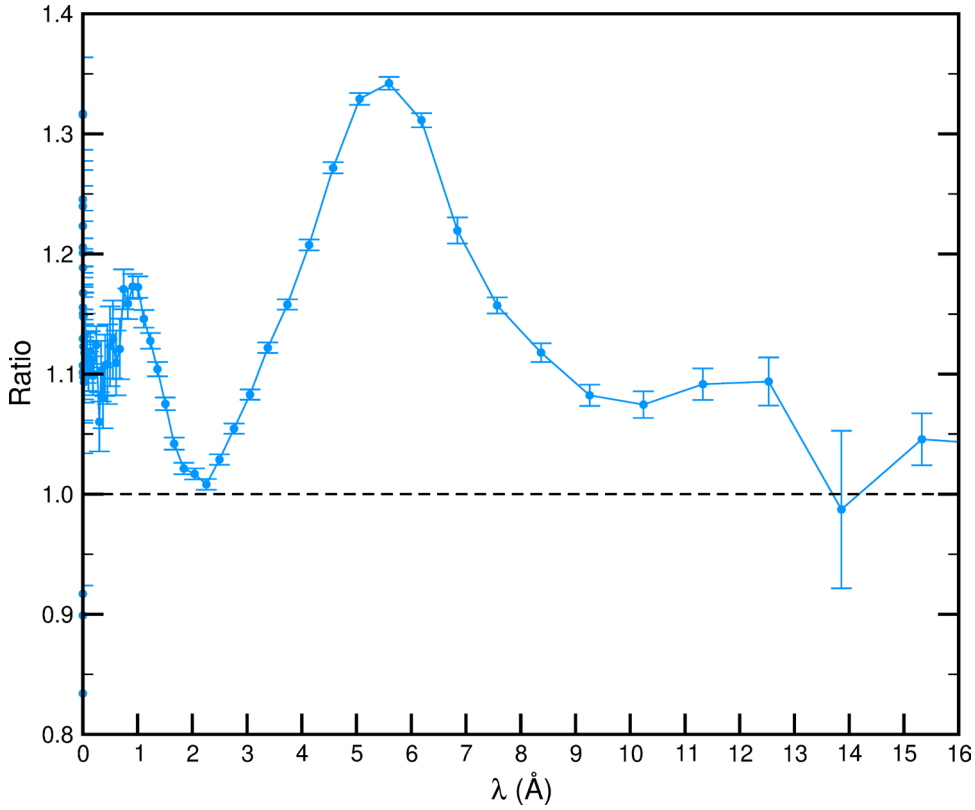



**Figure 8-8 Neutron Brightness Gain at the Cavity Side with Respect to the Non-Cavity Side of the CNS**

### 8.2.2 CNS Size and Neutron Guide Illumination

Irrespective of the size and type of cold moderator needed to obtain high cold neutron spectral gains, the CNS cross-sectional area also determines the neutron guide illumination, as illustrated schematically in Figure 8-9 for an ideal, long, straight neutron guide. “Long” in this context is for wavelengths satisfying $W/L < \vartheta_c$ (defined in the figure).

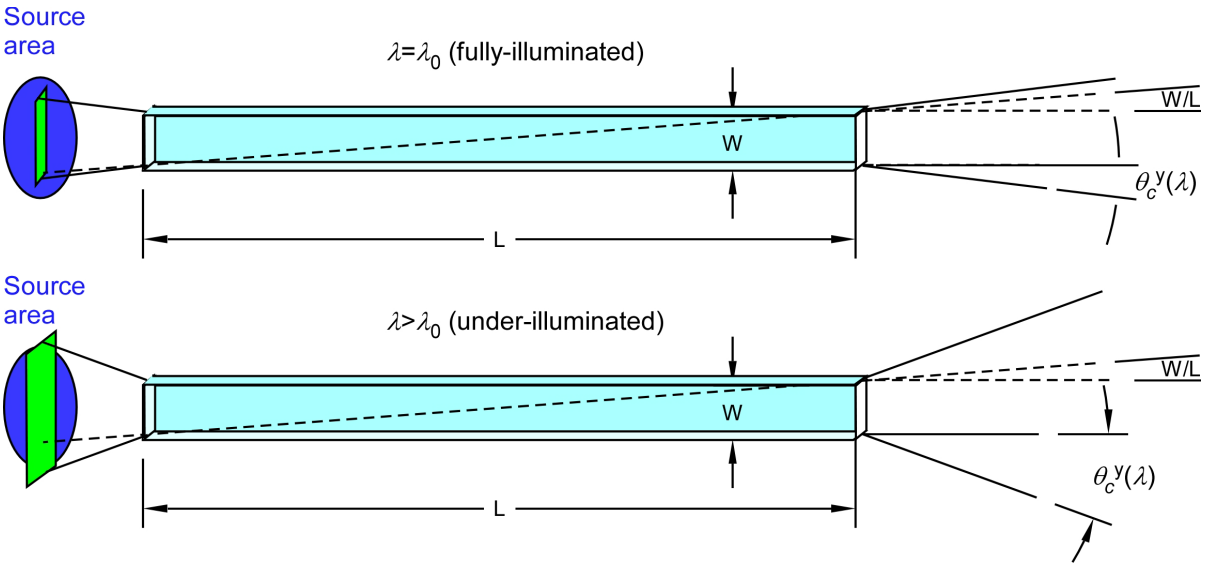



**Figure 8-9 Schematic of Full-Illumination (top) and Under-Illumination (bottom) of an ideal, Long, Straight Neutron Guide**

Figure 8-10 illustrates illumination by plotting the origins of successfully transmitted neutrons projected onto the source cross-section. The figure shows, for several neutron wavelengths, the neutron origins projected onto the cross-section of a vertical CNS $LD_2$ vessel cylinder of diameter 297 mm and height 305 mm for the challenging example of a tall, high-*m* guide (guide #4 of group 3 in reference [6]). Full details can be found in reference [4]. The results show full illumination up to about $\lambda$ = 0.8 nm. Therefore, the model CNS height is likely ample even for taller, high-*m* guides, and further increasing the vessel diameter serves only to increase the cold neutron brightness (see Section 8.2.1.3). Tall guides are favorable for extracting multiple beams from multiple levels or when a large initial beam height can be focused onto the sample.

### *8.2.2.1 Optimization of CNS Height*

The CNS height should be reasonably minimized for several reasons, including reduction of $LD_2$ inventory and the CNS heat load. Consequently, it will be no taller than necessary to produce optimal or near-optimal neutron transmission. This is further emphasized by the diminishing returns from the top and bottom of the CNS. The top and bottom of the source tend to contribute more divergent neutrons that are usually less useful at the instruments, incur increased transmission losses, or cannot reach the sample and cause an unwanted background. Furthermore, the vertical cold neutron flux profile at the CNS usually offers reduced brightness at the top and bottom than at the center.

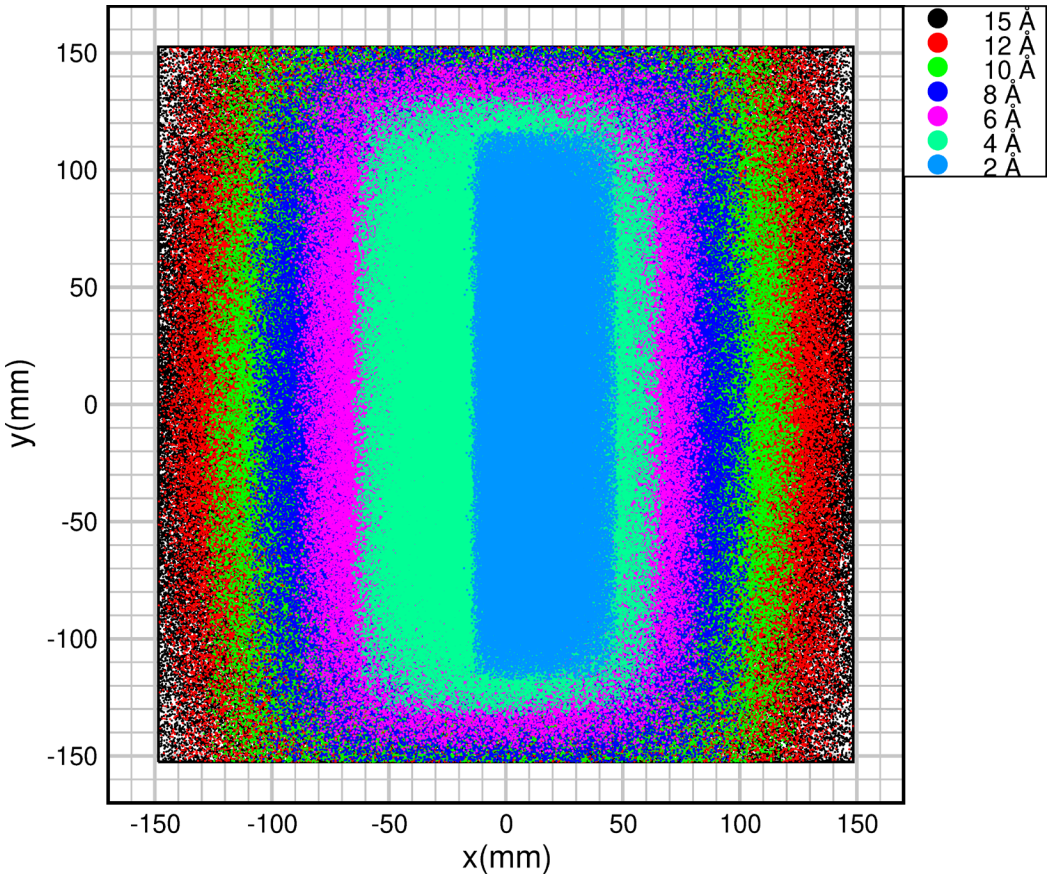



**Figure 8-10 Contributing Regions of a Rectangular Cross-Section Source**

### 8.2.3 $LD_2$ CNS Diameter and Nuclear Heat Load

A practical constraint on the volume of the CNS (other than deuterium inventory) remains the ability to remove sufficient heat from the CNS cryogenic circuit. This has been studied with MCNP simulations and details can be found in reference [4].

The results are summarized in Table 8-6 and Figure 8-11. The non-nuclear component of the heat load (thermal radiation and heat introduced by conduction and convection) was not estimated here but based on results for the OPAL CNS [7] would likely add about 10% to the totals shown in Table 8-6 (about 400 W for OPAL). The aluminum-6061 thickness for each model is assumed unchanged from the 30 cm model values.

It is observed that the increase in nuclear heat load (and of the heating due to individual radiation components) increases approximately quadratically with the CNS vessel diameter. This is illustrated in Figure 8-11. If the CNS diameter were increased to about 35 cm or 36 cm to gain cold neutron brightness (Figure 8-5), the nuclear heat load per CNS would increase to about 6.5 kW, requiring at least about 15 kW total cooling capacity.

**Table 8-6 Heating Contributions from Radiation Components and Total Minimum Cryogenic Heat Loads**

| Component | Total Nuclear Heating (W) as a Function of CNS Diameter | | | | | | |
|---|---|---|---|---|---|---|---|
| | 22 cm | 26 cm | 30 cm | 34 cm | 36 cm | 38 cm | 40 cm |
| Gamma | 1347 | 1782 | 2220 | 2857 | 3175 | 3512 | 3873 |
| Saturation $^{28}$Al beta | 1142 | 1439 | 1710 | 2084 | 2252 | 2423 | 25916 |
| Neutron | 219 | 358 | 583 | 885 | 1091 | 1340 | 1630 |
| TOTAL | 2708 | 3580 | 4513 | 5826 | 6518 | 7275 | 8093 |

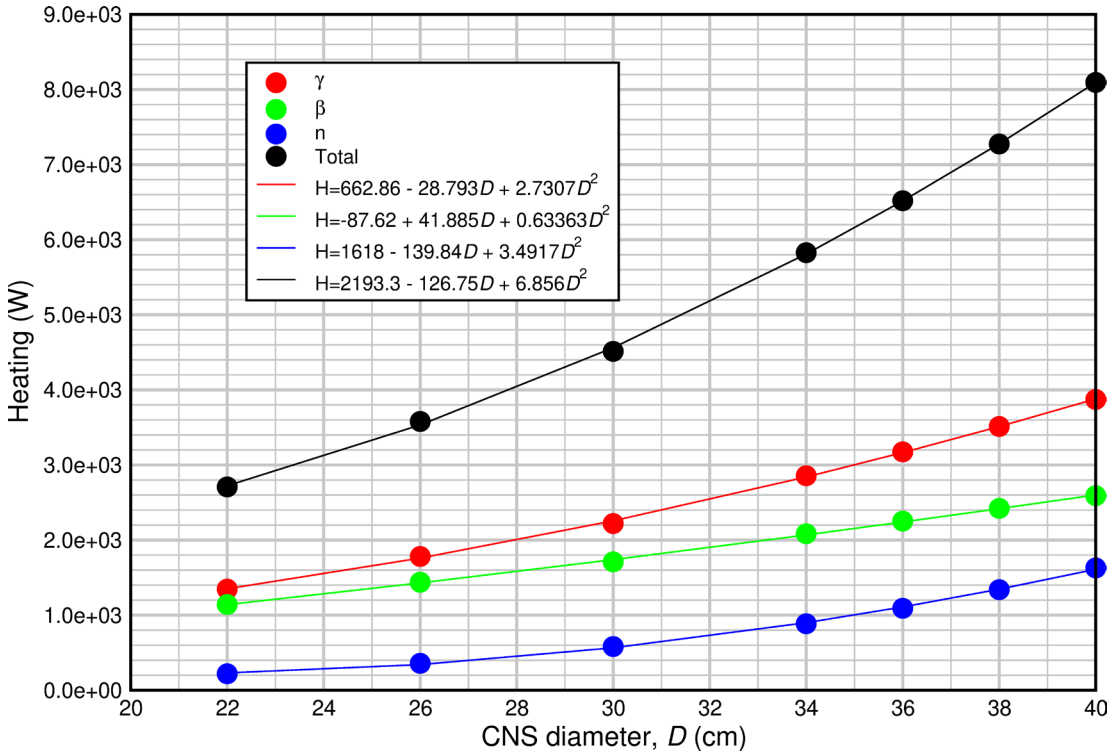



**Figure 8-11 Cryogenic System Radiation Heat Load as a Function of CNS Vessel Diameter**

## 8.3 Nuclear Heating of Al-Substrate Cold Neutron In-Pile Guides

An estimate of nuclear heating in Al-substrate in-pile cold neutron guides has been obtained for guides with entrances 1.5 m from the center of the CNS (see also reference [4]). The result, shown in Figure 8-12, includes heating from gamma rays, neutrons, and saturation-level $^{28}$Al beta particles produced following neutron absorption in the Al substrate, without a non-nuclear component. A very conservative absolute upper-temperature estimate, assuming heat loss only by radiation from the "exposed" surfaces to a sink temperature of 25°C, yields an estimated maximum temperature of 232°C for an emissivity ($\varepsilon$) equal to 0.1. For $\varepsilon$ = 0.2, the maximum estimated temperature reduces to 164°C. The former is close to the upper limit of stability of

reactively sputtered Ni-Ti supermirror layers and well above what is tolerable if not reactively sputtered. However, the highly conducting aluminum-6061 substrate and the addition of forced convection cooling from a helium flow lead to guide temperatures that should be well within tolerable ranges.

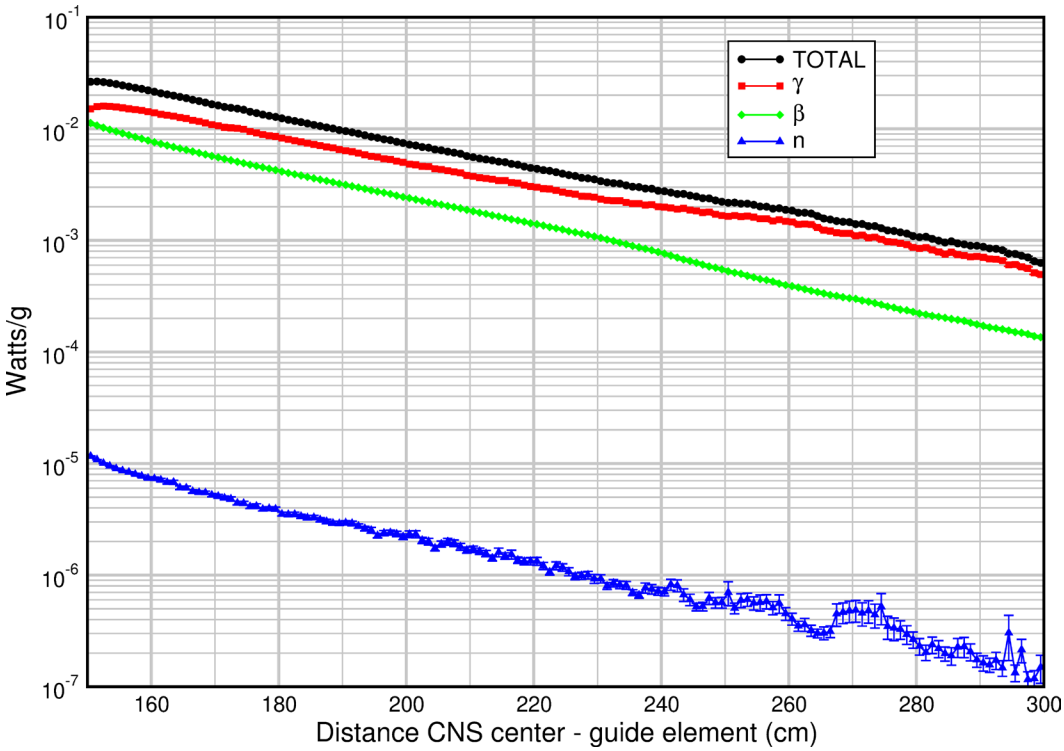



**Figure 8-12 Nuclear Heating for Al-Substrate In-Pile Cold Neutron Guides**

## 8.4 Thermal Beams

### 8.4.1 Thermal Spectral Brightness at Thermal Guide Entrance and Dependence on Tube Position

Preliminary investigations of the thermal neutron brightness along a thermal beam tube with a large enough cross-section to accommodate a 6 cm × 20 cm internal dimension thermal neutron beam have been carried out [4]. The thermal beam tube concept is shown in Figure 8-13. The thermal beam tubes are canted 5° to the fuel surface to view the thermal flux peak region of the reflector while avoiding a direct view of the fuel, thus significantly reducing the fast neutron and gamma contamination of the beam. However, the 5° angle facilitates thermal neutron instrument placement outside the reactor shielding (outer green layer in Figure 8-13).

The brightness results (with fitted Maxwellian functions to the thermalized part of the spectrum - solid curves) are compared with simulations for the NBSR thermal beam tube BT6 in Figure 8-14. The fitted effective temperature of 317 K for the NNS indicates that the contributing spectrum is well-thermalized. The results indicate a thermal brightness increase by

at least about a factor of two at equivalent (20 MW) reactor power. The position of the thermal tubes with respect to the fuel shown in Figure 8-13 appears close to the optimum location. Nonetheless, refinement of the position and thimble positioning will be performed as the core design evolves.

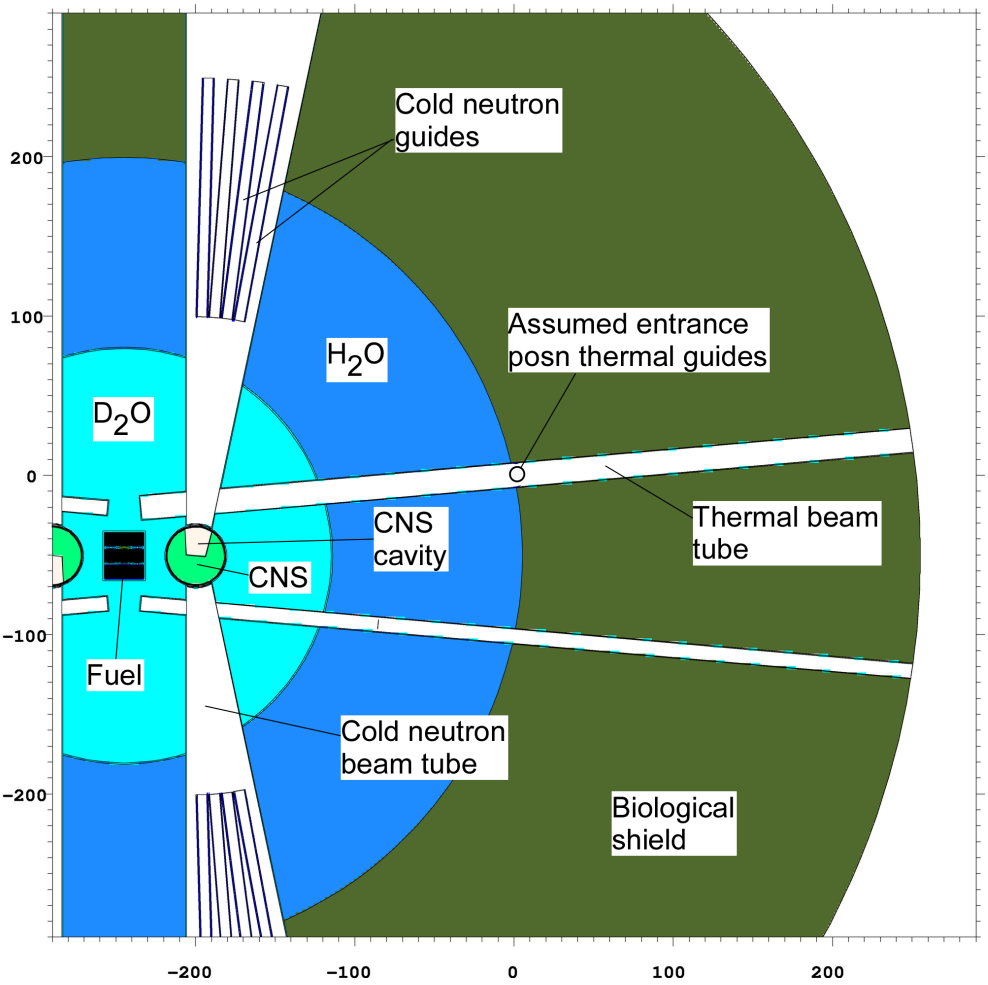



**Figure 8-13 Plan View Showing Placement of Thermal Beam Tubes**

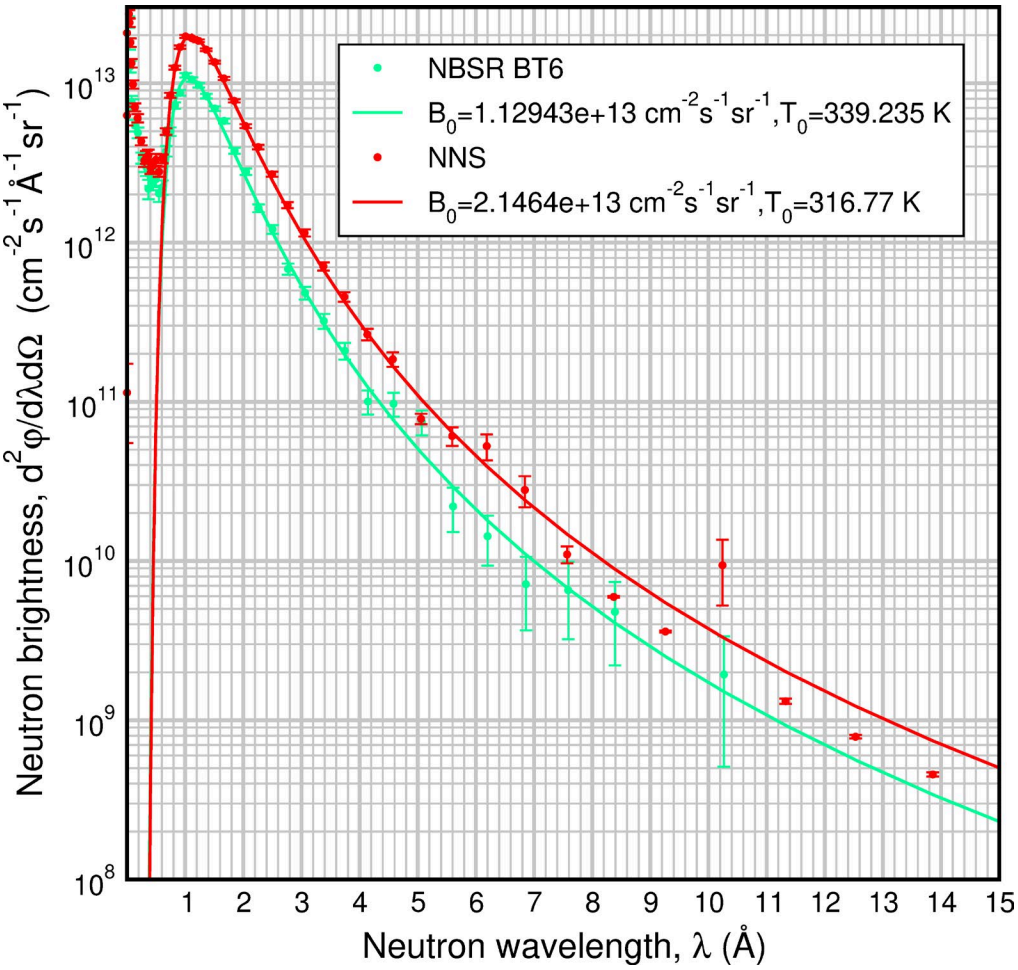



**Figure 8-14 Thermal Neutron Brightness vs Neutron Wavelength for NNS and NBSR BT6 at the Shield Exit**

### 8.4.2 Performance of Thermal Neutron Guides

Thermal neutron guides may facilitate instrument layout by enabling some to be placed further from the biological shield in lower background radiation with less penalty for the increased distance, particularly those instruments using longer wavelengths of the thermal range. To be effective, thermal neutron guides usually have high-*m* supermirror coatings to compensate for lower critical angles of shorter wavelength thermal neutrons. Furthermore, thermal neutron instruments sometimes use large beams. If the guide cross-section is large, thermal neutron guides likely only benefit instruments far from the source since the fraction of neutrons reflected from the guide surfaces is low for short guides of simple design.

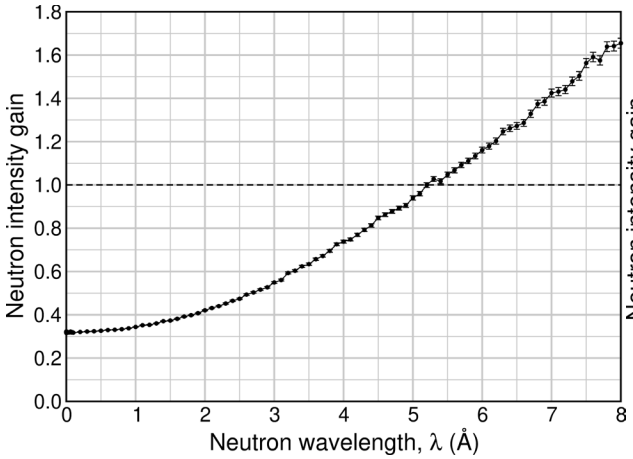
The following example illustrates their potential usefulness: The mean neutron flux is simulated on a 6 cm (w) × 20 cm (h) target area either:

(a) Through an empty 15 cm (w) × 25 cm (h) cross-section biological shield penetration

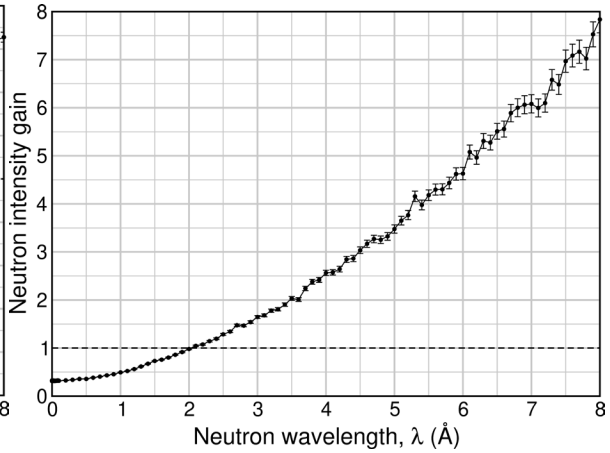
or

(b) With an intervening 6 cm (w) × 20 cm (h) thermal neutron guide (all $m$ = 4) whose entrance starts at the entrance to the biological shield (see Figure 8-13).

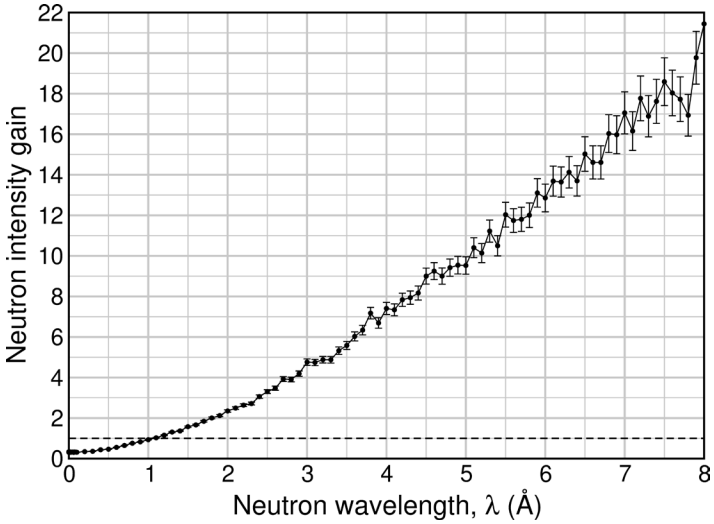
Simulations of the effectiveness of the thermal neutron guide with respect to an empty 15 cm (w) × 25 cm (h) biological shield penetration [4] are shown in Figure 8-15, comparing ratios of neutron flux as a function of wavelength on the 6 cm (w) × 20 cm (h) "sample" placed a distance $z$=0 m, 4 m, and 10 m from the exit of the (2.5 m thick) biological shield. These positions correspond to the guide exit positions for cases (b). In this example, the results show a threshold wavelength for net flux gains on-sample with a thermal neutron guide which reduces as the sample position moves away from the reactor ($\lambda \geq 5.25$ Å for $z$ = 0 m, $\lambda \geq 2$ Å for $z$ = 4 m, and $\lambda \geq 1$ Å for $z$ = 10 m). Increasingly large gains at a given wavelength above the threshold are obtained as $z$ increases. Thermal guides may not be able to compensate for intensity gains from placing instruments closer to the source (as the flux tends to vary as $1/z^2$). Indeed, for instruments close to the biological shield there appears to be no use for thermal neutron guides. However, in this example, for $z$ greater than about 8 m they provide useful gains for instruments using greater than 1.5 Å neutrons (with respect to the equivalent positions with no guide).




a) Sample Position at zero meters




b) Sample Position at 4 meters




c) Sample Position at 10 meters

**Figure 8-15 Flux Gains Using a Thermal Neutron Guide Over an Empty Penetration Through the Biological Shield**

## 8.5 References

[1] F. J. Webb, "Cold Neutron Sources," *Journal of Nuclear Energy. Parts A/B. Reactor Science and Technology,* vol. 17, no. 4, pp. 187-215, 1963-07-01 1963, doi: 10.1016/0368-3230(63)90021-1.

[2] N. Masriera *et al.*, "Development of the RRR Cold Neutron Source Facility," in *9th Meeting of the International Group on Research Reactors*, March, 2003, Sydney Australia.

[3] J. C. Cook *et al.*, "Neutron Delivery Systems Design of the Proposed NIST Neutron Source," in *2022 ANS Winter Meeting and Technology Expo*, November 13-17, 2022, Phoenix, AZ: American Nuclear Society, pp. 1020-1022, doi: doi.org/10.13182/T127-39643.

[4] J. C. Cook, C. F. Majkrzak, and H. E. King, "Pre-conceptual Design Activities of the NIST Neutron Source - Simulations of Neutron Beam Characteristics of the Proposed NIST Neutron Source," National Institute of Standards and Technology, Gaithersburg, MD, NIST TN 2284, February 2024, https://doi.org/10.6028/NIST.TN.2284.

[5] J. C. Cook *et al.*, "Proposed NIST Neutron Source User Facility," in *2022 ANS Winter Meeting and Technology Expo*, November 13-17, 2022 2022, Phoenix, AZ: American Nuclear Society, pp. 608-611, doi: doi.org/10.13182/T127-39654.

[6] J. C. Cook, H. E. King, C. F. Majkrzak, and D. A. Neumann, "Pre-conceptual Design Activities of the NIST Neutron Source: Preliminary Layout of Cold and Thermal Neutron Instruments," National Institute of Standards and Technology, Gaithersburg, MD, NIST TN 2280, February 2024, https://doi.org/10.6028/NIST.TN.2280.

[7] W. Lu and R. Thiering, "The OPAL Cold Neutron Source Heat Load Measurements," in *12th meeting of the International Group On Research Reactors*, October, 2009, Beijing, China.

# 9 Neutron Science Facilities

## 9.1 Introduction

The NNS will be tailored for neutron science using thermal and cold neutron beams. The reactor will provide thermal neutron beams and, with the use of two liquid deuterium ($LD_2$) cold sources, provide cold neutrons. At the initial startup (commissioning), the NNS will at least deliver the capabilities that exist with the NBSR as the neutron source. Once at full capacity, the facility should help alleviate the current over-subscription of scientific instruments through the combination of an increased number of instruments, incorporating two cold neutron sources possibly serving two guide halls, in addition to a substantial increase of the cold and thermal neutron source brightness. Additional capacity, (i.e., available neutron guide end positions) is desired to meet the ever-increasing demand from the scientific community for neutron measurement capabilities and to accommodate novel scientific instruments.

Experience gained from the operation of the NBSR as well as from other neutron sources throughout the world, confirms that the NNS's enhanced-brightness cold sources will revolutionize the impact of NCNR. Not only will NNS address the current oversubscription, but new science, not possible today, will emerge.

In this chapter, it is shown how existing neutron guide technology may be combined with today's cold neutron experiments. In addition, there is a discussion of how the thermal beam tubes will be used and how neutron activation analysis services could be accommodated.

## 9.2 Cold Neutron Beam Tube and Guide Network Layout

A preliminary layout for neutron guides and a broad suite of in-demand instruments has been been performed [1], [2]. The diverse range of instruments enhances the impact that the NNS will have. As design proceeds, groups of prospective users will be convened to optimize the instrument suite as well as the cold neutron sources and guides. A preliminary effort to obtain needs of the user community has already taken place [3] and results of that meeting will be incorporated in future design reports.

By having two major CNSs the number of cold neutron guides could be increased from 12 to at least 16 along with improvement in the usable acceptance solid angle [2]. This results in estimated transmittable cold neutron current gains at the guide entrances of 9.2 to 11.1 compared to what is currently available from the NBSR Unit 2 $LH_2$ cold source [4]. Further improvements are possible from optimization of the CNS positions and geometry (see Chapter 8). Additional gains for the instruments will be accomplished by customizing the neutron optics to transmit maximal beam flux within the area and divergence interval used by a particular instrument. This frequently has the advantage of increasing the instrument signal-to-noise ratio.

Figure 9-1 shows the region (in light blue) where the cold neutrons (CN) emanate from the cold neutron sources (dark blue dots). With 16 end-positions there will be four groups with four guides each from the two cold neutron sources. The red square represents the reactor core.

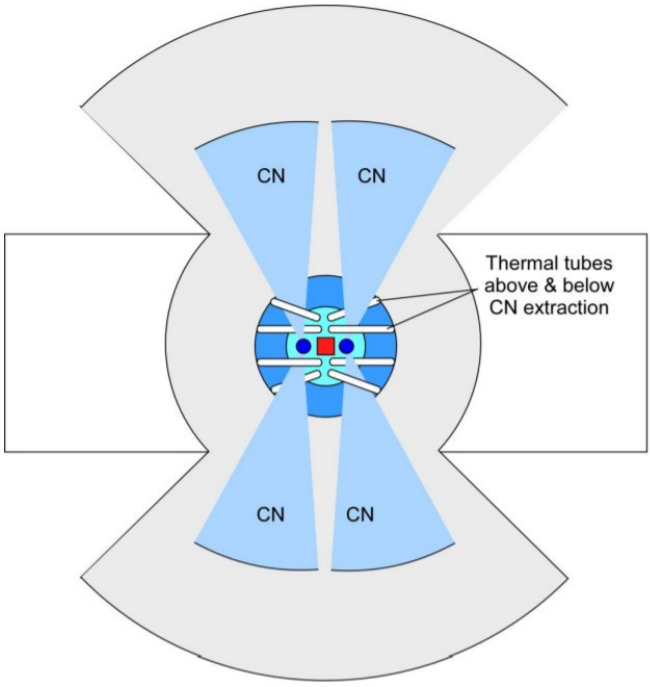



**Figure 9-1 Schematic Showing Access to the Two Cold Neutron Sources and Eight Thermal Beam Tubes [2]**

The instruments may be roughly classified as shown in Figure 9-2 for Groups 1 and 2 on the north side and Groups 3 and 4 on the south side. Definitions of the instruments in the figures are found in Table 9-1 and more details are in reference [2]. Additional end positions can be created with benders on guides whose end-position instruments do not require the full beam height (e.g., SANS instruments) and monochromatic positions may be created on the sides of the longer guides and on outer guides where the full beam height may not be required.

Reference [2] gives an indication of the assumed footprint for various instruments. If that footprint is “symmetrical,” that is, equal space is required on each side of the beam, then the next metric to consider is whether a significant range of scattering angle is required. This helps explain that the actual number of instruments will likely evolve as experiment placement is optimized. In Table 9-1 the experiments in the 16 end-position layouts are identified and some details on options for additional experiments are also given.

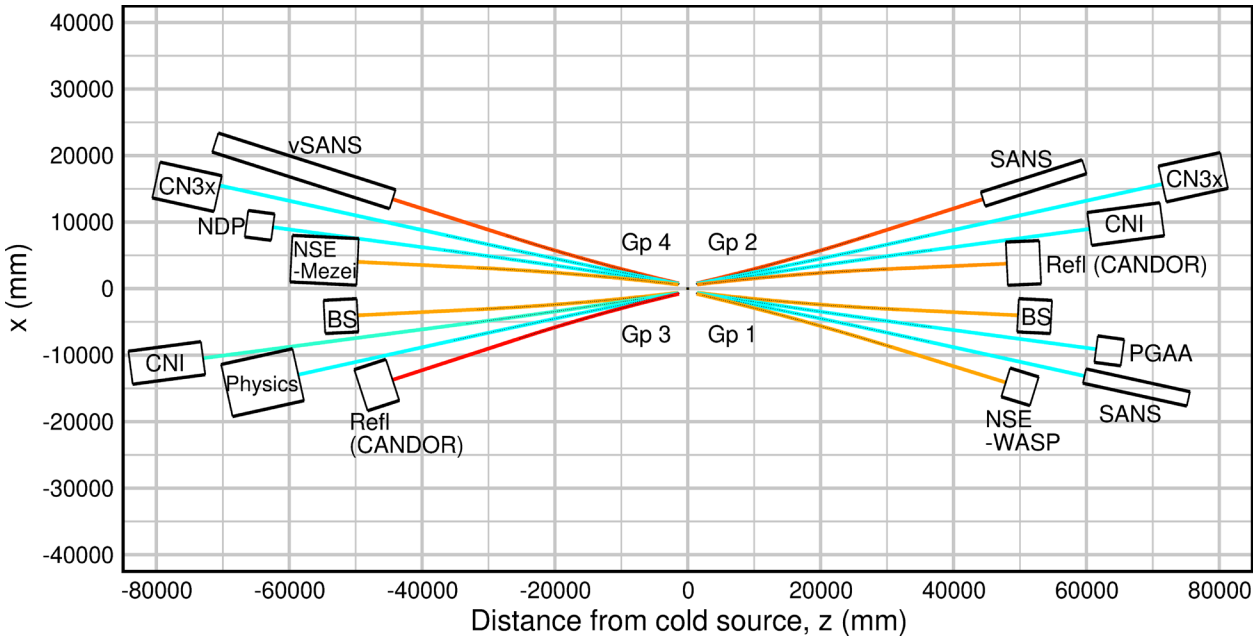



**Figure 9-2 Possible Instrument Layout for Groups 1-4 [2]**

**Table 9-1 Cold Instruments for Guide Halls**

| Instrument Type | Total Number | End Position |
|---|---|---|
| Small-Angle Neutron Scattering (SANS) | 3 | YES |
| Reflectometer (CANDOR type) | 2 | YES |
| Cold Neutron Imaging (CNI) | 2 | YES |
| Cold 3-Axis (CN3X) | 2 | YES |
| Backscattering (BS) | 2 | YES/NO? |
| Neutron Spin-Echo (NSE) (Mezei-type) | 1 | YES |
| Neutron Spin-Echo (NSE) (WASP type) | 1 | YES |
| High current physics experimental position (Physics) | 1 | YES |
| Prompt Gamma Activation Analysis (PGAA) | 1 | YES |
| Neutron Depth Profiling (NDP) | 1 | YES |
| Materials Diffractometer (> 3 Å) | 1? | YES |
| Interferometer | | NO |
| Monochromatic Physical Measurements Laboratory (PML) positions | 2-3 | NO |
| Miscellaneous monochromatic/test positions | 2-3 | NO |
| Very Small-Angle Neutron Scattering (vSANS) | 1 | NO |
| TOTAL | 23-24 | 16-17 |

## 9.3 Thermal Instruments

The shorter wavelengths (~0.1 nm) and higher energies (~0.025 eV) of thermal neutrons are essential for a certain class of experiments using a variety of scattering and imaging methods. Some instruments currently being considered for use in the thermal beams, along with their moniker, are listed in Table 9-2. There are currently six specialized instruments that provide unique structural information (e.g., an Ultra-Small Angle Neutron Scattering (USANS) diffractometer for microstructure up to about 100 nm) and dynamical information (e.g., Thermal Triple Axis Spectrometers with large double-focusing monochromators and interchangeable analyzers/detectors). At least nine thermal beam instruments will be accommodated at the NNS. This will possibly require several instruments being located on curved or straight high-*m* supermirror thermal neutron guides [2], [4].

**Table 9-2 Thermal Instruments Currently Being Considered**

| Instrument Type | Moniker |
|---|---|
| Prompt Gamma Neutron Activation Analysis | PGNAA |
| Neutron Microscope | Imaging |
| High-Res powder diffractometer | D |
| Triple Axis Spectrometer | 3X |
| Ultra-Small Angle Neutron Scattering | USANS |
| High Throughput, Fast Powder Diffractometer | D |
| White Beam Engineering Diffractometer (with CANDOR[h]-type detector) | ENG |
| High Current Physics Experimental Position | PHYS |

The compact core of the NNS produces a significant gain in the thermal neutron beam flux by allowing the thermal beam thimbles to be more optimally placed in the peak of the thermal flux. The NNS core will produce a minimum peak unperturbed thermal neutron flux in the reflector of about $5\times10^{14}$ $cm^{-2}s^{-1}$ at 20 MW, whereas the NBSR core, which has a peak thermal flux located at the center of the fuel, constrains the beam thimbles to be located at a radius where the peak unperturbed thermal neutron flux has fallen to about $2\times10^{14}$ $cm^{-2}s^{-1}$ at 20 MW power (see also reference [4]).

To take advantage of the increased neutron flux and to optimally configure instruments, a preliminary layout for the thermal beam suite of instruments is presented here. This serves as a guide to the impact that the NNS will have, recognizing that as construction proceeds and technology improves, user groups will be convened to help decide on the optimal instrument suite.

Unlike the current NBSR configuration, the thermal instruments (especially those employing longer neutron wavelengths in the thermal spectrum) may take advantage of high-*m* supermirror thermal neutron guide technology, allowing instrumentation to be placed at a distance from the reactor face, reducing constraints on instrument footprint. Currently, space for instrument deployment within the NBSR confinement building is severely limited. This also enhances performance due to lower background radiation as well as potentially reducing beam-dependent background by limiting transmission of neutrons outside of the divergence range of the instrument.

Detailed design calculations have been carried out [4]. Consideration of curved vs straight guides with existing *m* values of the supermirrors, suggests that, in many cases, the thermal

[h] CANDOR is the "Chromatic Analysis Neutron Diffractometer or Reflectometer" at the NIST Center for Neutron Research which employs detector multiplexing by using multiple energy analyzer crystals.

guides are likely to be straight with a large proportion of fast neutrons, often requiring bismuth gamma filters and fast neutron filters such as MgO, sapphire, or quartz.

Although designs for practical thermal beam tube placement in the core are preliminary, a configuration like that shown in Figure 9-3 is likely required with beams at split levels to facilitate cold neutron beam extraction from both sides of each cold source at a central level. The layout shows eight (roughly to-scale) instrument cartoons, some of which would be fed by thermal neutron guides penetrating the mid-pool region around the core. The benefits of introducing thermal neutron guides through the shield to optimize thermal neutron beam extraction as well as engineering constraints, such as providing sufficient cooling will be studied further as the instrument suite is refined.

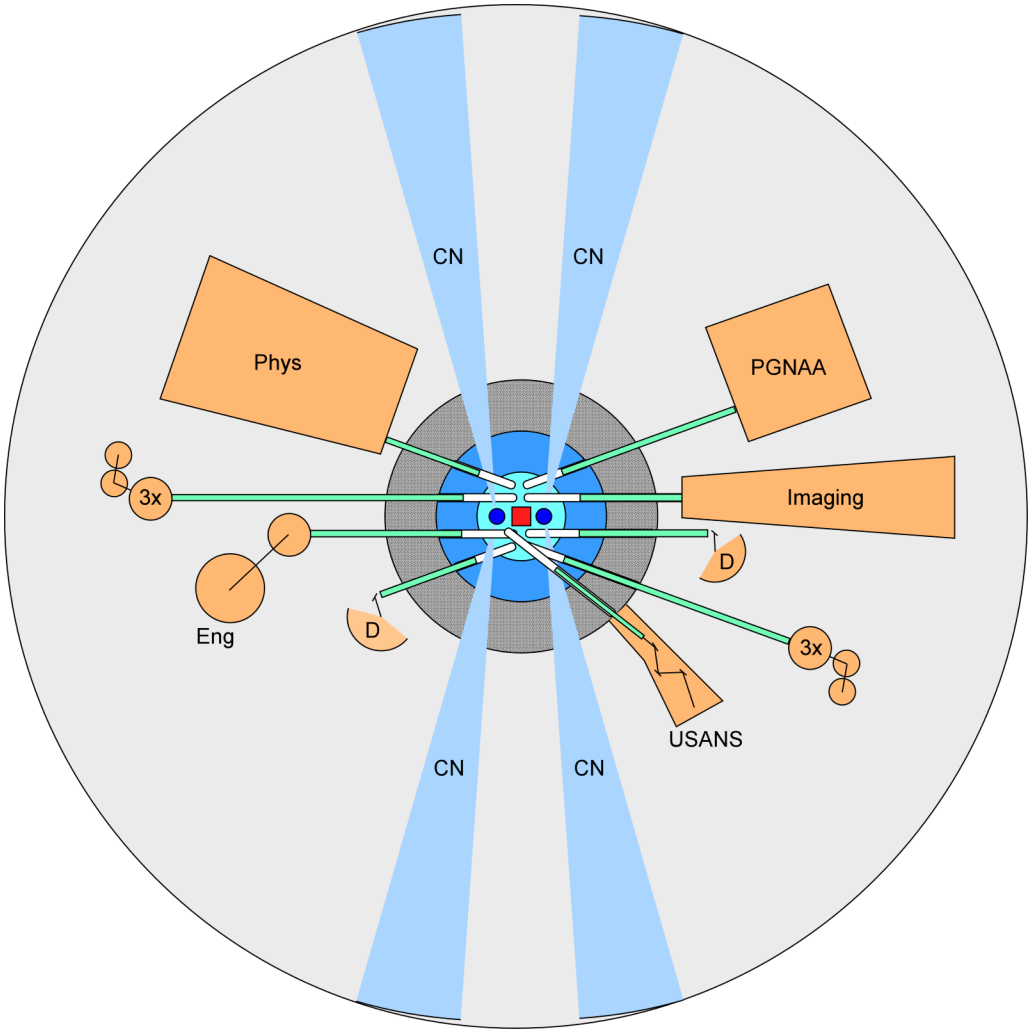



**Figure 9-3 Beam Guide Configuration and Thermal Instruments**

## 9.4 Neutron Activation Analysis

Thermal neutrons are essential for neutron activation analysis (NAA). Thermal-neutron irradiation facilities are critical to the mission needs of NIST for calibrations, activation analysis, and sample irradiations. This is in support of NIST's role as the nation's reference laboratory for measurements and standards of chemical composition. Neutron activation analysis often serves as one of the two independent measurements required for the certification of Standard Reference Materials®.

Although not shown in the pre-conceptual design layout in Chapter 3, detailed designs will have tubes in the reflector tank where, as stated above, the minimum peak unperturbed thermal neutron flux in the reflector will be about $5\times10^{14}$ $cm^{-2}s^{-1}$ or greater at 20 MW. The tubes, of different sizes, will be for pneumatic irradiation facilities as well as for other experiments. Not only will the thermal fluxes be higher than at the NBSR, but also the flux in the resonance region will be lower, another advantage reducing the noise.

Prompt gamma neutron activation analysis (PGNAA) will also be carried out at the NNS. However, PGNAA is performed employing thermal and cold neutrons, via the thermal beam tubes, and cold neutron guides, respectively (see PGNAA in Table 9-2).

## 9.5 References

[1] J. C. Cook *et al.*, "Proposed NIST Neutron Source User Facility," in *2022 ANS Winter Meeting and Technology Expo*, November 13-17, 2022 2022, Phoenix, AZ: American Nuclear Society, pp. 608-611, doi: doi.org/10.13182/T127-39654.

[2] J. C. Cook, H. E. King, C. F. Majkrzak, and D. A. Neumann, "Pre-conceptual Design Activities of the NIST Neutron Source: Preliminary Layout of Cold and Thermal Neutron Instruments," National Institute of Standards and Technology, Gaithersburg, MD, NIST TN 2280, February 2024, https://doi.org/10.6028/NIST.TN.2280.

[3] S. Wilson, M. Hore, and S. Kline, "Neutrons for the Future," National Institute of Standards and Technology, Gaithersburg, MD, NIST SP 2100-07, October 18-20, 2023, 2024, https://doi.org/10.6028/nist.sp.2100-07.

[4] J. C. Cook, C. F. Majkrzak, and H. E. King, "Pre-conceptual Design Activities of the NIST Neutron Source - Simulations of Neutron Beam Characteristics of the Proposed NIST Neutron Source," National Institute of Standards and Technology, Gaithersburg, MD, NIST TN 2284, February 2024, https://doi.org/10.6028/NIST.TN.2284.

# Appendix A List of Acronyms / Abbreviations

| Acronym or Abbreviation | Definition |
|---|---|
| 2D / 3D | Two-Dimensional / Three-Dimensional |
| 10CFRxx | Title 10 of Code of Federal Regulations Part xx |
| BNL | Brookhaven National Laboratory |
| BOC | Beginning-of-Cycle |
| CDF | Cumulative Distribution Function |
| CFD | Computational Fluid Dynamics |
| CHFR | Critical Heat Flux Ratio |
| CMS | Core Monitoring System |
| CNS | Cold Neutron Source |
| DT | Digital Twin |
| ECS | Emergency Control Station |
| EOC | End-of-Cycle |
| FA | Fuel Assembly |
| FE | Fuel Element |
| FP | Fuel Plate |
| FRM | Forschungsreaktor München |
| HMI | Human Machine Interface |
| HX | Heat Exchanger |
| IAEA | International Atomic Energy Agency |
| I&C | Instrumentation and Control |
| LCO | Limiting Condition of Operation |
| LEU | Low-Enriched Uranium |
| $LH_2$ / $LD_2$ | Liquid Hydrogen / Deuterium |
| LOCA | Loss of Coolant Accident |
| LOFA | Loss of Flow Accident |
| LOPA | Loss of Power Accident |
| LSSS | Limiting Safety System Setting |
| HEU | Highly-Enriched Uranium |
| MCNP | Monte Carlo N-Particle |
| MHA | Maximum Hypothetical Accident |
| MOC | Middle-of-Cycle |
| MTR | Materials Testing Reactor |
| NBSR | National Bureau of Standards Reactor |
| NCNR | NIST Center for Neutron Research |
| NIST | National Institute of Standards and Technology |
| NNS | NIST Neutron Source |

| Acronym or Abbreviation | Definition |
|---|---|
| NPR | Non-Power Reactor |
| OFIR | Onset of Flow Instability Ratio |
| ONBR | Onset of Nucleate Boiling Ratio |
| OPAL | Open-Pool Australian Lightwater (reactor) |
| PCS | Primary Cooling System |
| PPCS | Plant Process Control System |
| PPF | Power Peaking Factor |
| PSAR | Preliminary Safety Analysis Report |
| RCB | Regulating Control Blade |
| RCS | Reactor Control System |
| RELAP | Reactor Excursion Leak Analysis Program |
| RIA | Reactivity Insertion Accident |
| RMS | Reactor Monitoring System |
| RPCS | Reactor Pool Cooling System |
| RSPCS | Reactor and Service Pools Cooling System |
| RPS | Reactor Protection System |
| SSC | Structures, Systems, and Components |
| SU | Startup (beginning of fuel cycle before Xe buildup) |
| SCB | Shim Control Blade |
| SNR | Signal-to-Noise Ratio |
| SNS | Spallation Neutron Source (at Oak Ridge National Laboratory) |
| TRACE | TRAC/RELAP Advanced Computational Engine |
| U-10Mo | Uranium plus 10% Mass Fraction of Molybdenum |